A COMPARISON OF THE HEFT SUBSURFACE AND DELFIC PARTICLE SIZE DISTRIBUTIONS AND EFFECTS IN HPAC

THESIS

Eric T. Skaar, First Lieutenant, USAF

AFIT/GNE/ENP/05-13

DEPARTMENT OF THE AIR FORCE
AIR UNIVERSITY

AIR FORCE INSTITUTE OF TECHNOLOGY

Wright-Patterson Air Force Base, Ohio

A COMPARISON OF THE HEFT SUBSURFACE

AND DELFIC PARTICLE SIZEDISTRIBUTIONS

AND EFFECTS IN HPAC

THESIS

Presented to the Faculty

Department of Engineering Physics

Graduate School of Engineering and Management

Air Force Institute of Technology

Air University

Air Education and Training Command

In Partial Fulfillment of the Requirements for the

Degree of Master of Science in Nuclear Engineering

Eric T. Skaar, BS

First Lieutenant, USAF

March 2005

A COMPARISON OF THE HEFT SUBSURFACE AND DELFIC PARTICLE SIZE DISTRIBUTIONS AND EFFECTS IN HPAC
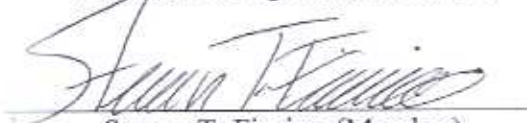
Eric T. Skaar, BS

First Lieutenant, USAF

Approved:

_____
Charles J. Bridgman (Chairman)

3/11/05
date

_____
Steven T. Fiorino (Member)

11 MAR 05
date

_____
Vincent J. Jodoin (Member)

11 Mar 05
date

Abstract

The Heft subsurface three component lognormal fallout particle size distribution is compared and contrasted with the single lognormal fallout particle size distribution used by the Defense Land Fallout Interpretive Code (DELFIC). Comparison of the two distributions is accomplished with results from the AFIT smear code and the Hazard Prediction and Assessment Capability (HPAC). The effect of the distributions is explored in HPAC for varying yield weapons, varying surfaces, precipitation conditions, varying wind effects and varying dose rate times. The results from the two distributions are quantitatively compared using the concepts of grounded source normalization constant and the rate at which activity is being deposited on the ground everywhere at time t.

The Heft subsurface three component lognormal fallout particle size distribution results in significantly less activity on the ground than does the DELFIC single lognormal particle size distribution. The grounded source normalization constant resulting from the Heft distribution is up to three times smaller than that observed when using the DEFLIC distribution.

Acknowledgments

I would like to thank my advisor, Dr. Charles J. Bridgman for his time, criticism, encouragement and humor. It has been an honor and a privilege to work under his tutelage. I'd also like to thank the members of my thesis committee, Lt. Col Vincent Jodoin and Lt Col Steve Fiorino for their feedback.

I am also indebted to all of those who went out of their way to help me, particularly Dr. Joseph T. McGahan and Major D. Brent Morris. Without their insight and assistance I could not have completed this thesis. A special thanks also to Major Steven Weber who helped me in the writing and editing of this thesis.

Eric T. Skaar

Table of Contents

List of Figures

List of Tables

A COMPARISON OF THE HEFT SUBSURFACE AND DELFIC PARTICLE SIZE

DISTRIBUTIONS AND EFFECTS IN HPAC

I. Introduction

Motivation

The possibility of a domestic nuclear event due to rogue nations or transnational threats demands vigilance from our law enforcement, intelligence and military communities to protect the citizens of this country from that danger. In order to assist these diverse groups, the scientific community has an obligation to understand the nature of the threat posed by nuclear weapons and the impacts that would result from a nuclear detonation.

The nuclear tests conducted in the 40's, 50's, and 60's have left us with a wealth of scientific knowledge concerning the effects of nuclear weapons. However, despite this vast amount of data, our ability to model the effects of a nuclear event is limited by our finite understanding of its physics, our imperfect mathematical tools used to describe the physics that we do understand, and our limited computational resources. Our limited computational ability requires that we greatly simplify the mathematics used to analyze nuclear events. As such, we strive to find the best mathematical representation of physical phenomena that gives us an understanding of what is happening without being overly complicated or time consuming.

Background

In order to mathematically represent a chemical, biological, radiological or

nuclear (CBRN) event, the Defense Threat Reduction Agency (DTRA) has overseen the development and maintenance of the Hazard Prediction and Assessment Capability (HPAC) software. HPAC is a modeling program that attempts to predict the effects from a CBRN event. HPAC is used for planning purposes by military strategists and emergency response personnel.

All fallout codes consist of two basic components: source definition and transport. Source definition takes into account all the variables from the moment of detonation through cloud rise until the formation of the stabilized nuclear cloud. Transport then takes the fallout defined in the stabilized nuclear cloud and uses weather and deposition phenomena to distribute the fallout over the ground. This will be described in greater detail in Chapter 3.

A single lognormal was suggested by the Defense Land Fallout Interpretative Code (DELFIC) to model the particle size range of fallout particles for surface bursts (19:16). A surface burst is a nuclear explosion where the fireball interacts with the surface of the earth. This single lognormal has been traditionally used to represent the particle size distribution typical of fallout that results from nuclear bursts in many subsequent fallout codes including HPAC. In 1968, Heft proposed a series of three lognormal distributions to represent the particle size distribution that would result from a subsurface nuclear detonation (12:271). Thanks to the work of McGahan of SAIC, the Heft subsurface tri-lognormal particle distribution has been incorporated into the most recent version of HPAC, HPAC 4.04 (14:1). All versions of HPAC previous to 4.04 use the DELFIC single-lognormal to model the particle size distribution from a nuclear burst.

Problem

This thesis compares and contrasts the Heft distribution with the DELFIC distribution in order to quantitatively and qualitatively describe the effects of the two particle distributions on the predictive fallout contours of HPAC.

Scope

  HPAC can be used to model a variety of CBRN scenarios. HPAC can model subsurface, surface and near-surface nuclear blasts up to 10 megatons. This research looks specifically at the differences between predictions of HPAC 4.03 and 4.04 generated by the nuclear weapon module as a result of differing particle size distributions. While cloud rise dynamics play an important role in fallout prediction, it is not considered here. Similarly, the discussion of HPAC's transport module, SCIPUFF, is limited to explanation as it pertains to fallout particle deposition and a brief critique of rain scavenging mechanisms in SCIPUFF. Validation of the accuracy of the fallout modeling by comparison with actual nuclear surface bursts is not considered here. For a more complete treatment of this subject please see "A Comparison of Hazard Prediction and Assessment Capability (HPAC) Software Dose Rate Contour Plots to a Sample of Local Fallout Data from Test Detonations in the Continental United States, 1945-1962" by Richard Chancellor (4).

General Approach

  This research begins with a discussion of the physics of fallout formation. First, emphasis is placed upon the concept of Freiling ratio and its implications for determination of radionuclide distribution in fallout particles. Next, particle distributions are considered with a focus on describing the DELFIC single lognormal and the Heft tri-lognormal particle size distributions. After this, a brief overview of HPAC is given with emphasis on particle distributions HPAC uses to model fallout particle sizes. Finally, the impact of the two particle distributions is considered on varying weapon yields, resolutions, surfaces, rainout and winds.

II. Literature Review

This chapter provides a brief overview of the physics of fallout formation and a brief description of the DELFIC and Heft subsurface distributions. Finally, an overview of HPAC is provided with a summary of how components of the nuclear weapons and transport module are calculated.

Physics of Fallout Formation

When a nuclear weapon is detonated the fission of fuel atoms (either ^{235}U or ^{239}Pu) causes a great deal of energy to be released in a very short amount of time. This release of energy translates into a dramatic increase in temperature and pressure. The energy translated into heat is referred to as thermal radiation and the visible light given off from a nuclear explosion is referred to as the fireball. The temperature of a nuclear explosion can reach up to tens of millions of degrees. Matter that interacts with this high temperature within the fireball is vaporized. After the moment of detonation, the temperature causes the fireball to rise after the pressure comes in to equilibrium with its surroundings during fireball expansion. The aforementioned expansion results in a temperature drop within the fireball (8:26-44).

At a bare minimum, debris from the weapon itself is present in the fireball of a nuclear explosion. This debris includes casing and components from the weapon itself as well as radioisotopes from the nuclear fuel of the weapon. These radioisotopes will include both unused atoms of either uranium or plutonium as well as radioisotopes that are the result of fission products or decay from fission products. However, since both ^{235}U and ^{239}Pu have relatively long half lives, we are primarily concerned with the activity of the fission products, which have much shorter half lives.

In the case of a surface burst the fireball interacts with the ground. As the fireball rises, it draws up soil from the surface below. As the soil interacts with the fireball it is vaporized. Eventually, the fireball cools to the boiling point of the local soil material. When this boiling point is reached, soil material starts to condense together. This particular temperature varies based on the atomic composition of the soil. The temperature within the fireball continues to fall below the boiling point of the local soil. When the fireball temperature reaches the melting point of the soil, the soil particles start to solidify (20:3-5). The melting point is generally assumed to be around 1400ºC (6:3).

As the soil material starts to condense, radioisotopes from the weapon start to condense onto the soil. The fission products do not condense onto each other because of the relative abundance of the soil material in comparison with the fission products. Fission fragments make up a very small proportion of the mass of debris in a nuclear explosion. The fraction of fission fragments in a surface burst will be in the range of parts per ten million (2:402). For this reason, the soil acts as a carrier for the fission product radioisotopes. Similar to the soil material, the temperature at which a fission product radioisotope will condense varies. Some radioisotopes have a condensation temperature that is greater than the melting temperature of the carrier soil material. Consequently, when the temperature of the fireball reaches the condensation temperature of the carrier soil material, these radioisotopes immediately begin to condense onto the carrier soil. These radioisotopes are known as refractories. Because refractories condense onto carrier while it is still molten and condensing, they have the opportunity to both condense with the carrier and diffuse throughout the volume of the soil particle. For this reason, refractories tend to be volume distributed within the condensed soil particles.

Conversely, radioisotopes that have boiling temperatures lower than the solidification point of the local soil, and hence condense at temperatures lower than the melting point of the local carrier material, are known as volatiles. Volatiles do not condense onto the local soil particles until the soil particles have formed and solidified. As a result of this, volatiles are surface distributed over the soil particles (6:3).

The relative abundance of different radioisotopes found in fallout particles varies based on many factors. One of these factors is the size of the fallout particles. Fallout particle size ranges from a few tenths of a micron to 1 millimeter or more. The first particles to be formed grow larger than particles formed at later times. As such, they scavenge the refractory radioisotopes which condense at a higher temperature, and hence form at a time sooner than the volatiles. When these early forming particles get large enough they fall out of the fireball and onto the earth. These early fallout particles often leave the fireball before it has cooled enough for certain volatiles to condense onto them. As such, they are refractory rich and volatile poor. Smaller soil particles, however, are often introduced into the nuclear fireball at a later time and may not even be melted depending on the temperature of the fireball at the time of their introduction. Because these smaller particles are formed at a later time, most of the refractories have already been scavenged and as a result, these smaller particles collect more volatiles. Fractionation is then the difference in the radioisotopic composition of fallout particles from the overall composition of fission fragments or as Freiling defines it, "any alteration of radionuclide composition occurring between the time of detonation and the time of radiochemical analysis which causes the debris sample to be nonrepresentative of the detonation products taken as a whole" (7:1991).

Description of the DELFIC Particle Distribution

The DELFIC lognormal particle distribution for surface bursts is given by the following equation:

$$f(d) = \frac{1}{\sqrt{2\pi}\beta d} e^{-\frac{1}{2}\left[\frac{\ln(d)-\alpha_0}{\beta}\right]^2}$$ (1)

where,

f(d) is the fraction of particles with diameter d

β is the natural logarithm of the standard deviation (ln(4.0))

α_0 is the natural logarithm of the median diameter in microns (ln(0.407)) (19:16).

Two implicit assumptions of most particle distributions are that the fallout particles are spherical and they have a constant density across the entire distribution.

One fortunate property of the lognormal number distribution is the relative ease of finding the surface area and volume distributions from the number distribution. The surface area distribution can be found by substituting α_0 with α_2 where $\alpha_2 = \alpha_0 + 2\beta^2$. The volume distribution can be found by substituting α_0 with α_3 where $\alpha_3 = \alpha_0 + 3\beta^2$ (2:405-406). It should be noted that volume and mass distributions are equivalent for spherical particles with constant densities over the distribution.

As seen in Figure 2, most of the mass contained in the distribution is to be found above 100 microns. Since volume distribution is assumed for larger particles (19:50), most of the activity will be found in this range as well.
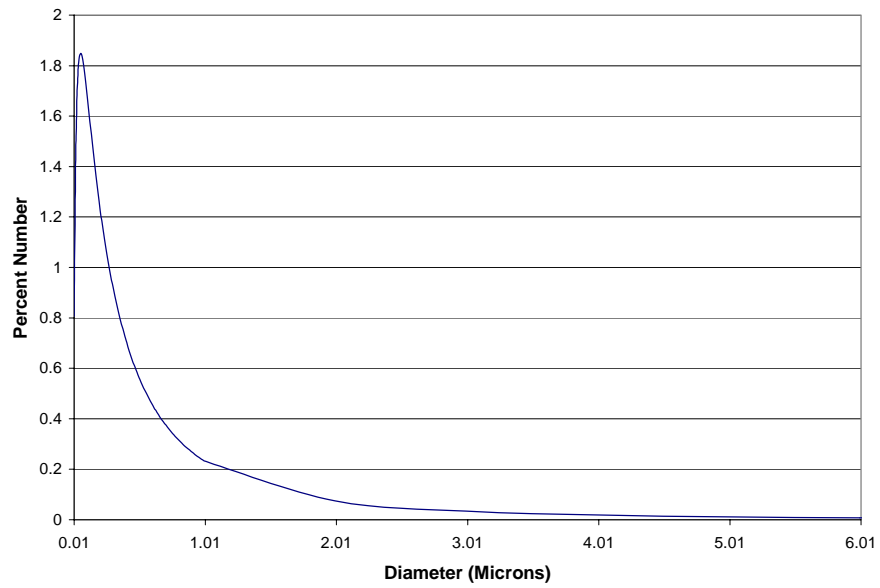
Figure 1: DELFIC Number Distribution

In terms of numbers of particles, 99% of fallout particles, according to the DELFIC number distribution shown in Figure 1, are found below 10 microns.
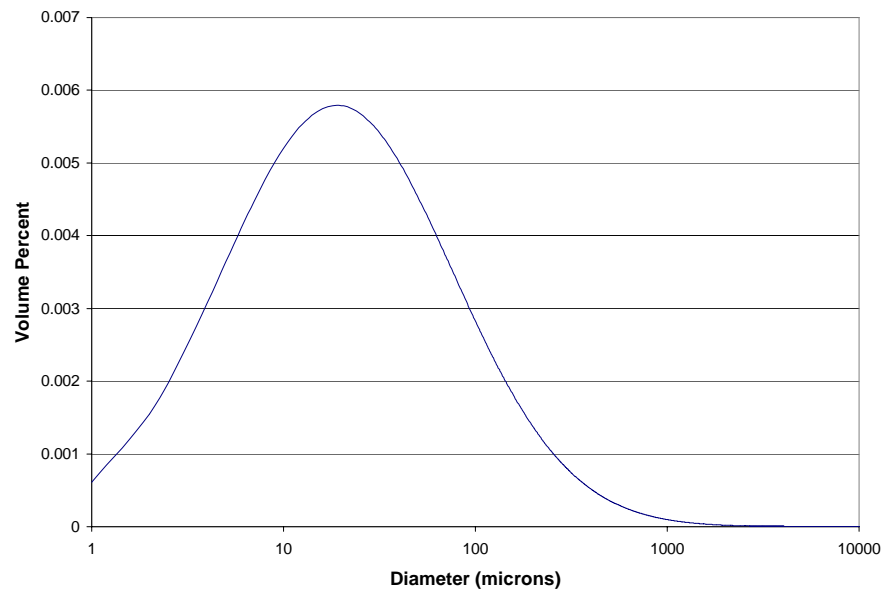
Figure 2: DELFIC Mass Distribution

Description of the Heft Subsurface Particle Distribution

The Heft subsurface mass distribution is given by the following equation:

$$\frac{dF_m}{dx} = \sum_{i=1}^{3}\left(\frac{\phi_i}{\sigma_i\sqrt{2\pi}}\right)\exp\left[-\left(\frac{\overline{x_i}-x}{\sigma_i\sqrt{2}}\right)^2\right] \tag{2}$$

where

ϕ_i is the percentage of mass for the ith population

σ_i is the standard deviation of the $\log_{10}$(diameter) for the ith population

$\overline{\chi_i}$ is the $\log_{10}$ of the average diameter in microns for the ith population

χ is the $\log_{10}$ of the diameter in microns (12:274).

The parameters for equation 5 are shown below in Table 1.

Table 1: Parameters for Heft Subsurface Log_{10} Mass Distribution

Population	ϕ_i	σ_i	$\overline{\chi_i}$
1 (Local)	0.40	0.57	2.48
2 (Glass)	0.474	0.23	1.26
3 (Crystalline)	0.126	0.28	0.83

The Heft subsurface distribution can be converted from a lognormal base 10 distribution to a lognormal base e distribution (see Appendix A). This results in the following formula:

$$f(d) = \sum_{i=1}^{3}\frac{\phi_i}{\sqrt{2\pi}\beta_i d}\, e^{-\frac{1}{2}\left[\frac{\ln(d)-\alpha_{0i}}{\beta_i}\right]} \tag{3}$$

where

Population	ϕ_i	β_i	α_0	α_3
1 (Local)	0.40	1.31	0.542	5.71
2 (Glass)	0.474	0.5296	2.06	2.9
3 (Crystalline)	0.126	0.6447	0.6699	1.92

Comparison of Heft Subsurface Crystalline Distribution with Baker Airburst

Distribution

For an airburst, Baker suggests a single lognormal distribution with a Beta equal to ln(2) and the median radius of 0.1 microns (2:404). This is shown along with the Heft subsurface crystalline component in Figure 3.

It can be seen from figure Figure 3 that while the crystalline particles are larger as a whole, there is considerable overlap between the airburst and the crystalline component. Even though Baker's small distribution assumes no carrier soil whatsoever, there is some similarity between the Baker small distribution and the Heft subsurface crystalline distribution. This means the transport of fallout particles due to the crystalline component will behave similarly to transport of fallout particles from an airburst. Since an airburst produces no local fallout, it is not an unreasonable expectation that the
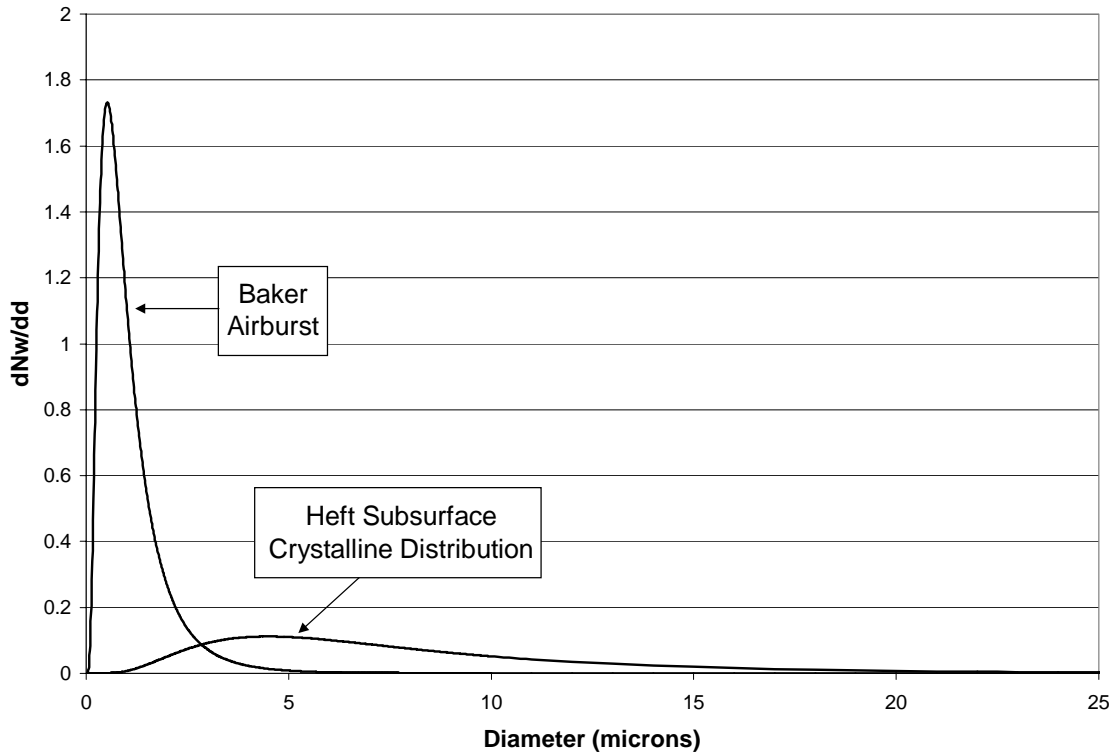
Figure 3: Volume Distribution for Heft Subsurface Crystalline and Baker Airburst

crystalline portion of the Heft three-component subsurface distribution will not contribute

significant amounts of activity to local fallout.

Comparison of the Heft Three-Component Subsurface Distribution with the

DELFIC Surface Distribution

An overlay of the mass distributions for the Heft three-component subsurface

distribution and the DELFIC surface distribution is shown in Figure 4.

It can be readily seen from Figure 4 that the Heft distribution has a much greater

proportion of its mass in particles less than 20 microns than does the DELFIC
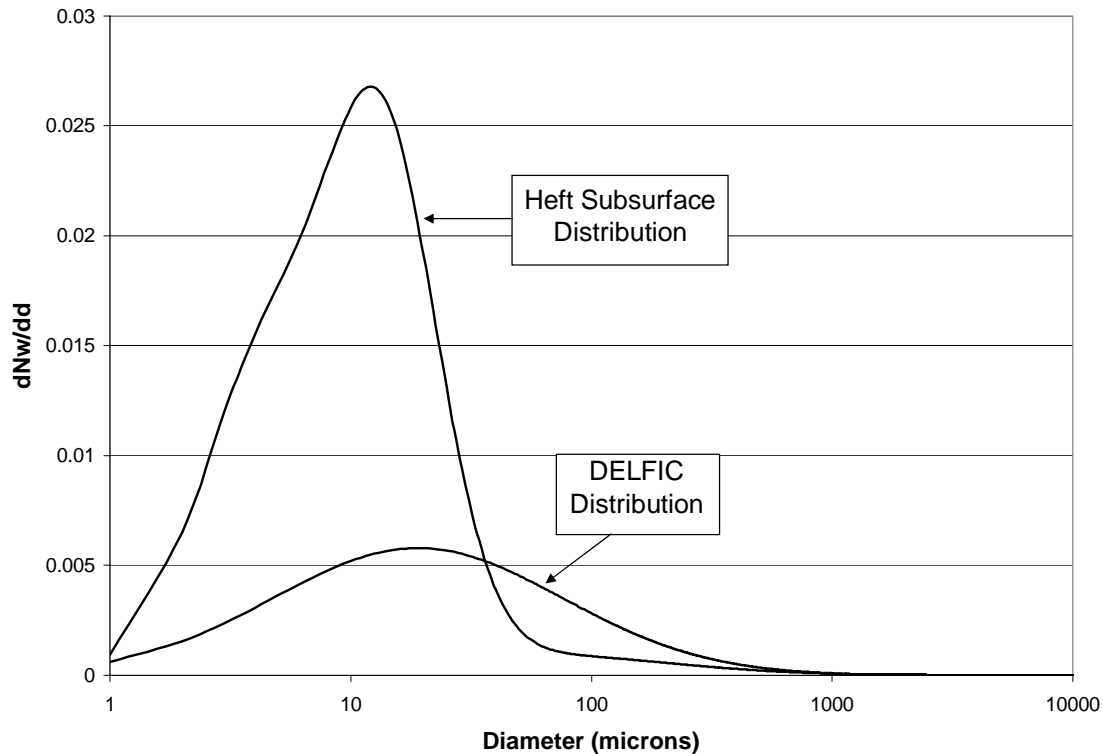
Figure 4: Comparison of DELFIC and Heft Three-Component Mass Distributions

distribution. Conversely, the DELFIC distribution contains much more of its mass in

particles greater than 20 microns than does the Heft three-component distribution. If the

highest dose rate is created by the fallout closest to ground zero and if the fallout closest

to ground zero is due to the larger particles that fall out faster than the smaller particles,

than the DELFIC distribution will generate higher dose rates close to ground zero than

the Heft three-component distribution.

HPAC Overview

The Hazard Prediction and Assesment Capability software predicts the effects of

a chemical, biological, radiological or nuclear incident and the collateral effects on

civilian population. This thesis concentrates on the nuclear weapon module, in particular

the impact of different particle size distributions. All HPAC calculations are composed
of three basic stages: hazard source definition, transport and effects.
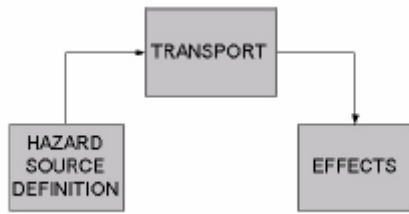
Figure 5: HPAC Stages (11: 4-1)

The hazard source definition defines the CBRN incident in terms of the location,
composition, size and time domain of the release. HPAC then uses the Second Order
Closure Integrated PUFF (SCIPUFF) to model the transport of the hazardous material
through the atmosphere and deposition on the ground. After this is accomplished, the
effects stage then calculates the impact the hazardous material would have on the local
civilian population (11:4-1). This thesis will not concern itself with the effects stage.

The nuclear weapon (NWPN) module is the hazard source definition module
within HPAC. This is based upon the cloud rise and activity definition modules of the
research code Newfall (11:6-5-17). Due to improved computer speeds and algorithms,
Newfall is able to replicate the Defense Land Fallout Interpretive Code (DELFIC) in a
faster running code. Newfall's cloud rise calculations are based on the DELFIC cloud
rise physics calculations (16:3).

Cloud Rise in Newfall/DELFIC

The DELFIC cloud rise initialization time is defined to be the time when the
fireball reaches pressure equilibrium with the atmosphere (19:9). This time is calculated

using the weapon yield. After this, the mass of the fallout in the cloud is calculated based on weapon yield and depth of burst. The mass of fallout in the initially stabilized cloud includes both weapon debris and lofted soil.

Another important time in DELFIC is when the soil particles in the fallout cloud stop scavenging fission products from the weapon debris within the volume of the fallout particle. This is taken to be the time where the average cloud temperature cools down to the soil solidification temperature. DELFIC distinguishes this temperature based on the type of soil over which the bomb is detonated. For siliceous soil, such as that found at the Nevada test site, the temperature is taken to be 2200K. For calcarious soil, such as the coral of the Pacific test site, the temperature is taken to be 2800°K (19:12).

The amount of energy available from the explosion to heat the cloud, H, is determined based on the weapon yield. The mass of air in the cloud at the cloud initialization time is determined based on the energy available, ambient and virtual temperature at initialization time and mass of fallout in the cloud. Virtual temperature is defined as the temperature that dry air must have in order to have the same density as the moist air at the same pressure (23:52). The mass of water in the cloud at cloud initialization time is determined based on the energy available, ambient and virtual temperature at initialization time, latent heat of vaporization of water, the mass of air in the cloud, the relative humidity, the ratio of molecular weights of air and water, the ambient pressure, the saturation water vapor pressure and mass of fallout in the cloud (19:12-15).

The initial shape of the cloud is assumed to be an oblate spheroid (19:26). The initial height of the cloud center is found based on the following equation:

$$z_i = z_{GZ} + z_{HOB} + 90W^{1/3}$$ (3)

where

z_{GZ} is the altitude of ground zero

z_{HOB} is the altitude of the height of burst above ground zero

W is weapon yield in kilotons (19:14).

Initial rise speed of the cloud is determined based on the initial cloud radius. Cloud rise is calculated using a set of coupled ordinary differential equations that solve for momentum, cloud center height, temperature, turbulent kinetic energy density, mass, soil mass mixing ratio, water vapor mixing ratio and condensed water mixing ratio (19:19-24).

As the initial stabilized cloud is defined, a particle cloud is defined for each particle size group. Each particle cloud is assumed to be a cylinder with a uniform shape that has a diameter and height equal to the major and minor axes of the stabilized nuclear cloud. This cylinder is then subdivided into disks which are then tracked through the atmosphere by the transport code (19:27-30).

Activity Calculation in DELFIC

This section will provide a brief overview of how activity is calculated and distributed in Newfall and therefore, by extension, HPAC. Since this thesis is primarily interested in comparing the Heft particle size distribution with the DELFIC particle size distribution, the following discussion will focus on the activity associated with the fallout particles formed from local soil material and bomb debris. Induced activity in the soil is modeled only for those neutrons that interact with the apparent crater. Induced activity in the device material is only considered in the case of neutron capture by ^{238}U and

15

subsequent decay.   Induced activity in the soil and induced activity in the device

materials will not be considered beyond the above mention. Newfall uses the same basic

technique for activity calculation and distribution as is used in the DELFIC code, except

the user has the option of using the DELFIC, Heft subsurface or other user input particle

size distribution.

12 different fissions are considered in the DELFIC code:

U233 High Energy Neutron Fission

U233 Thermal Neutron Fission

U233 Fission Spectrum Neutron fission

U235 Thermal Neutron Fission

U235 High Energy Neutron Fission

U235 Fission Spectrum Neutron Fission

U238 High Energy Neutron Fission

U238 Thermonuclear Neutron Fission

U238 Fission Spectrum Neutron Fission

P239 High Energy Neutron Fission

P239 Thermal Neutron Fission

P239 Fission Spectrum Neutron Fission.

The decay history of each member of a decay chain is calculated using the

Bateman equation, adjusted for branching (19:42-45).

DELFIC uses Freiling's simplifying assumption that a refractory will be volume

distributed throughout a fallout particle while a volatile will be surface distributed onto a

fallout particle (19:47). In reality, radionuclides attachment onto soil particles is a

diffusive process. As discussed in appendix B, Freiling ratios measure the amount of nuclides in a particular fission product mass chain that are refractory at the time when the temperature in the stabilized nuclear cloud reaches the soil solidification temperature.

DELFIC and Newfall look at each mass chain and apportions the effective fissions for each mass chain into the particle size groups based on the Freiling ratio of the mass chain. For a purely refractory mass chain, where all the isotopes would be volume distributed in a fallout particle, the equivalent fissions of mass chain i in particle size group k can be found by the following equation:

$$F_i(d_k) = F_T Y_i m_i(d_k) \qquad\qquad (4)$$

where

F_T is the total number of equivalent fissions in all size classes

Y_i is the fission yield of the ith mass chain

$m_k(d_k)$ is the mass fraction of the kth size group (19:48).

However, most mass chains are not purely refractory meaning that they exhibit a combination of volume and surface distribution. Therefore, the equivalent fissions from a particular mass chain for a given particle size group will not be proportional to the mass fraction of that size group. Instead, the equivalent fissions for a mass chain will be a combination of refractory atoms from that mass chain that were volume distributed and volatile atoms that were surface distributed.

In addition, smaller particle sizes favor volatiles and surface distribution while larger particles favor refractories and volume distribution. DELFIC makes the assumption that 100 μm is the "crossover point" where the number of apparent fissions that are volume distributed equals the number of apparent fissions that are surface

17

distributed. Freiling postulated that the specific activity of fallout particles is proportional to the (b_i-1) power of the particle diameter where b_i is the square root of the Freiling ratio for mass chain i. As a reminder, for a purely refractory mass chain b=1 while for a purely volatile mass chain b=0. Therefore, for a purely refractory chain, the specific activity is constant while for a purely volatile chain specific activity is radially distributed.

DELFIC divides the equivalent fissions of mass chain i into particle size group k by the following equation:

$$F_i(d_k) = F_T Y_i \left(R_i E_i d_k^{b_i-1} + S_i \right) m_k(d_k) \tag{5}$$

where

F_T is the total number of equivalent fissions in all size classes,

Y_i is the fission yield of the ith mass chain,

d_k is the geometric mean diameter of the kth particle-size group

$m_k(d_k)$ is the mass fraction of the kth size group

R_i is the fration of fissions in the ith mass chain that obeys radial distribution

S_i is the fraction of fissions in the ith mass chain that appears with constant specific activity

E_i is a normalization factor (19:48-51).

It should be noted that S_i plus R_i equals one. S_i and R_i takes into account both the volatile/refractory makeup of a mass chain as well as the tendency for smaller particles to scavenge volatiles while larger particles are more likely to scavenge refractories.

Basic Information Concerning SCIPUFF

After the DELFIC cloud rise model sets up the stabilized nuclear cloud and populates it with particle disks, these disks are then converted to Gaussian puffs and transported by the SCIPUFF code.

SCIPUFF is a Lagrangian dispersion model that tracks a collection of Gaussian puffs through various wind fields. These puffs are allowed to disperse, split, and even combine as they are transported by wind.

The Gaussian puffs created in SCIPUFF are transported through space according to the advection-diffusion equation for a scalar quantity in an incompressible flow field (21:4). The advection-diffusion equation is represented by:

$$\frac{\partial c}{\partial t} + \frac{\partial}{\partial x_i}\left(u_i c\right) = \varsigma \nabla^2 c + S \tag{6}$$

where

c is concentration of particulates

t is time

u_i is the wind velocity in the i direction

x_i is the distance in the i direction from source

ς is the molecular diffusivity

S is sources and sinks.

As can be seen by equation 6, changes in position for the puff is a function of the wind velocity and the concentration of the puff. Both the change in position and concentration of a puff is dependent upon the molecular diffusivity and sources and sinks. However, since a nuclear explosion has only one instantaneous source, the change in

concentration is simply a function of dispersion and particle deposition after the explosion takes place.

Unlike a disk tosser routine, SCIPUFF allows diffusion in both the vertical and horizontal axes for its puffs. The diffusion modeled in SCIPUFF is assumed to arise primarily from buoyancy forces and, in the case of the vertical direction, inhomogeneity in the boundary layer. SCIPUFF also accounts for changes in the vertical axis due to wind shear.

SCIPUFF is capable of tracking solid particle materials such as nuclear fallout. In order to do this, SCIPUFF first requires a description of the particle size distribution. This description is given to SCIPUFF by assigning a set number of size bins, N_p. Each size bin is associated with a unique puff. Puffs are only allowed to merge with other puffs of the same size bin. In addition to size bins, material density, ρ_p, must also be specified.

The fall velocity of the puffs is found by equating the gravitational force to the drag force according to:

$$\frac{4}{3}\pi g \rho_p r_p^{\,3} = F_p \tag{7}$$

where

r_p is the equivalent spherical particle radius

ρ_p is the particle material density

F_p is the drag force (21:48).

The drag force is then found using the following equation:

$$F_p = \frac{1}{2}\rho_a c_D \pi r_p^2 v_g^2 \tag{8}$$

where

ρ_a is the air density

c_D is the drag coefficient

v_g is the particle fall speed.

The drag coefficient, which is a function of velocity, is parameterized as a function of Reynold's number (21:49).

From these equations, the fall speed of the particles is determined for the average radius of each size bin (21:48-49).

SCIPUFF assumes a conservation of mass (21:5):

$$\frac{dQ}{dt} = 0 .$$
(9)

This is slightly modified by surface deposition of particles due to gravitational settling so that the conservation of mass equation now becomes:

$$\frac{dQ}{dt} = -F_s$$
(10)

where

F_s is the mass flux at the surface and is defined by

$$F_s = v_D \int_{z=0} c\,dA$$
(11)

where

v_D is the downward velocity of the particles

c is the concentration

A is Area (21:50).

The fall velocity calculated from gravitational settling is continually adjusted for vertical motions at the individual puffs due to atmospheric dynamics. For further discussion concerning modeling of dry deposition processes in SCIPUFF, see reference 21 pages 48-53.

Chapter 3: Methodology

This section begins with an introduction to the analytical tools grounded source normalization constant and the function g(t). The methodology for calculating the grounded source normalization constant and the function g(t) for HPAC outputs is discussed. This section is concluded with a discussion of the default parameters used in the HPAC runs presented in chapter four.

Introduction to Source Normalization Constant, k

The unit-time reference dose rate (URDR) is the dose rate that would occur if all of the activity over the ground were homogeneously distributed over one square kilometer and then converted to the dose rate one hour after the burst which would occur at a detector one meter above the ground. The source normalization constant (k) is the URDR divided by the yield of the nuclear explosion (2:425). The units for the source normalization constant are $[R\text{-}km^2/hr\text{-}kT]$.

The activity that results from a nuclear explosion is from the fission fragments and the unused fuel. The particular radioisotopes that make up the fission fragments are a result of the type of fuel used. The amount of fuel that is used for a particular device is based upon the yield. Therefore, the source normalization constant should only depend upon the yield of the device and the type of fuel. However, since fine particles are carried great distances, they will not be accounted for in local fallout representations. The integration of activity on the ground due to fallout cannot be extended out infinitely due to computational limitations. Additionally, SCIPUFF cannot track puffs of fine particles for extended times. For these reasons, the grounded source normalization constant calculated from the dose rate data sets generated by HPAC or any fallout code

will be less than the actual source normalization constant for a particular nuclear

explosion. There is a range of accepted values for the source normalization constant.

These values range from 2590 to 7544 [R-km^2/hr-kt] (2:436). The Castle Bravo test field

measurements, which do not include global fallout, show a source normalization constant

ranging from 2590 to 3880 [R-km^2/hr-kt] (8:494).

Due to the impact of smaller particles on the effective source normalization

constant, it is reasonable to expect HPAC 4.04, with its great number of fine particles, to

exhibit a smaller grounded source normalization constant in comparison with HPAC

4.03, which has less fine particles. This is indeed what is observed between the

comparisons of different contours as will be shown by the results presented in this

chapter.

Method for Calculating Source Normalization Constant from HPAC Output

First a particular set of conditions are input into HPAC and the calculation is

completed. After this, the dose rate at the time of the final puff is plotted using the

default dose rate contours. The boundaries for the longitude and latitude are then

carefully noted. Next, the dose rate at the last puff is exported into a text file using a data

grid (typically 200 by 200 points) defined by the latitude and longitude boundaries.

Then using the Way-Wigner approximation, these dose rates are adjusted to the

unit time, which is assumed to be one hour. The Way-Wigner formula is

$$\dot{D}_{Gd}(t) = \dot{D}_{Gd}(1)t^{-1.2} \tag{12}$$

where

$\dot{D}_{Gd}(1)$ is the Dose Rate on the ground at the unit time (2:424).

After this, the distance between latitude points and the distance between longitude points are calculated in kilometers. Then the unit-time reference dose rate is calculated by integrating the unit-time dose rates over the entire area using Simpson's double integral (3:232-234). Finally, the unit-time reference dose rate is divided by the yield of the nuclear explosion to find the grounded source normalization constant. For more detail on these calculations, please see Appendix E.

Introduction to g(t)

g(t) is a quantity which represents the fractional rate of activity deposition on the ground per unit time everywhere at time t (2:413-414). Clearly it follows from this that g(t) integrated over all time will yield unity. If the fallout cloud is approximated as a two dimensional cloud (a wafer) with no distribution of particle size in the vertical direction and gravitational settling is assumed to be the only particle deposition mechanism, then only one size group would be arriving on the ground at time t. In this case, g(t) can be approximated by

$$g(t) = A(d) \left| \frac{-dd}{dt} \right|$$ (13)

where

A(d) is the activity distribution as a function of fallout particle diameter

d is fallout particle diameter

t is time (2:414).

This is the simplifying assumption used in the AFIT smear code. In HPAC A(d) is determined based on individual mass chains and as such there is not a simply activity distribution by which to calculate g(t). In addition, dd/dt is not known. However, if a

constant wind is input into the model, then the fallout cloud center can be approximated

by assuming that after weapon detonation the fallout cloud travels at the same speed as

the constant wind. It can then be assumed that the activity is deposited on the ground

when the fallout cloud center is directly overhead. If the dose rate of the fallout particle

activity on the ground is integrated in horizontal slices transverse to the constant wind

and then divided by the source normalization constant, g(t) can be approximated for an

HPAC fallout contour with the following equation:

$$g(t)dt = g(x)\frac{dx}{dt} \tag{14}$$

where

   x is downwind distance in km

   t is time in hours.

   From this relationship, it follows that

$$g(t) = \frac{\int_0^\infty UDR}{kW} \cdot \frac{dx}{dt} \tag{15}$$

where

   UDR is the unit-time dose rate [R-km/hr]

   t it time in hours

   k is the source normalization constant in [R-km^2/hr-kT]

   Wis yield in kilotons.

   This is the basis for the g(t) code found in Appendix D which is used to analyze

the HPAC constant wind fallout contours.

Method for Calculating the Function g(t) from HPAC Outputs

A particular set of conditions are input into HPAC and the calculation is completed. After this, the dose rate at the time of the final puff is plotted using the default dose rate contours. The boundaries for the longitude and latitude are then carefully noted. Next, the dose rate at the last puff is exported into a text file using a data grid (typically 200 by 200 points) defined by the latitude and longitude boundaries.

Then using the Way-Wigner approximation, these dose rates are adjusted to the unit time, which is assumed to be one hour.

After this, the distance between latitude points is calculated in kilometers. The unit-time dose rates transverse to the wind direction are then integrated using Simpson's rule. Dividing the integrated unit-time dose rates by the yield times the source normalization constant (assumed to be 4000 [R-km^2/hr-kt]) results in g(x). The function g(x) can then be multiplied by the speed of the constant wind, which is used to approximate dx/dt. This results in an estimation of the function g(t). See Appendix D for the FORTRAN code documenting this calculation.

General Information Concerning HPAC Runs

Unless otherwise noted, the nuclear weapon parameters used in all HPAC runs are shown in Figure 6. Time of burst is important to note because when a fixed wind is used, the historical data for humidity, temperature and pressure profile is used based on that time.

Figure 6: Nuclear Weapon Parameters Used in HPAC Runs

Unless otherwise noted, the fixed wind parameters used in all HPAC runs are

shown in Figure 7.

Figure 7: Fixed Wind Parameters Used in HPAC Runs

Unless otherwise noted, the general weather parameters used in all HPAC runs are shown in Figure 8.

Figure 8: General Weather Parameters Used in HPAC Runs

There are a number of dose rate contour plots in this chapter. In order to avoid obscuring any of the features of these plots, the legend is not included on many of them. Figure 9 shows a typical HPAC dose rate contour plot with the default contour legend included. Any time that the default contours are not used, a legend indicating the value of each contour is included.
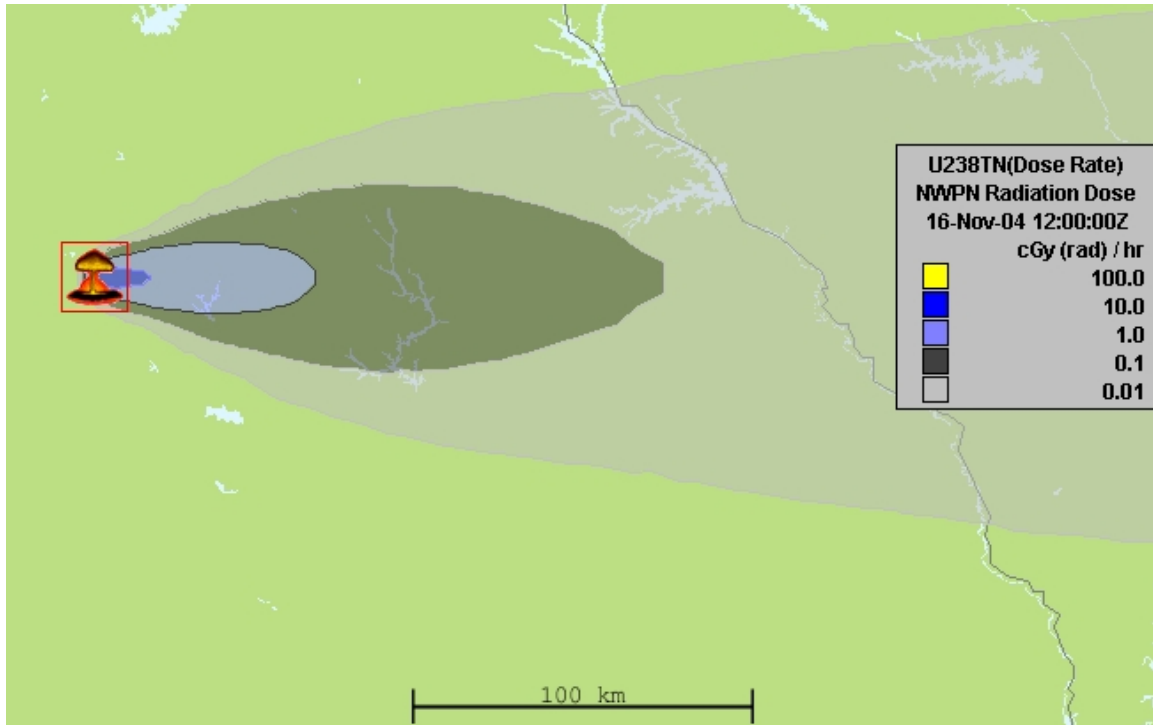
Figure 9: Typical HPAC Dose Rate Contour with Default Dose Rate Values Shown in Legend

Unless otherwise noted, the contours in all HPAC figures will be the default dose rate contour values. These values are summarized in Table 2.

Table 2: HPAC Default Dose Rate Contour Values

Color	Dose Rate Value (rad/hr)
Yellow	100.0
Dark Blue	10.0
Light Blue	1.0
Dark Grey	0.1
Light Grey	0.01

IV. Results and Data Comparison

This chapter compares fallout dose rate contours from HPAC 4.03, which uses the DELFIC particle distribution, with fallout dose rate contours from HPAC 4.04, which uses the Heft subsurface particle distribution. These contours are compared visually, by the grounded source normalization constant and by g(t) for selected contours.

Results of the AFIT Smear Code for DELFIC Surface and Heft Subsurface Particle Distributions

The AFIT Smear Code is a highly simplified fallout code. The only transport mechanism considered is a constant wind. The only particle collection mechanism considered is simple gravitational settling. Particle cloud horizontal dispersion is modeled using a combination of dispersion due to cloud rise, diffusion and wind shear. The net result is that the nuclear cloud grows and disperses over time. The 30 day dose on the ground is given by the following equation:

$$D_{Gd}(x, y, t) = kY_f \int_0^{720} t^{-1.2} f(y, t_a) \frac{g(t_a)}{v_x} dt \qquad (16)$$

where

$\dot{D}_{Gd}$ is the dose rate on the ground

k is the source normalization constant in units of $\dfrac{R - km^2}{hr - kT}$

Y_f is the fission yield in kilotons

t is time since the nuclear detonation in hours

$f(y, t_a)$ is the effective "time width" of the cloud

$g(t_a)$ is the rate at which activity is being deposited on the ground everywhere at

32

time t_a

t_a is the time of arrival of the nuclear cloud in hours

v_x is the velocity of the constant wind (2:425).

It should be noted that the exponent to which the time is raised is the Way-Wigner approximation. This approximation accounts for radioactive decay. The 30 day dose is shown in the following smear code contours because it is a convenient activity comparison in the smear code.

The result of an AFIT smear code 30 day dose calculation for the DELFIC distribution is shown in Figure 10:
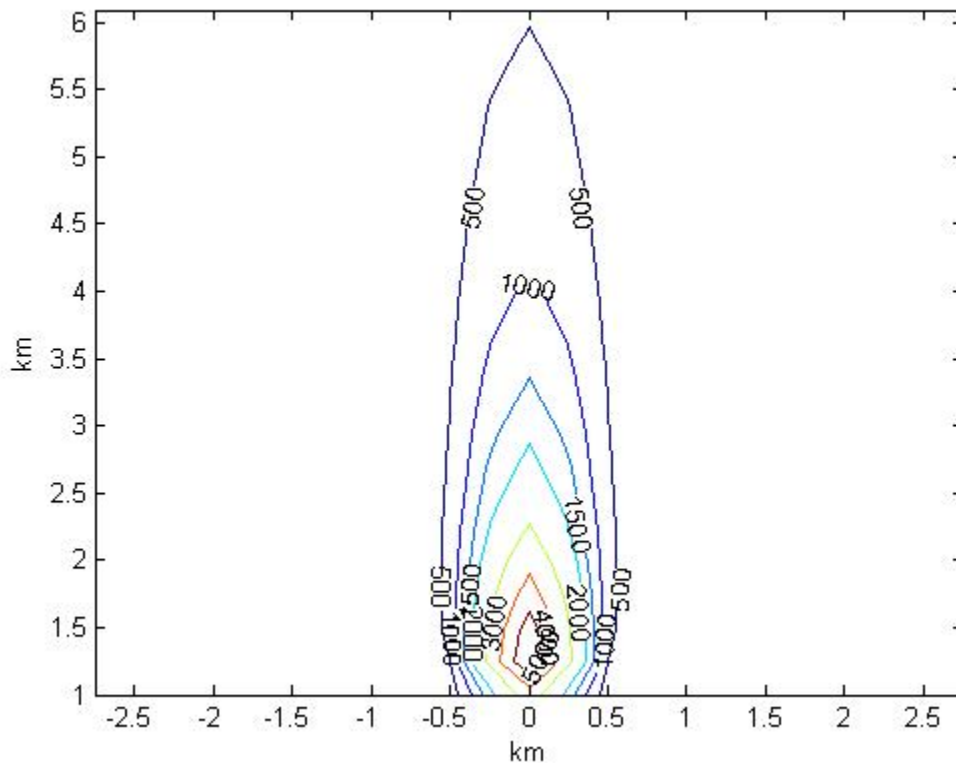
Figure 10: AFIT Smear Code 30 Day Dose Contour for 1kt Surface Burst using DELFIC

Distribution with 10kph Constant wind (Units in Roentgen)

Note that the DELFIC particle distribution extends the 500-Roentgen contour out to 6 km downwind.

The result of the Heft tri-lognormal subsurface burst particle distribution in the AFIT smear code is shown in Figure 11:
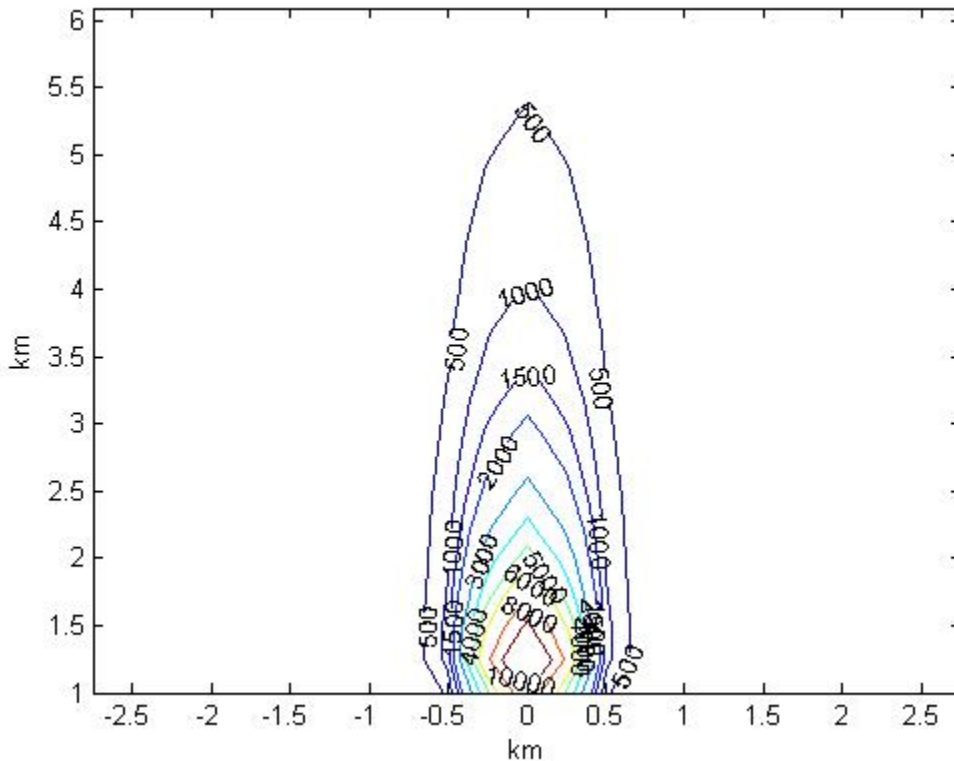
Figure 11: AFIT Smear Code 30 Day Dose Contour for 1kt Surface Burst using Heft Subsurface Distrubution with 10kph Constant Wind (Units in Roentgen)

As seen in Figure 11, the dose rate contours generated by the AFIT smear code using the HEFT subsurface distribution is significantly higher close to ground zero than the DELFIC Particle size distribution. However, farther downwind, the DELFIC distribution deposits more activity. This is demonstrated by the location of the 500-

Roentgen contour from the Heft subsurface distribution only extends to 5.5 km as compared to 6km for the DELFIC distribution.

The result of exclusively using the crystalline particle component of the Heft subsurface distribution as the particle size distribution in the AFIT smear code for a 1kt surface burst is shown in Figure 12:
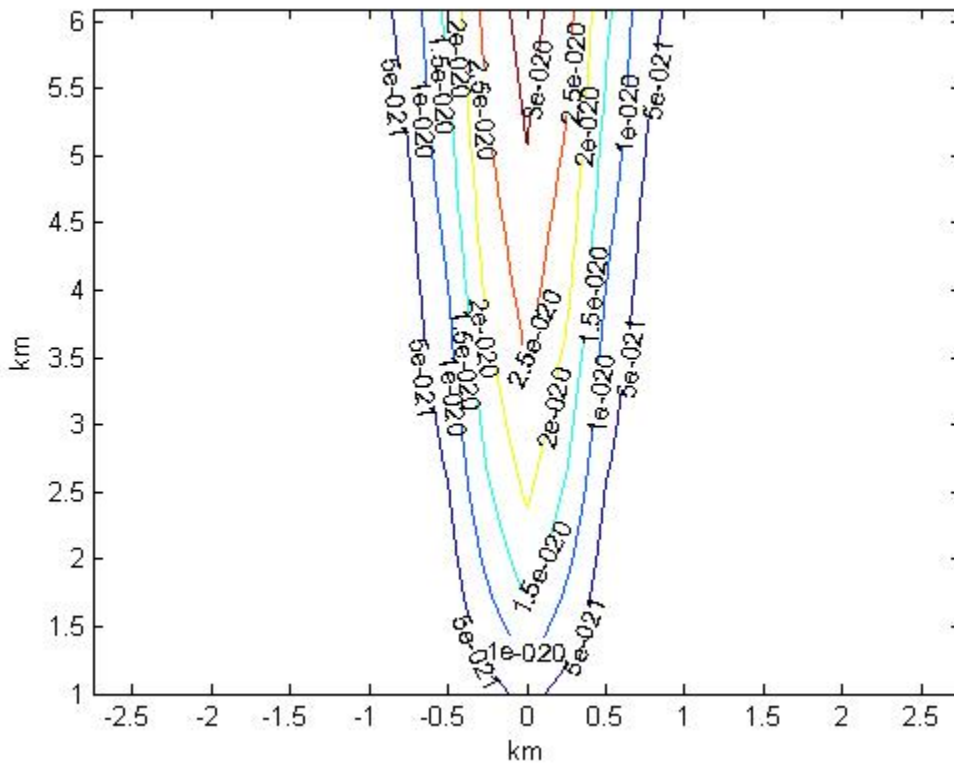
Figure 12: AFIT Smear Code 30 Day Dose Contour for 1kt Surface Burst using Crystalline Distribution with 10kph Constant Wind (Units in Roentgen)

As can be seen in Figure 12, the crystalline distribution deposits very little activity locally and as such makes no meaningful contribution to the activity in the Heft distribution.

The result of using the glass component of the Heft subsurface distribution as the particle size distribution in the AFIT smear code for a 1kt surface burst is shown in Figure 13:
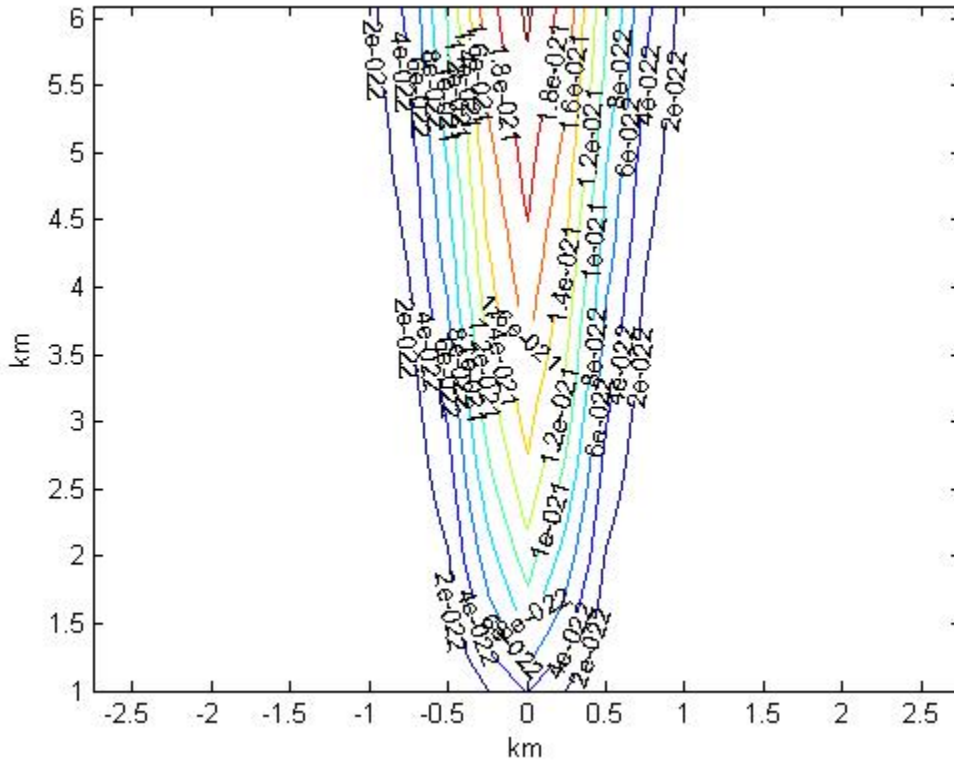
Figure 13: AFIT Smear Code 30 Day Dose Contour for 1kt Surface Burst using Glass Distribution with 10kph Constant Wind (Units in Roentgen)

Similar to the crystalline distribution, the glass distribution adds very little activity to the resulting smear from the Heft particle distribution.

The result of using the local particle component of the Heft subsurface distribution as the particle size distribution in the AFIT smear code with a 1kt surface burst is shown in Figure 14:
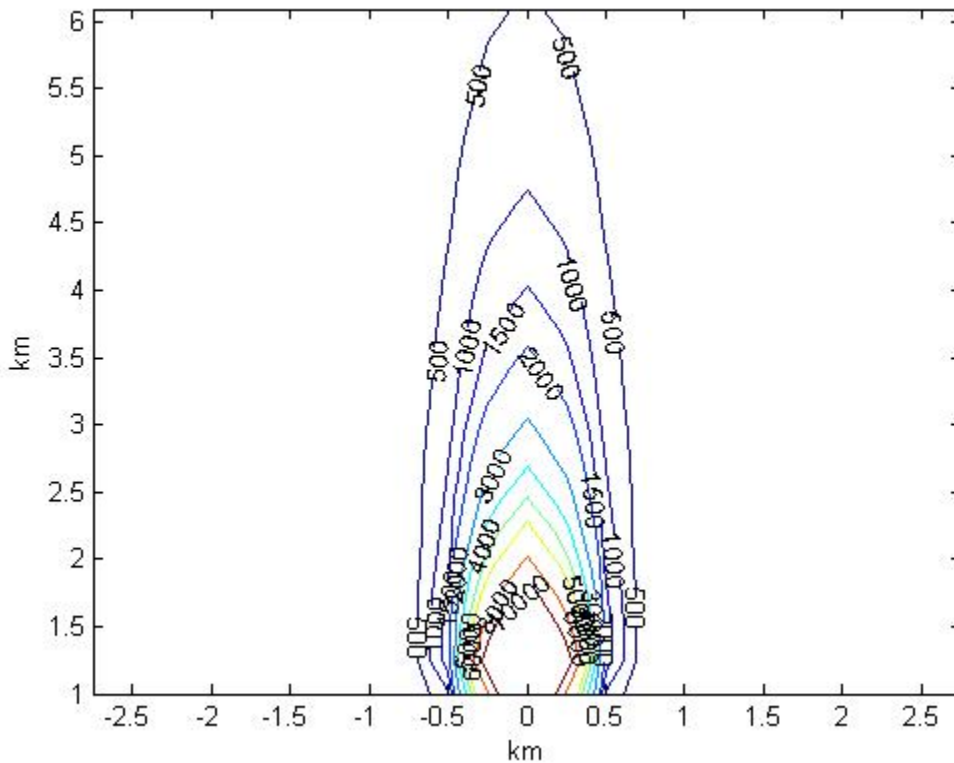
Figure 14: AFIT Smear Code 30 Day Dose Rate for 1kt Surface Burst using the Local

Distribution with 10kph Constant Wind (Units in Roentgen)

When compared with the Heft subsurface particle size distribution, the local

particle size distribution is very similar. The AFIT smear code results for both the Heft

tri-component subsurface distribution and the Heft local component subsurface

distribution show a similar shape. However, at similar locations, the smear code results

for the Heft local component show that the contours are approximately twice the value of

the smear code results from the Heft tri-component distribution. This is because the local

component makes up a little less than half, or about 40% of the mass of the Heft tri-

component subsurface distribution. Clearly, the local distribution is the driving force for any significant activity concentrated around ground zero.
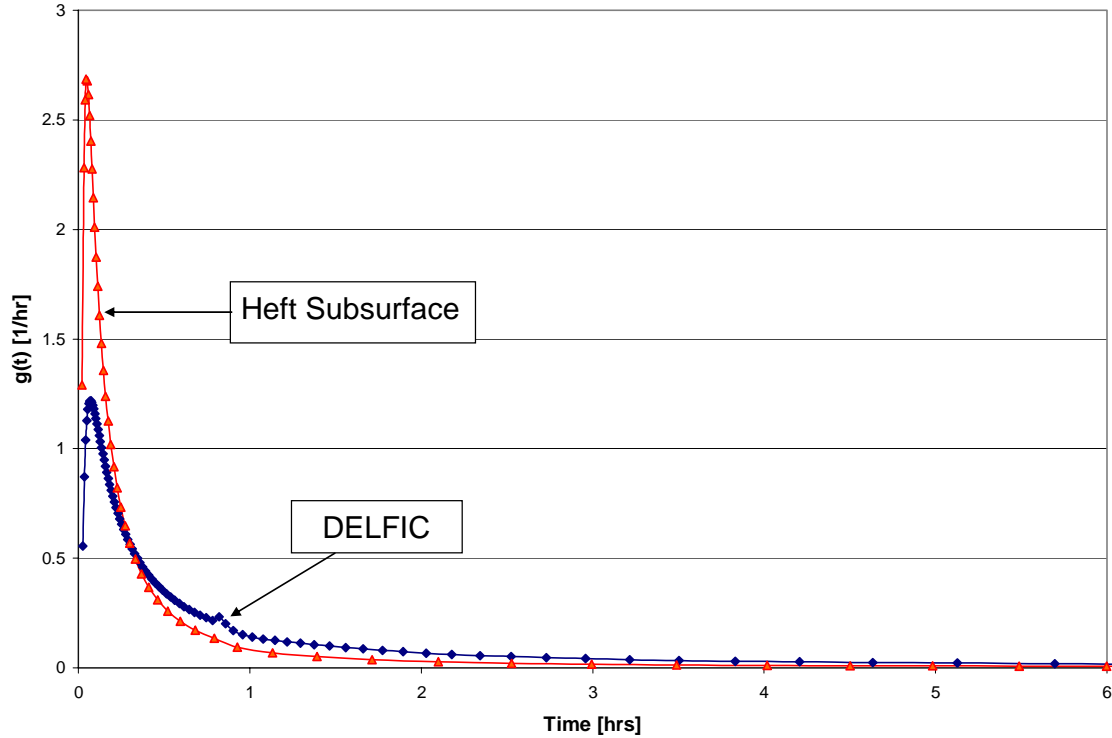
Figure 15: G(t) Comparison for 1kt Surface Burst using Heft Subsurface and DELFIC Particle Distributions in AFIT Smear Code

Figure 15 shows a g(t) comparison for the Heft subsurface and the DELFIC subsurface particle distributions. The Heft subsurface distribution clearly has a greater peak particle deposition than does the DELFIC distribution. As a result it deposits much more activity in the local area than does the DELFIC distribution. However, starting at about 30 minutes the DELFIC distribution starts depositing more activity than does the Heft distribution. Not shown on this graph is that the Heft distribution again deposits more activity on the ground after 20 hours, which corresponds to 200 km downwind.

From this point until the end of the run, the Heft distribution deposits more activity. The

DELFIC distribution deposits its last size bin at about 472 hours while the Heft

subsurface distribution doesn't deposit its last size bin until 1831 hours. This shows a

significant difference in the amount of small particles between the two distributions.

A Comparison of the DELFIC and Heft Subsurface Particle Distributions for

Varying Yields and Resolutions

As discussed in chapter two, a nuclear weapon surface burst produces a stabilized

cloud. The height of this stabilized cloud as well as its dimensions are dependent upon

several factors including the yield of the nuclear explosion, atmosphere, relative humidity

of the atmosphere and the altitude of the tropopause. In their book The Effects of

Nuclear Weapons, Glasstone and Dolan provide an approximate stabilized cloud height

as a function of the yield of a nuclear device for a surface blast.
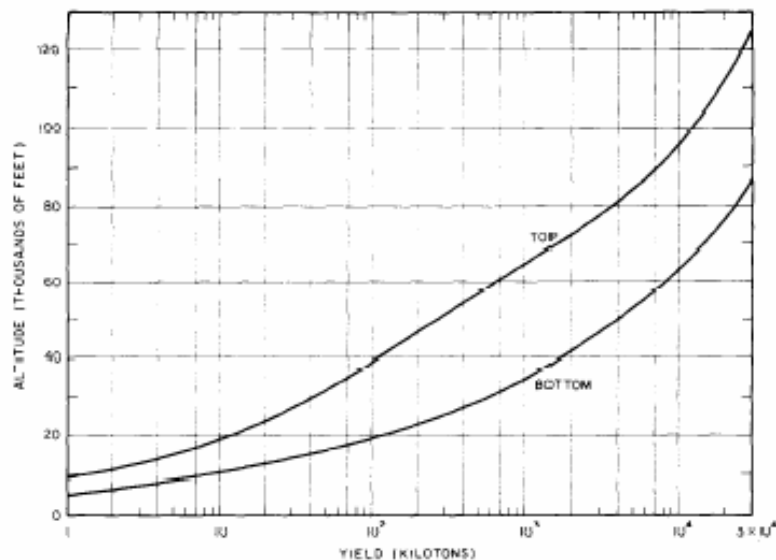
Figure 16: Altitudes of the Stabilized Cloud Top and Cloud Bottom Based on Yield for

Surface Bursts (9: 431)

For a 1kt surface burst, HPAC 4.03 ran until the last puff was stopped at 12.75 hours. The resulting dose rate contour plot at 12.75 hours is shown in Figure 17.
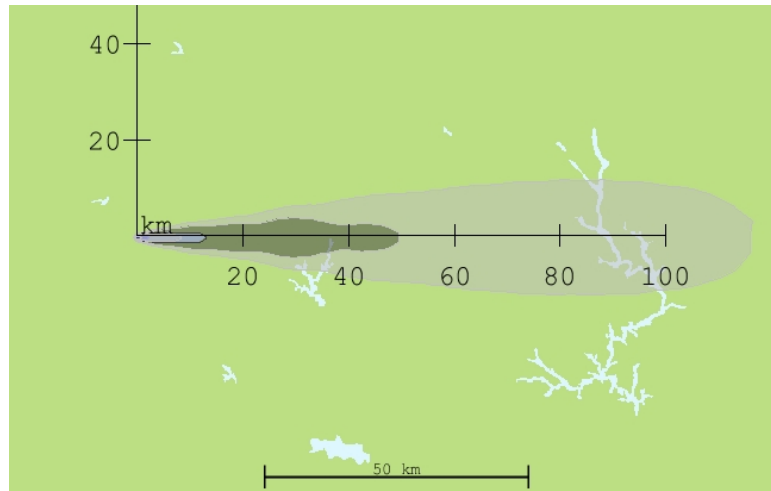
Figure 17: HPAC 4.03 Dose Rate Contour for 1kt Surface Burst at 12.75 Hours

HPAC 4.04, by comparison, stopped tracking its final puff at 12.25 hours for a 1kt surface burst. The 4.04 contour plot for a 1kt surface burst at 12.25 hours is shown in Figure 18.
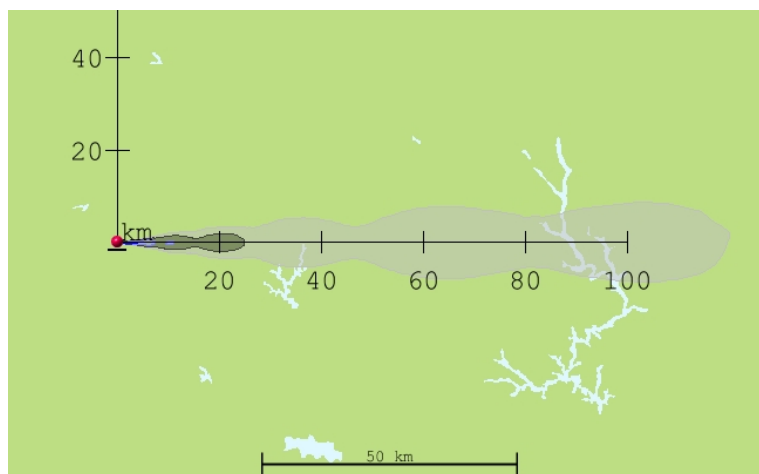
Figure 18: HPAC 4.04 Dose Rate Contour for 1kt Surface Burst at 12.25 Hours

The most noticeable similarity between the two contours is that they both extend downwind to approximately 120km. However, the 4.03 contour is 30 minutes later than the 4.04 contour. In those 30 minutes, a small portion of the activity would have decayed away leaving a smaller total dose rate than is present at the time where the 4.04 contour is taken from. While both contours extend approximately the same distance downwind, the 4.03 contour shows a larger spread in the north/south direction. This spread is approximately twice the size of the 4.04 contour. This is apparent in the close up views of ground zero from 4.03 and 4.04, which are discussed below.

Since the Heft subsurface distribution contains 40% of its mass in the local distribution, which is made up of large particles with short fall times, it is worth examining the contours close to ground zero. The dose rate contour at 12 hours for HPAC 4.03 is shown in Figure 19. Ground Zero is indicated by the yellow dot.
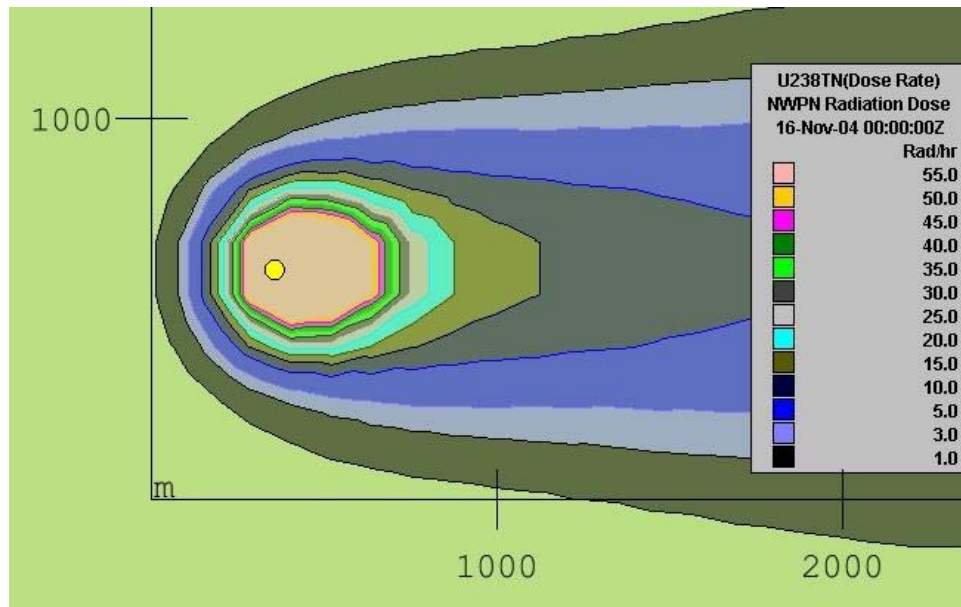
Figure 19: HPAC 4.03 Ground Zero Dose Rate Contour for 1kt Surface Burst at 12

Hours

The dose rate increases until it reaches its peak value of 120 rad/hr. For the sake of readability, the maximum dose rate contour in Figure 19 is 55 rad/hr. However, it is evident in Figure 19 how sharply the dose rate increases as ground zero is approached.

The dose rate contour at 12 hours for HPAC 4.04 is shown in Figure 20.
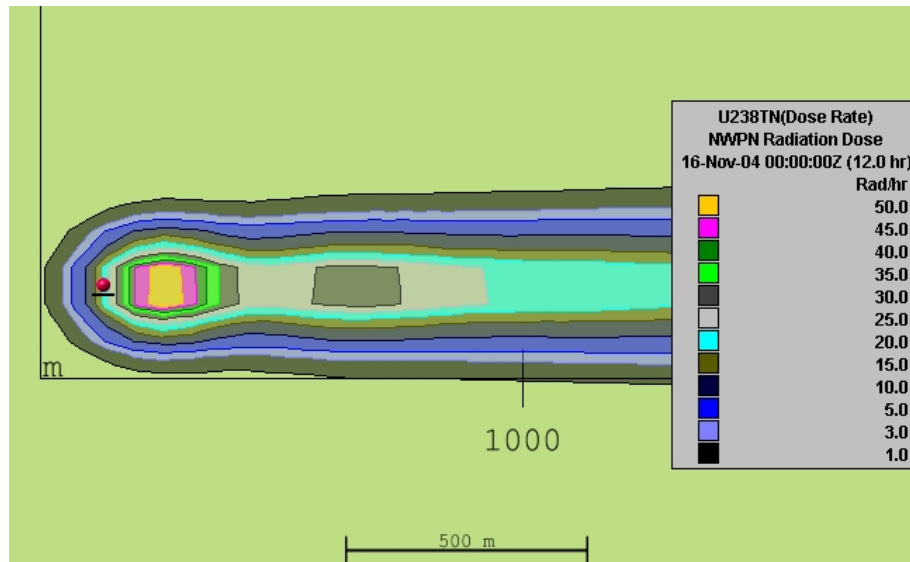
Figure 20: HPAC 4.04 Ground Zero Dose Rate Contour for 1kt Surface Burst at 12 Hours

The dose rate increases until it reaches its peak of 55 rad/hr just east of ground zero. This is a much smaller maximum dose rate at 12 hours than is generated by HPAC 4.03. It should also be noted how much smaller the high dose area is in both the North-South direction and the East-West direction than the 4.03 contour plot. Not only does the 4.03 contour extend out farther than the 4.04 output, it has a much higher concentration of radiation close to ground zero than the 4.04 output.

Another distinguishing feature is the surge in activity at 20 kilometers east of ground zero for the 4.04 contour. This surge in activity is a result of the discrete number of size bins used to model the particle distribution. The 4.03 contour, on the other hand, appears to decrease monotonically downwind. This feature is confirmed when g(t) comparisons between the two plots are made.
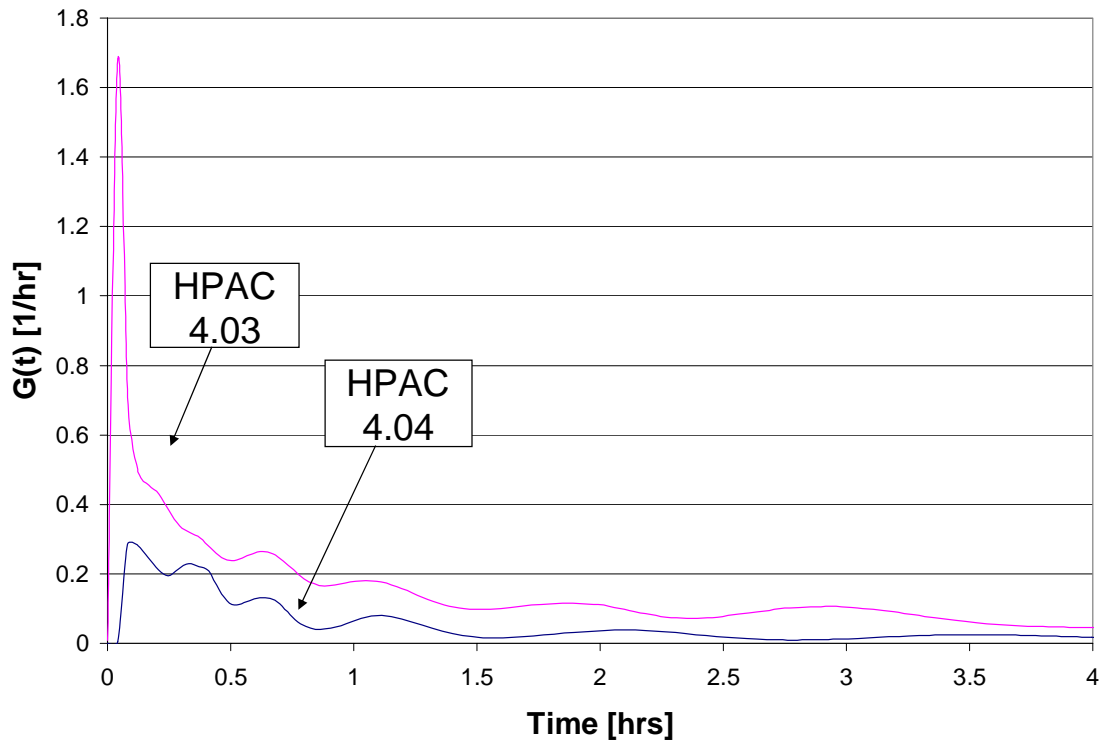
Figure 21: g(t) for 1kt Surface Burst in HPAC 4.03 and 4.04

It should be noted that the g(t) for the HPAC 4.04 run is consistently lower than the g(t) for HPAC 4.03. This indicates that 4.03 consistently delivers more activity as activity is integrated transversely to the wind. See Appendix D for details concerning this calculation.

Due to the sharp dose rate increase close to ground zero, the grounded source normalization constant was calculated using a series of finer resolutions for both HPAC

4.03 and 4.04. A resolution of up to 600 by 600 could be produced by HPAC 4.04, however, HPAC 4.03 would only produce a resolution of 300 by 300. The results are shown in Table 3.

Table 3: Comparison of k for 1kt Surface Burst in HPAC 4.03 and 4.04

Resolution	HPAC 4.03	HPAC 4.04
100 x 100	3450	1170
200 x 200	3330	1180
300 x300	3460	1190
400 x 400		1190
500 x 500		1210
600 x 600		1210

For a 10kt surface burst, HPAC 4.03 ran until the last puff was stopped at 23 hrs. The resulting contour is shown in Figure 22.
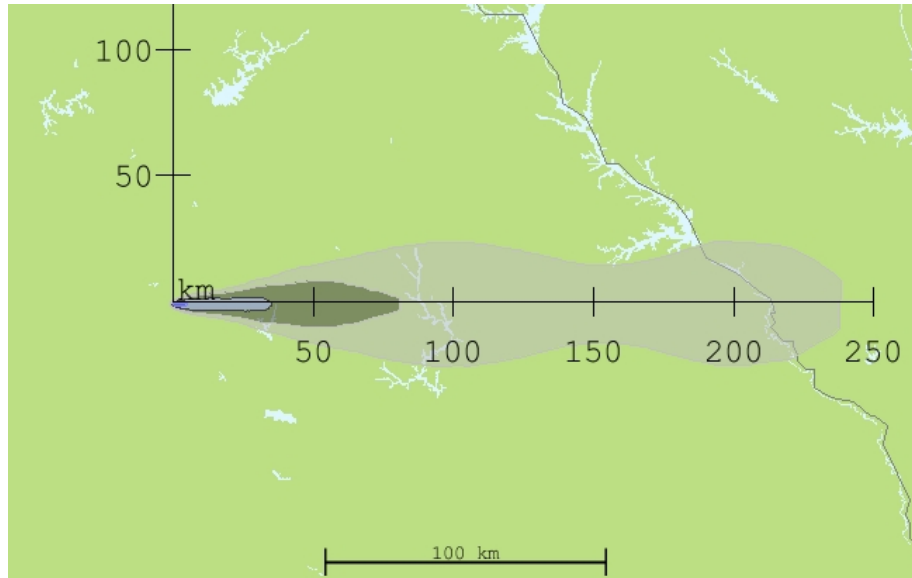
Figure 22: HPAC 4.03 Dose Rate Contour for 10kt Surface Burst at 23 Hours

For a 10kt surface burst, HPAC 4.04 ran until the last puff was stopped at 22hrs. The resulting contour at 22 hours is shown in.
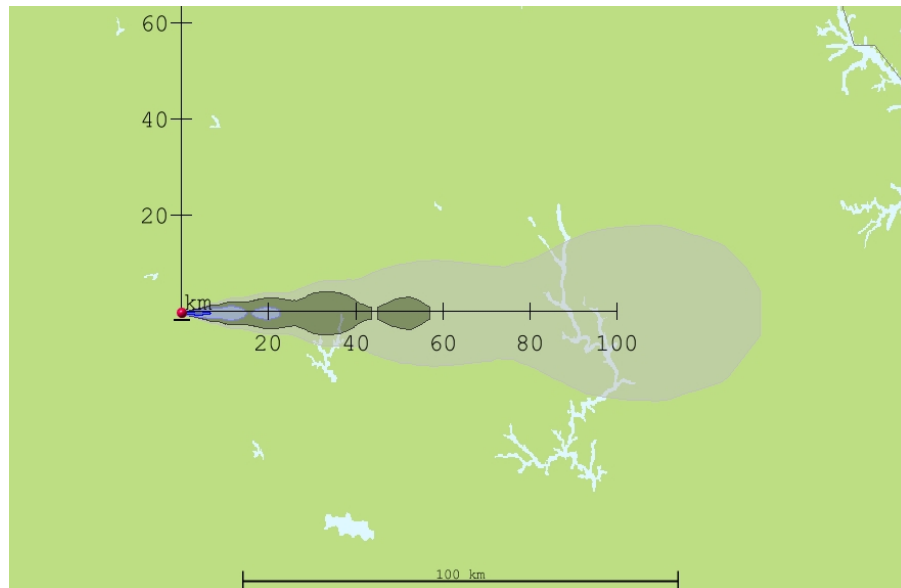
Figure 23: HPAC 4.04 Dose Rate for 10kt Surface Burst at 22 Hours

Many of the features discussed in connection with the set of 1kt bursts are also present in the set of 10kt bursts. Similar to the 1kt burst set, the 4.03 dose rate contour for the 10kt burst extends further downwind than does the 4.04 dose rate contour for the 10kt burst. The HPAC 4.03 10kt burst has an grounded source normalization constant of 3020 while the HPAC 4.04 10kt surface burst has a grounded source normalization constant of 970. These values are much lower than the values of the grounded source normalization constants found for 1kt blasts. This indicates that as the yield increases, more activity is lost through dispersion beyond the local area.

For the 100kt run in HPAC 4.03, the run ended when it reached the temporal domain at 48hrs. The contour plot generated by HPAC 4.03 by the 100kt surface burst is shown in Figure 24.
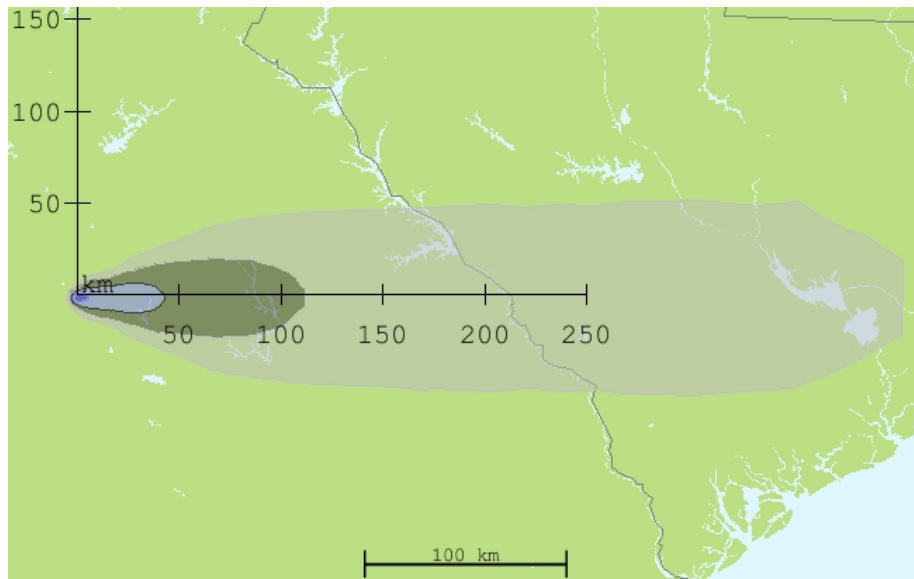
Figure 24: HPAC 4.03 Dose Rate Contour for 100kt Surface Burst at 48 Hours

For the 100kt run in HPAC 4.04, the run ended when it reached the temporal domain of 48hrs.
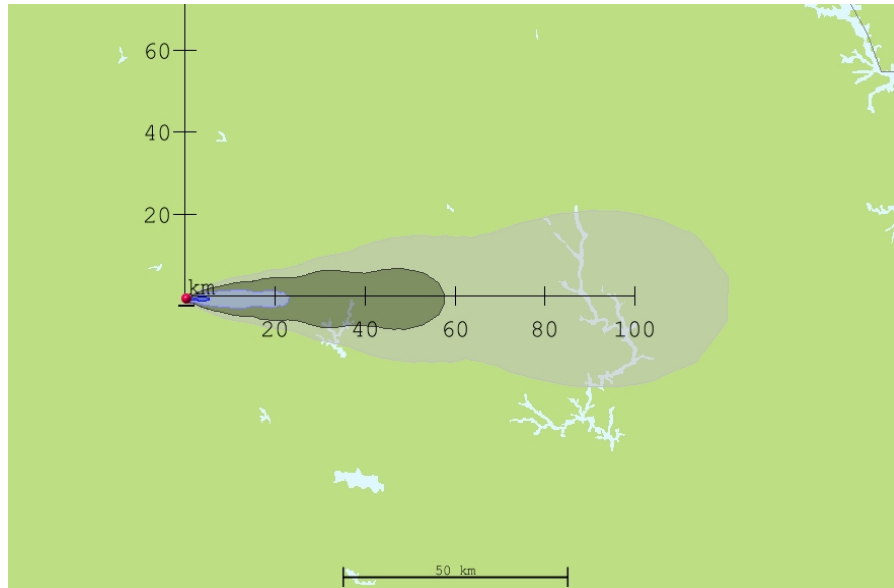
Figure 25: HPAC 4.04 Dose Rate Contour for 100kt Surface Burst at 48 Hours

The difference in the dose rate contours seems to be exaggerated for the 100kt yield case. For the exact same dose rate time (48 hrs), the DELFIC contour (4.03) extends out to about 400km while the Heft subsurface contour (4.04) only extends to approximately 120km. A difference of over 3:1.

The other noticeable feature for the 100kt surface bursts is that the grounded source normalization constants continue to drop from the values seen with the 1kt surface bursts. For HPAC 4.03, the grounded source normalization constant for a 100kt surface burst is 1470 [R-km^2/hr-kt], a decrease of 43% from the 1kt grounded source normalization constant. For HPAC 4.04, the grounded source normalization constant for a 100kt surface burst is 460 [R-km^2/hr-kt], a decrease of 39% from the 1kt grounded source normalization constant.

Variation in the Grounded Source Normalization Constant When Computed from Different Late Time Dose Rates

The analytical tools used to evaluate the effects of the two distributions under consideration have used the Way-Wigner formula to find the unit reference dose rate. The Way-Wigner approximation is a simplification that is used to give a rough approximation of the radioactive decay of the over 300 radioisotopes that are present from the time of the explosion to six months after the detonation. The actual decay of the fission products varies from the $t^{-1.2}$ law as shown in Figure 26, but Way-Wigner is an accepted approximation.

It is not possible to compute URDR directly from HPAC. Typically the earliest possible computation is four hours after burst. Thus it is necessary to use these later dose rates and adjust them back to one hour using the Way-Wigner formula. However, as shown in this section, one obtains different results when computing the URDR from different later modeling times. One reason that HPAC cannot easily compute a direct URDR is that most of the activity is still in the air at one hour. The URDR is intended to be used to compute later dose rates (and doses). Therefore, this suspended activity must be included in the URDR calculation. The computation of airborne activity is a difficult computation which is not attempted in HPAC, or most other fallout codes.
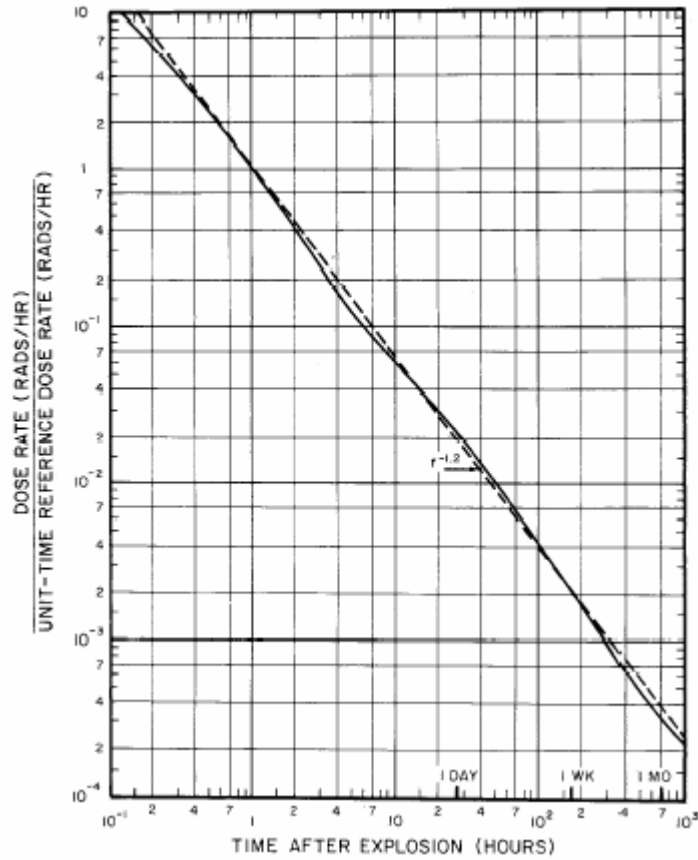
Figure 26: Dose Rate vs. Time (Dashed Line Represents the Way-Wigner

Approximation) (9:392)

For a 100kt explosion in HPAC 4.04, SCIPUFF stops tracking the puffs after

48hrs. The results of the early time decay are evident from examining the decay on the

ground, as shown by the following six figures starting with Figure 27 and ending with

Figure 32. A similar series is shown for HPAC 4.04 starting with Figure 33 and ending

with Figure 38. The red dot on each figure indicates the cloud centerline location for a

constant 10km/hour wind.
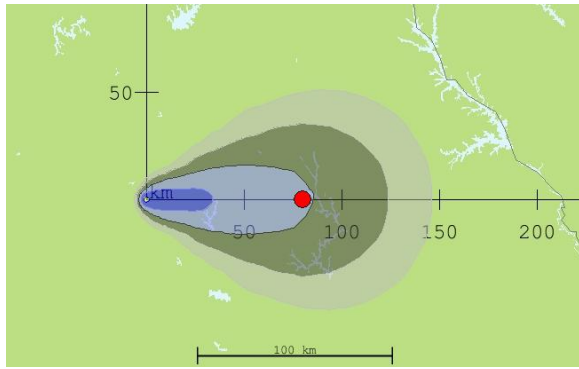
Figure 27: HPAC 4.03 Dose Rate Contour
for 100kt Surface Burst at 8 Hours
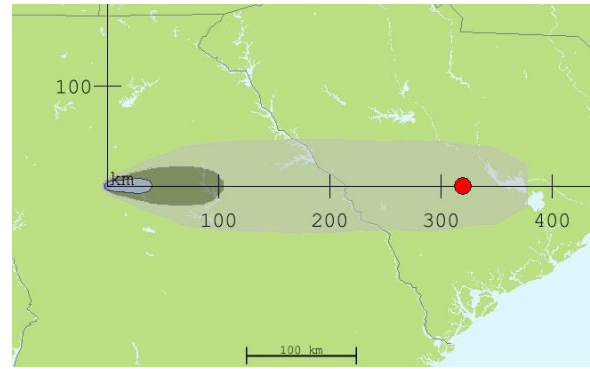
Figure 30: HPAC 4.03 Dose Rate for 100kt
Surface Burst at 32 Hours
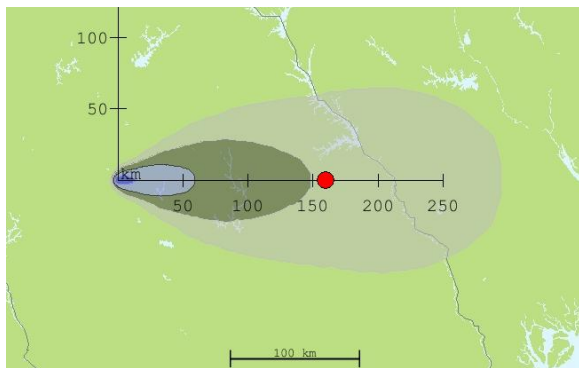
Figure 28: HPAC 4.03 Dose Rate Contour
for 100kt Surface Burst at 16 Hours
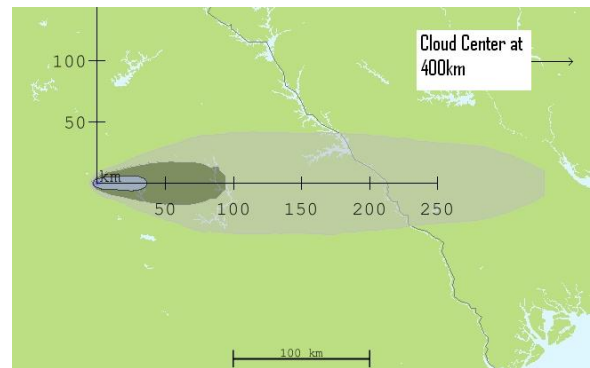
Figure 31: HPAC 4.03 Dose Rate Contour
for 100kt Surface Burst at 40 Hours
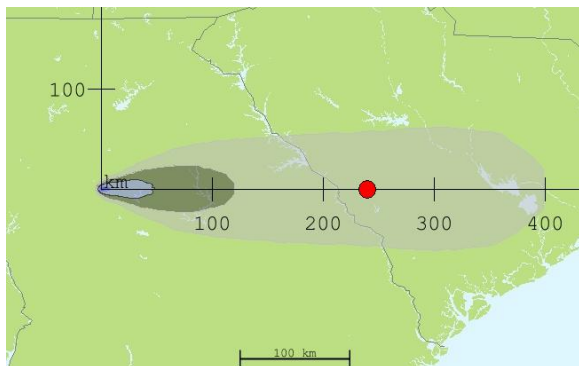
Figure 29: HPAC 4.03 Dose Rate Contour
for 100kt Surface Burst at 24 Hours
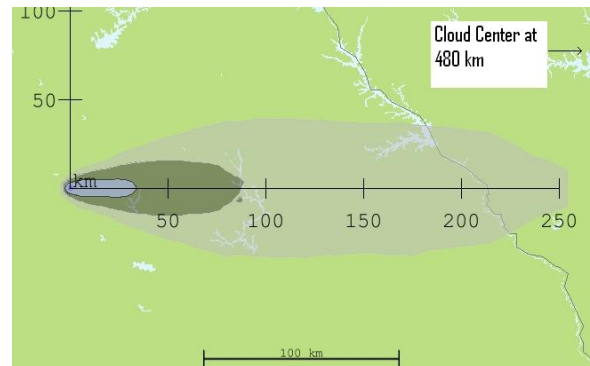
Figure 32: HPAC 4.03 Dose Rate Contour
for 100kt Surface Burst at 48 Hours
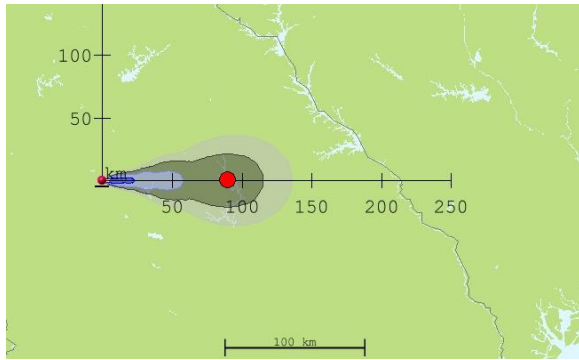
Figure 33: HPAC 4.04 Dose Rate Contour

for 100kt Surface Burst at 8 Hours
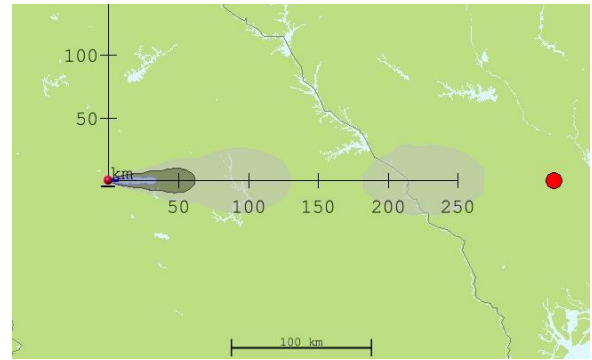
Figure 36: HPAC 4.04 Dose Rate Contour

for 100kt Surface Burst at 32 Hours
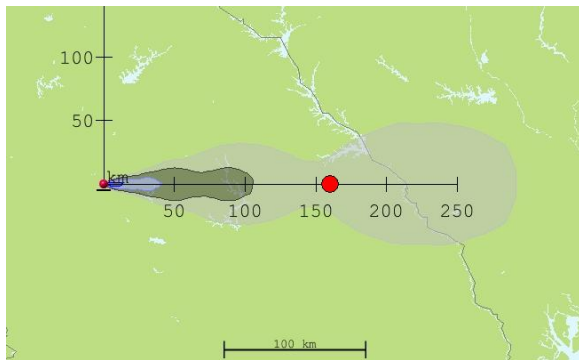
Figure 34: HPAC 4.04 Dose Rate Contour

for 100kt Surface Burst at 16 Hours
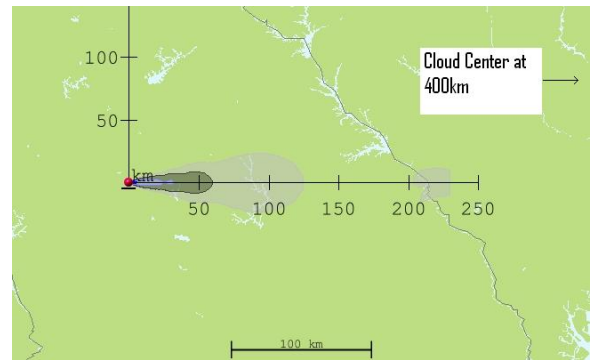
Figure 37: HPAC 4.04 Dose Rate Contour

for 100kt Surface Burst at 40 Hours
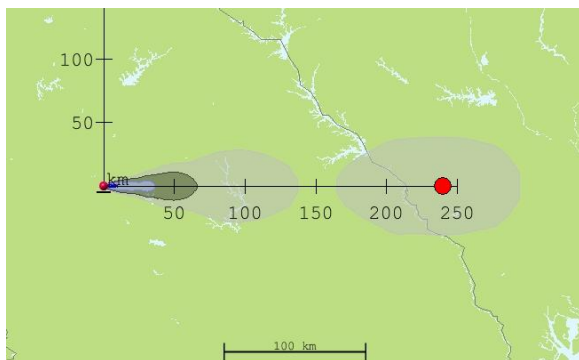
Figure 35: HPAC 4.04 Dose Rate Contour

for 100kt Surface Burst at 24 Hours
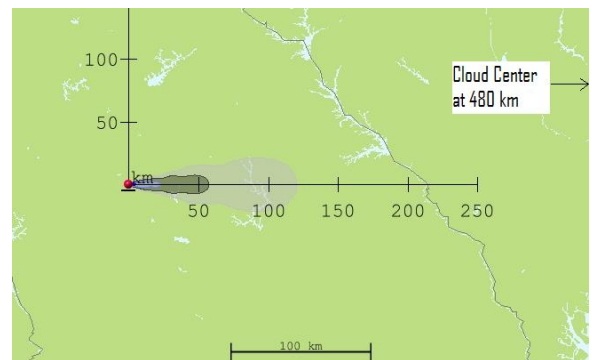
Figure 38: HPAC 4.04 Dose Rate Contour

for 100kt Surface Burst at 48 Hours

In this series of bursts, the dose rate contours grow in the easterly direction (the direction the wind is blowing to). However, as the fallout contour grows in the easterly direction with the passing of time, the fallout contour is actually decreasing in the north-south direction. This is due to the decay of radionuclides.

From these fallout patterns and the grounded source normalization constants in Table 4, it is once again noticeable how much less activity is deposited on the ground with HPAC 4.04, which uses the Heft subsurface particle distribution, than with HPAC 4.03, which uses the DELFIC particle distribution. The HPAC 4.03 fallout contour extend to a much larger maximum east-west distance of 400 km at 24 hours vs. the 300 km distance that the HPAC 4.04 fallout contour extends to in the east-west direction at 24 hours.

Table 4: Grounded Source Normalization Constant vs. Time Comparison for 100kt Blasts

4.03	Hrs	8	16	24	32	40	48
	Grounded k	1380	1510	1560	1530	1440	1470
4.04	Hrs	8	16	24	32	40	48
	Grounded k	470	500	490	480	470	460

As shown in Table 4, for HPAC 4.03 the maximum value of URDR occurs at 24 hours while the maximum value of the source normalization constant for HPAC 4.04 occurs at 16 hours. The growth of the source normalization constant from 8 hours up until the maximum value can be attributed to particles falling out of the stabilized cloud.

Considering how little activity the crystalline and glass populations add to the local area, a greater proportion of the activity for the Heft subsurface distribution that makes it to the ground is found in larger particles than is the case for the DELFIC distribution. This is because the majority of the activity in the local fallout contours generated by the Heft subsurface distribution is due to the local fallout lognormal. This means that percentage wise, a greater proportion of the activity is falling out at an earlier time for the Heft subsurface distribution than is true for the DELFIC distribution. Because of this, it is logical that the maximum dose rate for the Heft subsurface distribution would occur at an earlier time than for the DELFIC distribution, which is observed.

The time when the grounded source normalization constant is at a maximum is also the time where the center of the stabilized cloud is depositing significant activity to the outer edge of the 0.01 contour. This is seen in Figure 29 for 4.03 and Figure 34 for 4.04. The stabilized cloud continues to grow with time and the maximum grounded source normalization constant point is when the smallest particles that add significant activity are being deposited. After this point, the stabilized nuclear cloud is becoming too dispersed to add significant fallout to the local area.

The source normalization constant decrease after 24 hours for 4.03 and 16 hours for 4.04 is less intuitive than the increase up to those times. One possible explanation is that a proportion of the smaller particles is being resuspended by the constant wind and therefore being scattered. Smaller particles, which fall out later, would have a greater probability of resuspension than larger particles. Thus when the source normalization constant is calculated at later times, these resuspended particles have left the local area which is being considered. However, to the author's best knowledge, SCIPUFF does not

53

take resuspension of particles into account. Another possible explanation for this

phenomenon is that when the unit reference dose rate time is calculated using the Way-

Wigner approximation, there is error introduced when some of the activity has decayed

completely away as this lost activity is not corrected back to the unit reference time.

Varying time dose rate contours were also generated for both HPAC 4.03 and

4.04 with 1 kt surface bursts. The results are shown starting in Figure 39 and continuing

through Figure 46.

Similar to the 100kt bursts, the 1kt bursts in the preceding figures show the dose

rate contours grow in the easterly direction (the direction the wind is blowing to) as well

as the decay of short lived radionuclides. The grounded source normalization constants

calculated from the dose rates at various times is reported in Table 5.

Table 5: Grounded Source Normalization Constants for Varying Time 1kt Surface Bursts

4.03	Hrs	4	8	12	12hrs 15min
	Grounded k	3080	3650	3580	3460
4.04	Hrs	4	8	12	12hrs 15min
	Grounded k	1080	1220	1210	1210
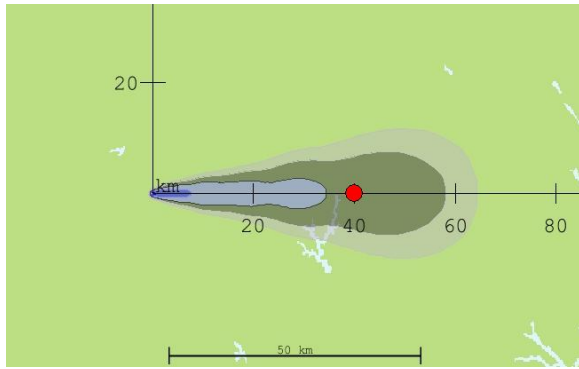
Figure 39: HPAC 4.03 Dose Rate Contour

for 1kt Surface Burst at 4 Hours
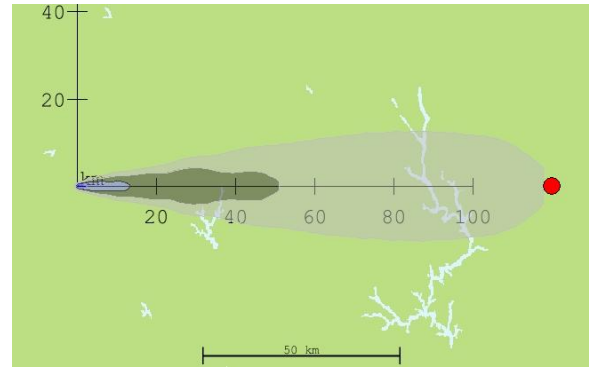
Figure 41: HPAC 4.03 Dose Rate Contour

for 1kt Surface Burst at 12 Hours
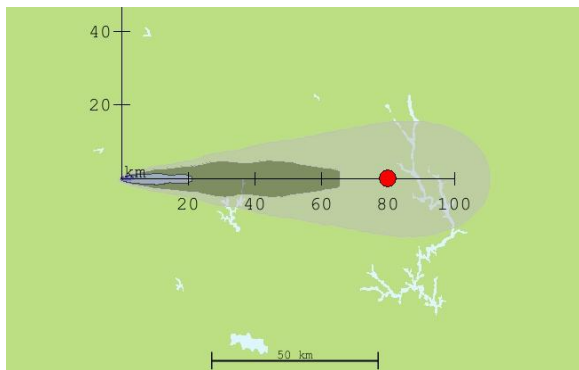
Figure 40: HPAC 4.03 Dose Rate Contour

for 1kt Surface Burst at 8 Hours
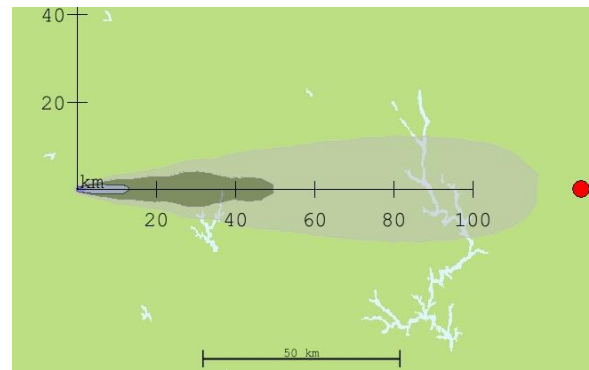
Figure 42: HPAC 4.03 Dose Rate Contour

for 1kt Surface Burst at 12.75 Hours
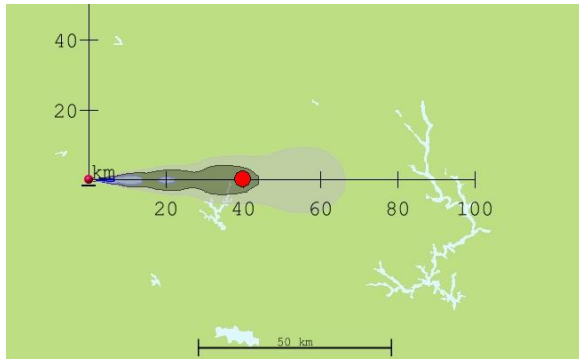
Figure 43: HPAC 4.04 Dose Rate Contour

for 1kt Surface Burst at 4 Hours
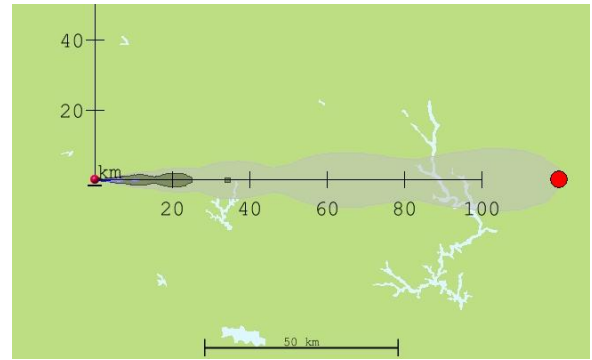
Figure 45: HPAC 4.04 Dose Rate Contour

for 1kt Surface Burst at 12 Hours
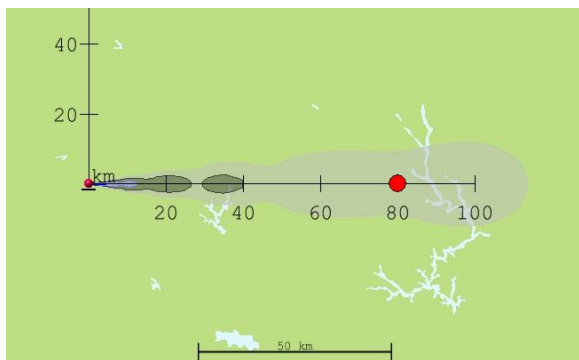
Figure 44: HPAC 4.04 Dose Rate Contour

for 1kt Surface Burst at 8 Hours
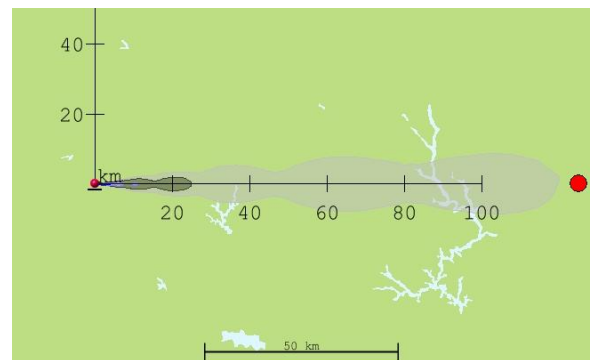
Figure 46: HPAC 4.04 Dose Rate Contour

for 1kt Surface Burst at 12.25 Hours

In both HPAC 4.03 and 4.04, the highest grounded source normalization constant occurs at eight hours. This is an indication that most of the activity has fallen from the stabilized cloud to the ground at the eight hour point for both HPAC 4.03 and 4.04. Whereas the 100kt bursts showed a different time for max k with an eight hour time interval, the one kt bursts do not show a difference with a four hour time step. The lower stabilization altitude of the nuclear cloud may help to account for this since the shorter fall distance for the particles will compress the fall time differences that different particle sizes exhibit. While the highest grounded source normalization constant does occur at 8 hours, it should be noted that there is little difference between the eight hour grounded source normalization constants and the grounded source normalization constants for 12 hours and later since the shorter time steps help to minimize the effects of decay.

V. Interaction of Particle Size Distribution with Other Variable Parameters in HPAC

This section looks at how the particle size distributions in HPAC 4.03 and 4.04 interact with other parameters in HPAC. Specific consideration is given to the effects of varying surfaces, rain scavenging and varying constant winds.

Effects of Varying Surfaces

In SCIPUFF differing surfaces such as vegetative canopies are affected by dry deposition processes and so the type of surface over which the fallout cloud is traveling helps to determine the mass flux of particles at the surface or how fast the fallout is deposited onto the ground. The roughness of the surface can also result in self-shielding by the ground of the radiation reaching the one meter high detector.

The default surface in HPAC 4.03 is the cultivated surface. This surface has a relatively high canopy height as well as a relatively low bowen ratio and albedo (See Table C-1 in Appendix C). The low bowen ratio indicates that cultivated is a fairly moist surface. The low albedo means that it absorbs most of the radiation from the sun that is incident upon it.

When a 1kt blast was run in HPAC 4.03, the last puff was tracked until 12.75 hours. The grounded source normalization constant for this run is 3460 [R-km^2/hr-kt]. For HPAC 4.04, the last puff was tracked until 12.25 hours with a grounded source normalization constant of 1210 [R-km^2/hr-kt]. The resulting contour plots for a cultivated surface at 12 hours are shown in Figure 47 and Figure 48.

58
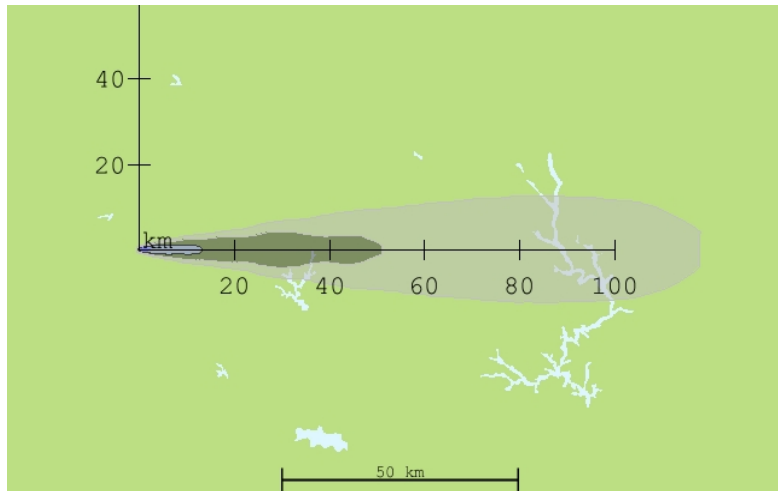
Figure 47: HPAC 4.03 Dose Rate Contour for 1kt Surface Burst with Cultivated Surface
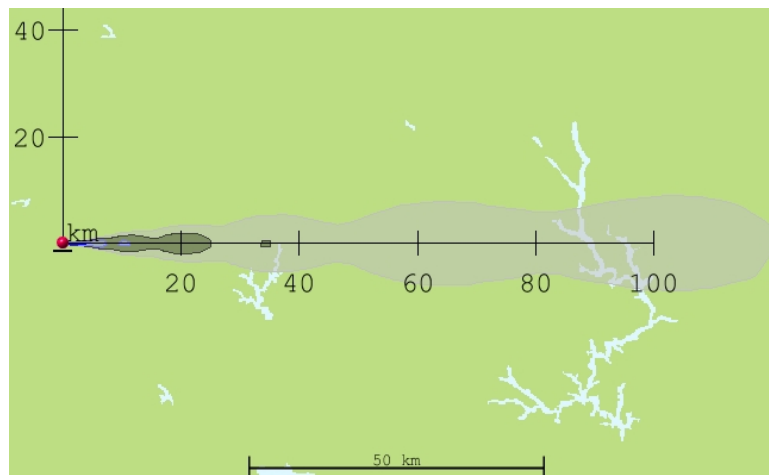
at 12 Hours

Figure 48: HPAC 4.04 Dose Rate Contour for 1kt Surface Burst with Cultivated Surface

at 12 Hours

The forest surface has the highest canopy of all the surfaces at 10m. It also has a

relatively high Bowen ratio and low Albedo. In HPAC 4.03, the last puff was tracked

until 11.5 hours. In HPAC 4.04, the last puff was tracked until 11.0 hours. This is the

shortest run time for any of the surfaces as would be expected since forest has the largest canopy. The large canopy of forest means there is more friction induced effects, such as eddies, over that surface as compared to the other surfaces. This results in the fallout particles traveling slower over this surface and thus being more likely to be deposited per unit area. The grounded source normalization constant for a forest surface in HPAC 4.03 is 3720 [R-km^2/hr-kt] while in HPAC 4.04 it is 1240 [R-km^2/hr-kt]. This is the highest grounded source normalization constant for any surface in both 4.03 and 4.04. This would seem to indicate that radiation shielding as a result of the surface isn't being taken into account in the HPAC dose rate calculations. The contour plots at 12 hours for a 1kt surface burst with a forest surface for both 4.03 and 4.04 is shown in Figure 49 and Figure 50. As seen in Figure 49 and Figure 50 the areas of the 0.001 fallout contour is larger for both the HPAC 4.03 and 4.04 1kt forest runs when compared to their HPAC 4.03 and 4.04 cultivated surface counterparts in Figure 47 and Figure 48 respectively. This is because of the increased activity deposition on the ground due to the forest surface in comparison to the cultivated surface.

The urban surface has a canopy height that is smaller than either the forest surface or the cultivated surface, but it is larger than the water, desert and grassland surfaces. As such, in HPAC 4.03 the time that its last puff was tracked until was longer than either forest or cultivated, but shorter than grassland, desert and water. In HPAC 4.03, the last puff was tracked until 13.25 hours. However, in HPAC 4.04, the last puff was tracked until 11.5 hours, which is the same amount of time that the forest surface was tracked until and less time than the puff was tracked over the cultivated surface.

Figure 49: HPAC 4.03 Dose Rate Contour for 1kt Surface Burst with Forest Surface at
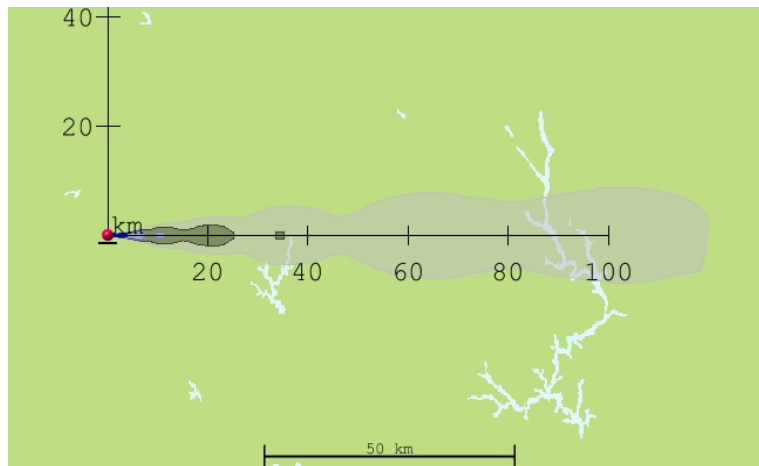
12 Hours

Figure 50: HPAC 4.04 Dose Rate Contour for 1kt Surface Burst with Forest Surface at

12 Hours

One possible explanation for this is that the deposition velocity is increased by having not

only a high canopy, but also a much higher bowen ratio than either the forest surface or

the cultivated surface has. This higher bowen ratio affects the smaller particles by

increasing their deposition velocity. Since the Heft distribution has a greater amount of

these smaller particles than does the DELFIC distribution, HPAC 4.04 tracked the last

puff over the urban surface than it did the last puff over the cultivated surface. The

grounded source normalization constant for HPAC 4.03 Urban run is 2730 [R-km^2/hr-kt]

while for the HPAC 4.04 run it is 1330 [R-km^2/hr-kt].
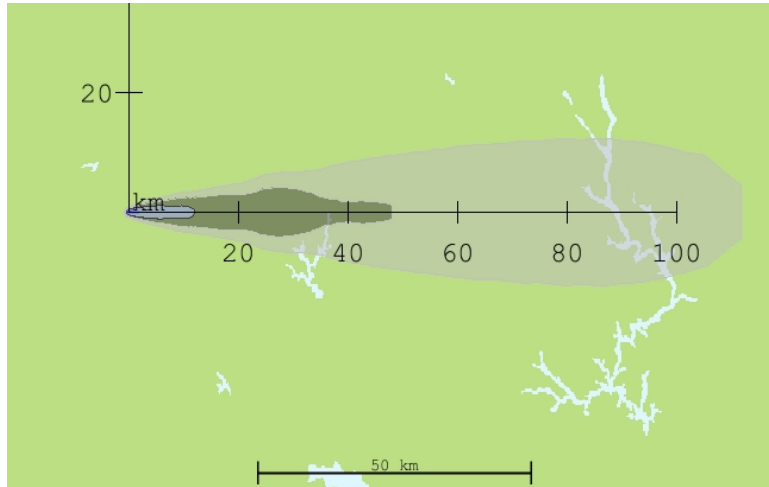
Figure 51: HPAC 4.03 Dose Rate Contour for 1kt Surface Burst with Urban Suface at 12

Hours

Figure 52: HPAC 4.04 Dose Rate Contour for 1kt Surface Burst with Urban Surface at

12 Hours

The grassland surface has a relatively small canopy at only 0.25 meters, but it is a much higher canopy than either desert or water. For the HPAC 4.03 run the last puff was tracked until 14.0 hours. For the HPAC 4.04 run the last puff was tracked until 12.25 hours. This follows the general trend of a lower canopy having a slower deposition velocity. The grounded source normalization constant for 4.03 grassland is 3310 [R-km^2/hr-kt] while for 4.04 it is 1240 [R-km^2/hr-kt].

Figure 53: HPAC 4.03 Dose Rate Contour for 1kt Surface Burst with Grassland Surface at 12 Hours
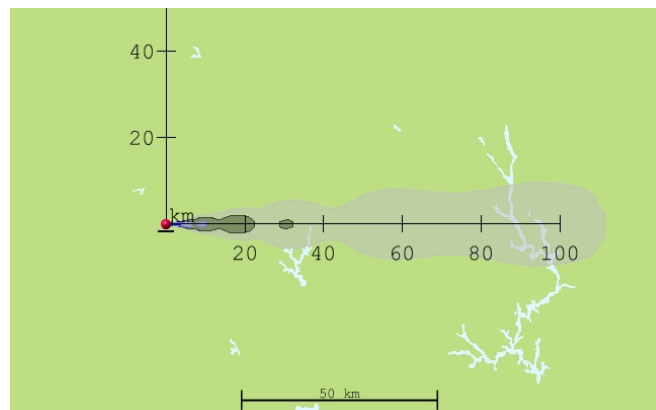
Figure 54: HPAC 4.04 Dose Rate Contour for 1kt Surface Burst with Grassland Surface at 12 Hours

The desert surface has a very small canopy of only 0.01 meters. Consequently, the time until the last puff landed is substantially longer for both 4.03 and 4.04. For both 4.03 and 4.04 the last puff was tracked until 17.75 hours. The source normalization constant for HPAC 4.03 desert run is 3350 [R-km^2/hr-kt] while for HPAC 4.04 is 1110 [R-km^2/hr-kt].

Figure 55: HPAC 4.03 Dose Rate Contour 1kt Surface Burst with Desert Surface at 12 Hours
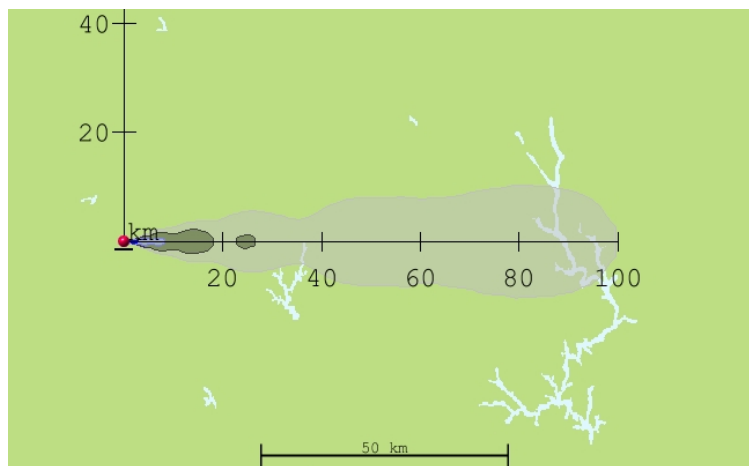
Figure 56: HPAC 4.04 Dose Rate Contour for 1kt Surface Burst with Desert Surface at 12 Hours

Water is a very smooth surface with no canopy. Therefore, like the desert surface, it will track puffs for a long time in comparison with the other surfaces. For HPAC 4.03, the last puff was tracked until 16.5 hours while for HPAC 4.04 the last puff was tracked until 16.25 hours. The grounded source normalization constant for the HPAC 4.03 water surface is 3230 [R-km^2/hr-kt] while for HPAC 4.04 it is 1150 [R-km^2/hr-kt].

Figure 57: HPAC 4.03 Dose Rate Contour for 1kt Surface Burst with Water Surface at 12 Hours
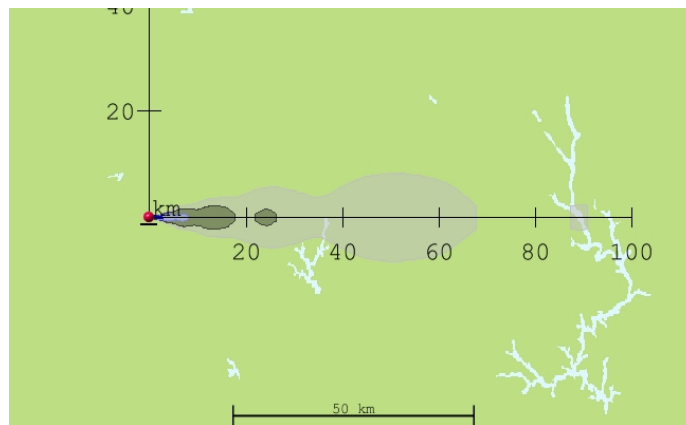
Figure 58: HPAC 4.04 Dose Rate Contour for 1kt Surface Burst with Water Surface at 12 Hours

The results for the following surface runs are summarized in the following table

Table 6: Comparison of Effects for Varying Surfaces

	HPAC 4.03		HPAC 4.04	
Surface	Last Puff (hrs)	k	Last Puff (hrs)	k
Cultivated	12.75	3460	12.25	1210
Forest	11.5	3720	11.0	1240
Urban	13.25	2730	11.5	1330
Grassland	14.0	3310	12.25	1240
Desert	17.75	3350	17.75	1110
Water	16.25	3230	16.5	1150

As shown in Table 6 and Table C-1 in Appendix C, canopy height is the greatest single factor in determining when the last puff lands for a given surface. Additionally, those with the highest canopies tend to have the highest grounded source normalization constants. The noticeable exception to this is the urban surface. The Urban surface has the second largest canopy after forest, but in the 4.03 run it has the lowest grounded source normalization constant while for 4.04 it has the highest source normalization constant. It is not clear why this is the case.

This relationship between increasing canopy height increasing the grounded source normalization constant is not intuitive. A terrain with a high canopy height, such as a forest or cultivated surface also has the greatest likelihood for shielding of radioactive fallout particles. For this reason, the grounded source normalization constants should decrease for these surfaces with greater inherent shielding. Neglecting

the effects of washout in water, one would expect desert and water to show the highest grounded source normalization constants instead of the lowest.

Effects of Rain Out

Precipitation scavenging by rain is a major removal mechanism for aerosols (particles ranging from 10^{-4} μm to tens of micrometers). Precipitation scavenging accounts for the removal of approximately 80-90% of the mass of aerosols in the atmosphere. Most of the remaining aerosol mass is removed through gravitational settling (23:153-154). Larger aerosol particles, aerosol particles greater than 1 μm, are collected more efficiently than smaller ones since the smaller aerosols will follow the streamlines around the raindrop instead of being impacted by the collecting raindrop (23:174).

If a fallout cloud encounters precipitation, a large portion of that cloud could be brought down by the precipitation (8:416). Based on the results of the AFIT smear code, all of the crystalline particles in the Heft subsurface distribution are dispersed into the atmosphere and a good portion of the glass distribution as well. One would expect a significant increase in the activity on the ground when there is precipitation present.

Fallout close to ground zero that is due to larger particles should not be greatly influenced by precipitation scavenging. This is because precipitation scavenging will not significantly affect the larger particles that fallout quickly by ground zero. However, downwind precipitation scavenging should cause surface deposition of smaller particles that would otherwise totally escape the local area.

Another consideration that should be accounted for is the yield of the blast. Typically rain clouds can be found between 10,000 to 30,000 feet (9:416). Generally

speaking, lighter rain clouds are found at the lower end of the altitude range while heavy rain clouds are at the higher end of the altitude range. Since that altitude that the nuclear cloud stabilizes at depends upon the yield of the burst, scavenging has less effect on high yield weapons. At 10kt the top of the stabilized cloud is usually about 19 kft while the bottom of the cloud is usually about 10 kft. At this yield, the entire stabilized cloud will usually be encompassed by the rain cloud or be completely below the rain cloud. At 100kt the top of the stabilized nuclear cloud is at about 40,000 feet while the bottom is at about 20,000 feet. This would mean that for a light rain there would be little to no scavenging of a 100kt burst, however, for a heavy rain, there would most likely be at least some scavenging. For nuclear explosives with yield greater than 100kt, scavenging will have little effect on the source normalization constant itself but might rearrange where the fallout lands.

A good historical example of the effect of precipitation scavenging causing fallout activity on the ground is the precipitation scavenging that occurred after the airburst shot associated with the bombing of Nagasaki. An airburst is not expected to result in any appreciable local fallout, however, after the Nagasaki airburst, there were some torrential rains. Measurements were made after the bombing and appreciable fallout was found on the ground. Krieser (13:15) assumes that 100% of activity should be scavenged in a rain storm. McGahan assumes that scavenging is 100% for particles with fall velocities less than the velocity of the rain itself (15:4).

SCIPUFF, which is the transport model used by HPAC, accounts for precipitation washout by adding a new sink term that must be accounted for in SCIPUFF's

conservation of mass. This new factor further modifies the conservation of mass

equation to

$$\frac{dQ}{dt} = -\left(F_s + F_R\right) \tag{17}$$

where

FR is the mass flux due to rain out (21:56). FR is defined by the following

equation:

$$F_R = \frac{Q}{\tau_R} \tag{18}$$

where

τ_R is the washout time scale.

The washout time scale is the inverse of the scavenging coefficient, ω_s. The

scavenging coefficient is defined by

$$\omega_s = \frac{p_o}{2/3D_r} E\left(D_p, \overline{D}_r\right) \tag{19}$$

where

p_o is the precipitation rate in mmh^{-1},

D_r is the raindrop diameter (an assumed range) in microns,

E is the collision efficiency,

D_p is the particle diameter in microns (21:57).

The precipitation rate, p_o, is assumed to be 0.5 mmh^{-1} for a light rain, 10 mmh^{-1}

for a moderate rain and 25 mmh^{-1}for a heavy rain (21:59-60). These are settings that the

user can specify within HPAC.

The Marshall Palmer raindrop distribution is assumed so that

$$N_r = 0.08e^{-\varepsilon D_r} \tag{20}$$

where $\varepsilon = 41(p_o)^{-21}$ (21:57).

The average raindrop diameter is then assumed to be

$$\overline{D_r} = \frac{3}{\varepsilon} \tag{21}$$

The collision efficiency is a function of the raindrop diameter, the Reynold's number, the Stokes number and the Schmidt number (21:57-58).

Sykes et al suggest that the model overestimates washout and as such they multiply the scavenging coefficient by 1/3. The authors of the SCIPUFF Technical Documentation offer the following to illustrate how the SCIPUFF rain scavenging agrees with the rain scavenging model proposed by Neito et al.
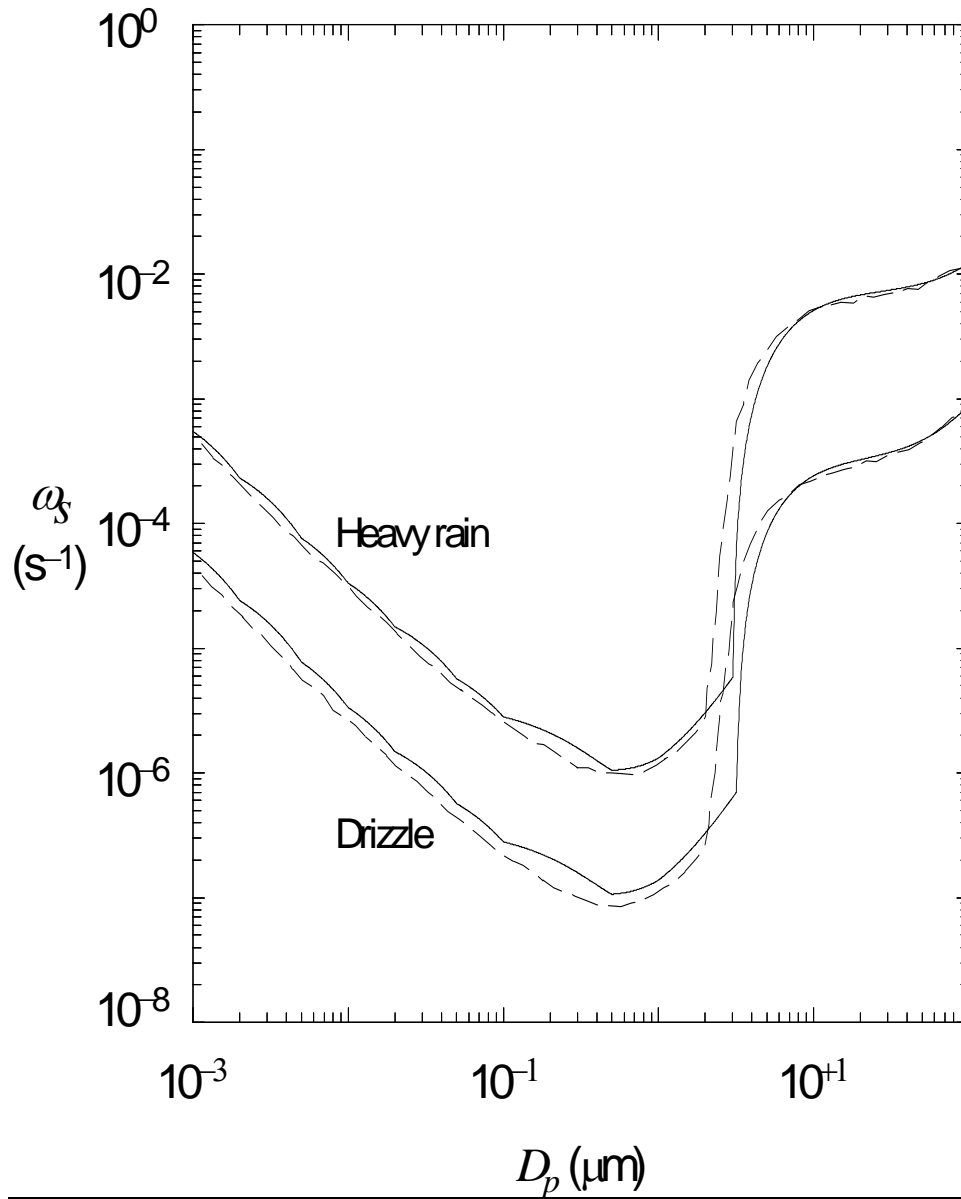
Figure 59: Scavenging Coefficient vs. Particle Diameter [From Sykes et al 59]

The solid lines in Figure 59 denote the model described above and the dashed lines denote the model of Nieto et al.

A series of HPAC runs was conducted for both light rain and heavy rain for a 1kt surface burst for both 4.03 and 4.04. The results are shown from Figure 64 to Figure 65:
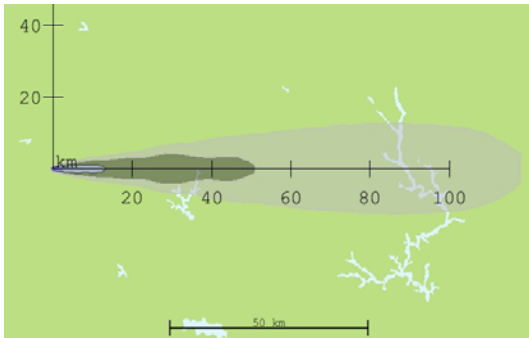
Figure 60: HPAC 4.03 Dose Rate Contour for 1kt Surface Burst with No Rain
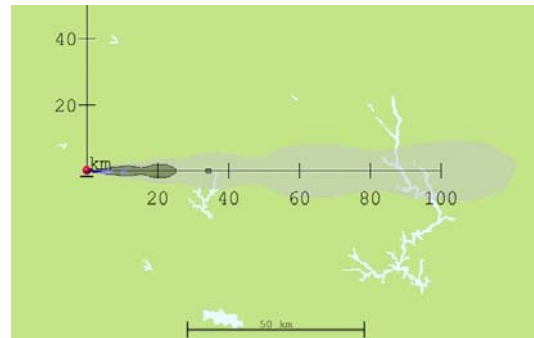
Figure 63: HPAC 4.04 Dose Rate Contour for 1kt Surface Burst with No Rain at 12 Hours
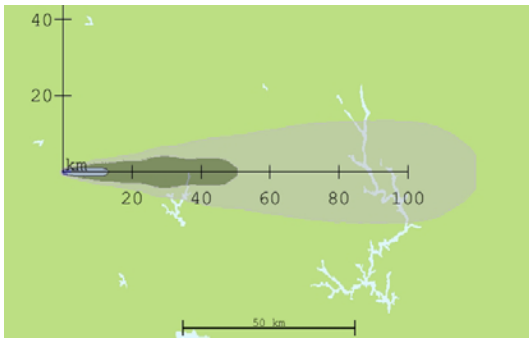
Figure 61: HPAC 4.03 Dose Rate Contour for 1kt Surface Burst with Light Rain at 12 Hours
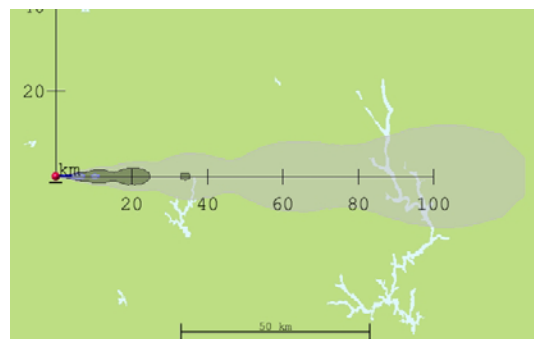
Figure 64: HPAC 4.04 Dose Rate Contour for 1kt Surface Burst with Light Rain at 12 Hours
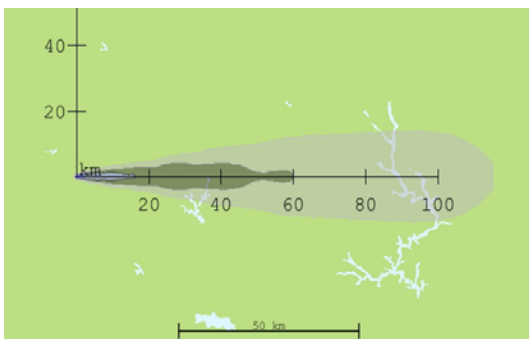
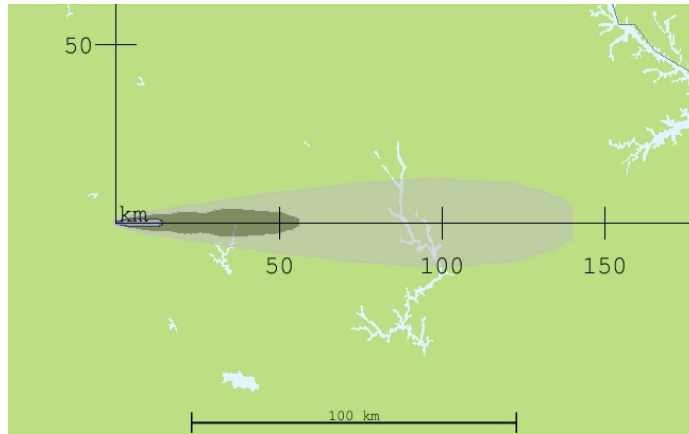Figure 62: HPAC 4.03 Dose Rate Contour 1kt Surface Burst with Heavy Rain at 12 Hours
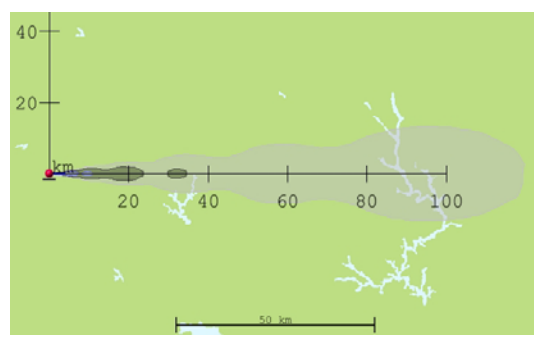
Figure 65: HPAC 4.04 Dose Rate Contour for 1kt Surface Burst with Heavy Rain at 12 Hours

Table 7: Grounded Source Normalization Constant Comparison for Rain Scavenging of Varying 1kt Surface Bursts

	HPAC 4.03	HPAC 4.04
No Rain	3460	1240
Light Rain	3710	1320
Heavy Rain	3810	1410

Rain scavenging should cause the fallout particles to fallout from the stabilized nuclear cloud at an earlier time than they otherwise would. This leads to the expectation that not only would there be more activity on the ground due to the scavenging of smaller fallout particles that does not normally fallout in the local area, but the area affected by fallout should be considerably reduced as activity is concentrated closer to ground zero due to rain scavenging. Table 7 shows a clear increase in the grounded source normalization constant for both HPAC 4.03 and 4.04 for rainout due to scavenging. For HPAC 4.03, there is a 7.4% from no rain to light rain while an increase of 10.2% is observed from no rain to heavy rain. For HPAC 4.04, there is a 6.1% increase from no rain to light rain and a 13.1% increase from no rain to heavy rain.

There is a clear reduction in the size of the fallout contour from the 4.03 no rain contour in Figure 64 to the heavy rain dose rate contour found in Figure 66. However, there is little appreciable reduction in the size of the fallout contours for the 4.04 series.

A series of HPAC runs was repeated for 10 kt bursts. The results are shown from Figure 70 through Figure 75.
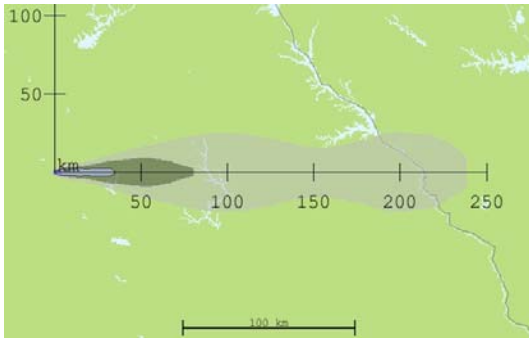
Figure 66: HPAC 4.03 Dose Rate
Contour for 10kt Surface Burst with No
Rain at 23 Hours
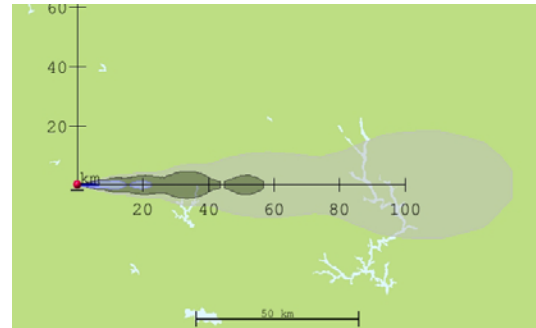
Figure 69: HPAC 4.04 Dose Rate
Contour for 10kt Surface Burst with No
Rain at 22 Hours
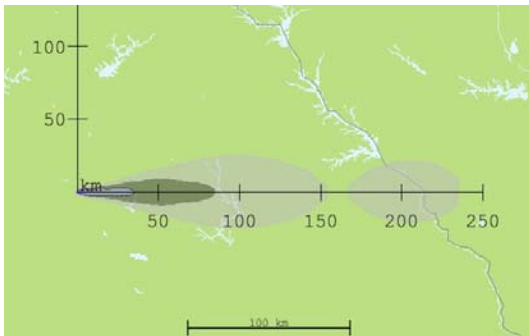
Figure 67: HPAC 4.03 Dose Rate
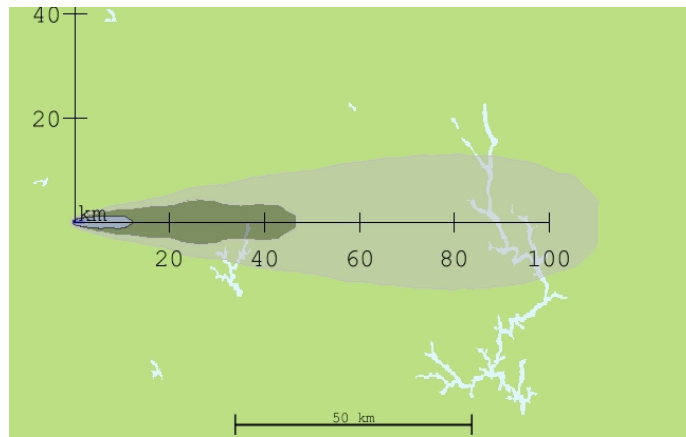Contour for 10kt Surface Burst with
Light Rain at 23 Hours
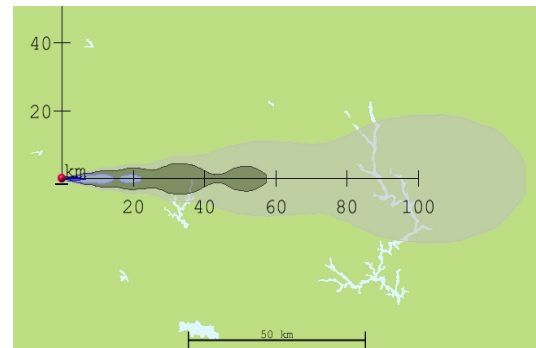
Figure 70: HPAC 4.04 Dose Rate
Contour for 10kt Surface Burst with
Light Rain at 22 Hours
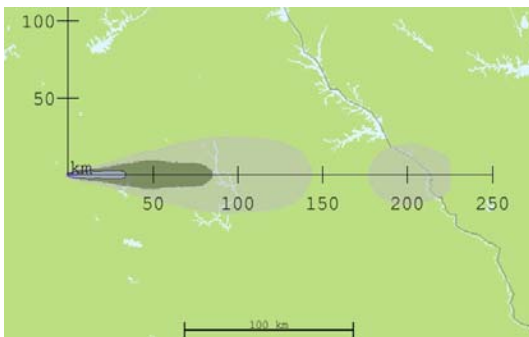
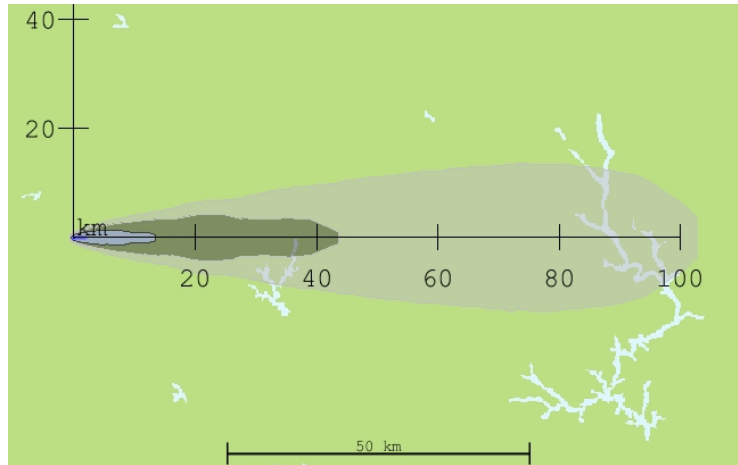Figure 68: HPAC 4.03 Dose Rate
Contour for 10kt Surface Burst with
Heavy Rain at 23 Hours
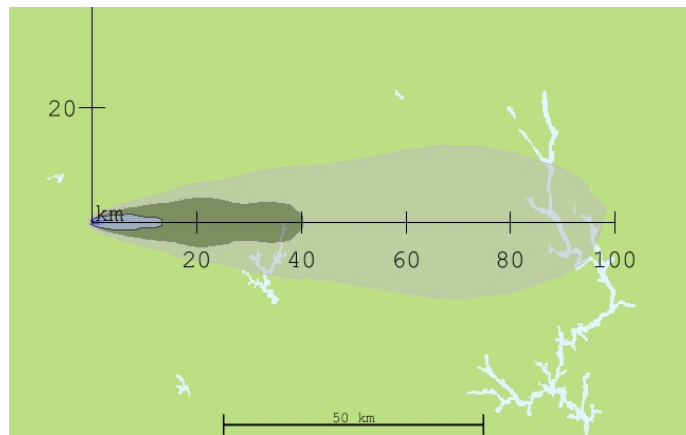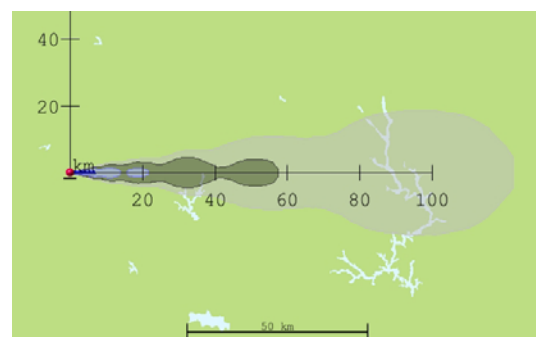

Figure 71: HPAC 4.04 Dose Rate
Contour for 10kt Surface Burst with
Heavy Rain at 22 Hours

From a visual standpoint there is very little difference in the 10 kt blast with no rain, light rain and heavy rain.

Table 8: Grounded Source Normalization Constant for 10kt Surface Burst with Varying Levels of Rain

	HPAC 4.03	HPAC 4.04
No Rain	3030	970
Light Rain	3050	990
Heavy Rain	3090	1000

Table 8 shows very little difference in activity deposition on the ground due to rainout for a 10kt surface burst. The difference from no rain to heavy rain is only 2% for 4.03 while for 4.04 the difference is only 3.4%. Visually there is some difference in the sizes of the dose rate contour for the 4.03 sequence, but again, there is no noticeable difference in the 4.04 10kt series.

While HPAC shows that the rain is a scavenging activity, it is not scavenging enough activity to be a realistic representation of the effect rainout would have on the airborne fallout that doesn't normally fall to the local area. Based on historical examples of washout, it is not unreasonable to assume that a heavy rain would effectively scavenge all of the activity in a fallout cloud. It is evident that the true source normalization constant must be at least 3800 [R-km^2/hr-kt] since this is the source normalization constant that is achieved from an HPAC 4.03 1kt surface burst with heavy rain. The AFIT smear code indicates that in the Heft subsurface particle distribution, that neither

the crystalline nor the glass particles contribute significant activity to the local fallout area. If it is assumed that none of the crystalline population, which makes up 17% of the mass, falls in the local area and that the crystalline population makes up 17% of the activity, then there is at lest 17% of the true activity that should be deposited in the local area due to rain scavenging. 17% of 3800 gives an increase of 650 in the HPAC 4.04 source normalization constant from no rain to heavy rain. However, there is an increase of merely 160 [R-km^2/hr-kt] for the 1kt surface burst and only 30 [R-km^2/hr-kt] for the 10kt surface burst, even though the stabilized clouds for both yields would most likely be within a rain cloud. The author cannot explain this anomaly.

Effects of Different Constant Wind Speeds for DELFIC and Heft Three Component Particle Distributions

As discussed earlier, SCIPUFF tracks a Gaussian puff of particle through the advection-diffusion equation (Equation 19). Wind velocity not only moves the puff, but also affects the concentration of puffs. The stronger the wind that acts upon an individual puff, the more diffusion and the lower the concentration that puff will have over time.

A series of runs was accomplished using both HPAC 4.03 and 4.04 using a constant wind of 5kph, 10kph and 15kph. The results for HPAC 4.03 are shown from Figure 72 through Figure 74. The results for HPAC 4.04 are shown from Figure 75 through Figure 77.

76
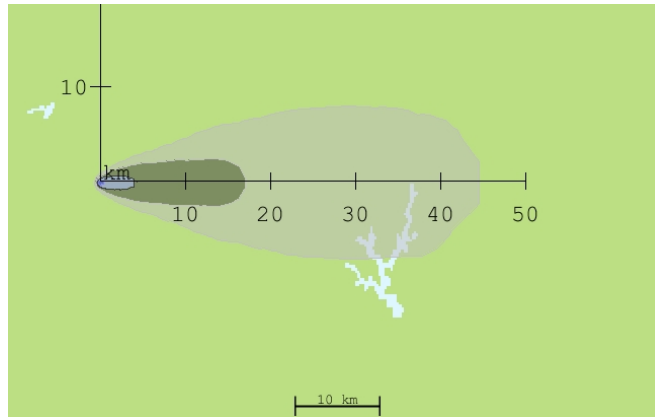
Figure 72: HPAC 4.03 Dose Rate Contour for 1kt Surface Blast with 5kph Constant Wind
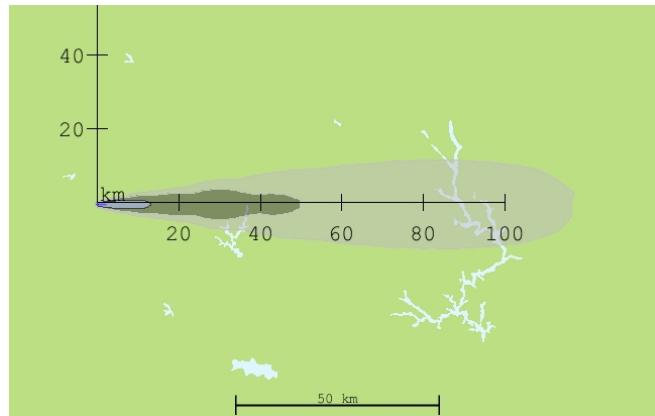
Figure 73: HPAC 4.03 Dose Rate Contour for 1kt Surface Burst with 10kph Constant Wind
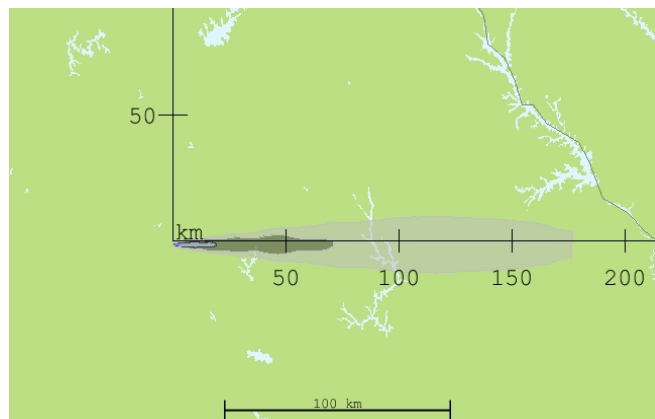
Figure 74: HPAC 4.03 Dose Rate Contour for 1kt Surface Burst with 15kph Constant Wind
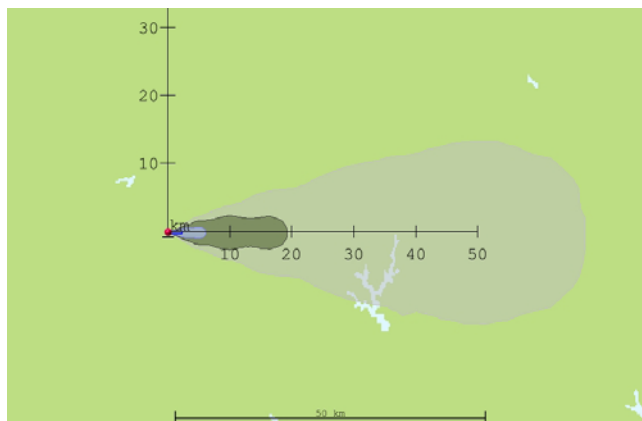
Figure 75: HPAC 4.04 Dose Rate Contour for 1kt Surface Burst with 5kph Constant Wind
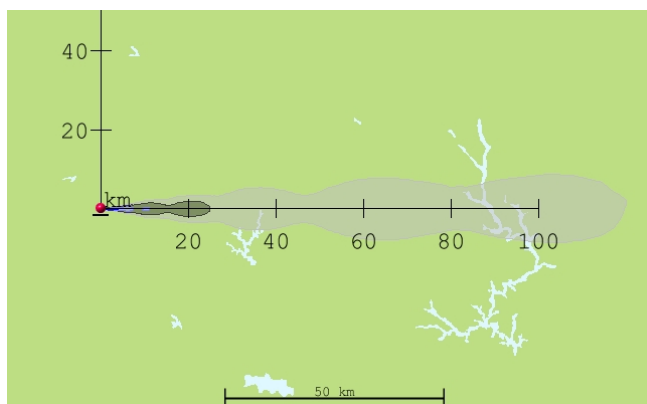
Figure 76: HPAC 4.04 Dose Rate Contour for 1kt Surface Burst with 10kph Constant Wind

Figure 77: HPAC 4.04 Dose Rate Contour for 1kt Surface Burst with 15kph Constant Wind

As can be seen, the slower the wind, the less the fallout cloud is dispersed and the more activity falls to the ground in amounts significant enough to be counted. As the wind increases, the fallout smear increases in the east-west direction, but drastically decreases in the north-south direction.

Table 9: Grounded Source Normalization Constant Summary for 1kt Surface Bursts with Different Winds

Wind Speed (kph)	HPAC 4.03	HPAC 4.04
5 (Dose Rate taken at 12 hrs)	3510	1310
10	3460	1210
15	3380	1160

Table 9 shows the summarization of grounded source normalization constant for Different Winds. There is a trend that the less wind, the higher the grounded source normalization constant. If the wind acts to diffuse the stabilized nuclear cloud, then slower wind allows more of the activity to be deposited in the local area. While there is a definite trend for increasing grounded source normalization constant with decreasing wind, it should be noted that the differences are not major.

Figure 78 and Figure 79 show g(t) for differing winds for HPAC 4.03 and 4.03 respectively.

The noticeable feature of Figure 78 and Figure 79 is that g(t) doesn't vary much with different wind speeds. This indicates that gravitational settling is the major

deposition mechanism and that the diffusion of the stabilized nuclear cloud is not a major

concern for total activity deposition.
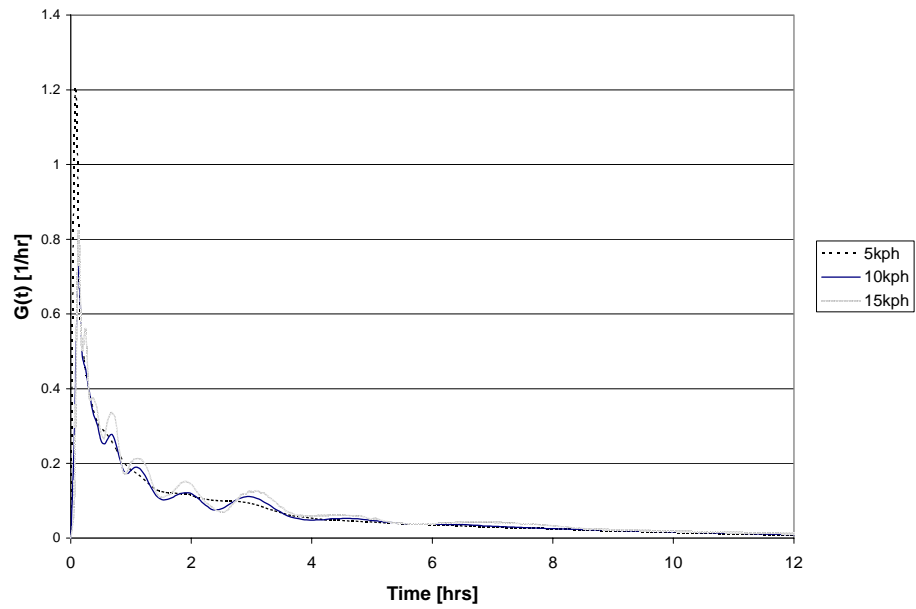
Figure 78: G(t) Comparison for HPAC 4.03 1kt Surface Burst with Different Winds
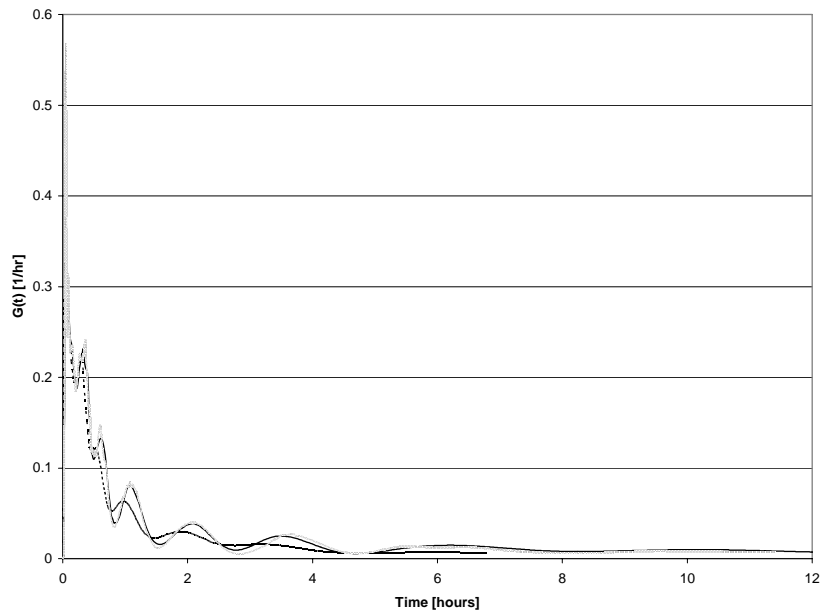
Figure 79: G(t) Comparison for HPAC 4.04 1kt Surface Burst with Different Winds

VI. Research Summary and Conclusions

This final chapter provides a summation of and conclusions drawn from the preceding research. Recommendations for further research on related topics are also included.

Research Summary

This research compared the DELFIC and Heft subsurface particle distributions for nuclear fallout modeling in HPAC. Since the Heft subsurface particle distribution is created from a low yield test shot in the Nevada desert, it is important to understand the implications of using this distribution as the sole distribution in HPAC for all surface burst fallout modeling. Through a series of HPAC runs using visual analysis, grounded source normalization constant and the rate of arrival function $g(t)$, the variation in HPAC output was analyzed for varying yields, varying times, varying surfaces, rainout and different wind speeds.

Conclusions

HPAC 4.04, which uses the Heft subsurface distribution, consistently deposits about a third of the activity in the local area as compared to HPAC 4.03, which uses the DELFIC particle distribution. Based on the CASTLE BRAVO test, the expected source normalization constant should be between 2590 and 3880 [R-km^2/hr-kt] (8:494). It should be noted that CASTLE BRAVO was a 15 Megaton shot (9:63). Some of Castle Bravo's fallout penetrated the tropopause and did not contribute to local fallout. Thus, the amount of fallout in the local area would be much less per kiloton of yield than for lower yield bursts, which have no global component. The highest source normalization constant generated was about 3720 [R-km^2/hr-kt] for a 1kt burst with forest surface in

81

HPAC 4.03. This is well within the expected source normalization constant based on CASTLE BRAVO. The highest source normalization constant generated by HPAC 4.04 is 1240 [R-km^2/hr-kt] and this also was for a 1kt surface burst with the forest surface. This value is far lower than that expected based on the CASTLE BRAVO source normalization constant.

When varying the yield of the nuclear detonation two things stand out. The first is that the grounded source normalization constant drops dramatically with increasing yield. In HPAC 4.03 it drops from 3460 to 1470 [R-km^2/hr-kt] and a similar drop is seen in HPAC 4.04 from 1210 to 458 [R-km^2/hr-kt]. These grounded source normalization constants are very low and seem to indicate that the fallout activity is being underestimated at higher yields or more of it is escaping the local area. The second noticeable feature is the area affected by fallout for varying yields. For 1kt, the HPAC 4.03 0.01 rad/hr dose rate contour extends a little less than twice the downwind distance that the HPAC 4.04 0.01 rad/hr dose rate contour extends. However, for 100kt, the HPAC 4.03 0.01 rad/hr dose rate contour extends more than three times the downwind distance that the HPAC 4.04 0.01 rad/hr dose rate contour extends. This indicates that either HPAC 4.03 is vastly overestimating the area affected by fallout for high yield weapons, or HPAC 4.04 is grossly underestimating that area.

The effects of varying times on the grounded source normalization constant showed that HPAC 4.04 stops adding significant activity to the local area at a much sooner time than does HPAC 4.03. This can also be inferred from the difference in area affected by fallout between HPAC 4.03 and 4.04.

Varying surfaces in HPAC produced differing concentrations of fallout. In general, the higher the canopy height, the greater the deposition rate of fallout particles is. While the varying surfaces do appear to affect the deposition rate of fallout, there is no indication that differing surface roughness factors are taken into consideration amongst the various surfaces. Surface roughness factors should pose a large contribution to the grounded source normalization constants seen from fallout modeling. This issue should be addressed in HPAC.

Rainout is an efficient scavenging mechanism for particles greater than 1 micron in diameter. Since the Heft distribution places a considerable portion of its mass in the fine crystalline distribution with a mass median diameter of 6.8 microns, rainout should greatly increase the grounded source normalization constant observed from HPAC 4.04 and greatly decrease the fallout area seen by both HPAC 4.03 and 4.04. However, the series of 1kt and 10kt rain runs showed only a slight increase in the grounded source normalization constant for both HPAC 4.03 and 4.04. Additionally, there was little difference in the area affected by fallout from surface bursts without rain and surface bursts with rain.

The effects of different constant winds on HPAC 4.03 and 4.04 is primarily to change the area affected by fallout. The function g(t) is not greatly influenced by different constant winds for either HPAC 4.03 or 4.04. This indicates that gravitational settling is the dominant mechanism for particle deposition in HPAC.

Recommendations for Future Research

This thesis leads to four recommendations for future research.

First, the Heft subsurface distribution should be benchmarked against historic test data for both high yield bursts and bursts over differing soils. The Heft subsurface distribution should be benchmarked against both the DELFIC distribution and the Heft two-component surface distribution for Pacific test shots. The research should seek to answer the question of which distribution is most appropriate for high yields, silicate soil and coral soil.

Second, the effects of rain scavenging in SCIPUFF should be investigated more thoroughly. A validation of rain scavenging of airburst and crystalline fallout particles by SCIPUFF could be accomplished by benchmarking SCIPUFF particle deposition against the historical example of rainout seen at Nagasaki.

Third, the activity distribution used with the Heft subsurface distribution should be analyzed. Heft's activity distribution could be modeled for each equal mass size class by integrating both the refractory and volatile distributions for each size group to find the percent of volatile and refractory in each size group. After this, the Freiling ratio for each mass chain could be determined. Knowing the cumulative yield and the Freiling ratio for each mass chain, the number of volatiles in a particular mass chain could then be apportioned for a given equal mass size group based on the percentage of volatiles and refractories in that equal mass size group determined by the Heft subsurface refractory and volatile distributions. The results of fallout based on the Heft subsurface activity distribution could then be compared with the current activity distribution by benchmarking against historic test shots.

Fourth, the SCIPUFF transport code should be benchmarked against a classic disk tosser routine (such as DELFIC) for fallout modeling. SCIPUFF may globally disperse

more of the activity from a nuclear detonation than a disk tosser and for this reason this research should focus on the difference in both the amount of activity deposited by each transport code and the area affected by fallout by benchmarking both transport codes against historic test shots.

Fifth, comparison should be made between a traditional fallout model such as HPAC that transports fallout based on current weather conditions and predictions and an inline weather fallout model that considers the effects a nuclear burst has on the weather and then transports fallout particles based on the updated weather predictions.

Sixth, SCIPUFF should be examined to track the puffs as a function of time and space, both vertically and horizontally. In this way, activity could be integrated vertically in order to determine how much activity is still in the air as a function of time after detonation. This activity should be tracked until it is grounded. By doing this integration immediately after detonation, the source normalization constant for HPAC could be determined. Then by tracking the activity until it lands and integrating the activity over all ground, a determination could be made of whether or not HPAC conserves activity.

Glossary

A - Area

A(d) - the activity distribution as a function of fallout particle diameter

a_i - the number of atoms of isotope i in a sample

c – concentration of puff

c_D – coefficient of drag

$\dot{D}_{Gd}$ - Dose Rate on the ground at the unit time.

$\overline{D_r}$ - average raindrop diameter

d – diameter of fallout particle

DELFIC – Defense Land Fallout Interpretative Code

F_T - the total number of equivalent fissions in all size classes

F_i - the total number of equivalent fissions in the ith size class

F_p - the drag force

F_R - mass flux due to rain out

f_i - the number of fissions needed to create the number of radioisotopes observed

      in the fallout particle

k – grounded source normalization constant [R-km^2/hr-kt]

kt - Kiloton

M - the mass of the puff

m_k – mass fraction of the kth size group

N(d) –the number of particles of diameter d

Q – total mass of all puffs

R_i - the fration of fissions in the ith mass chain that obeys radial distribution

$r_{i,j}$ - the ratio of the number of fissions needed to create the number of radioisotopes

      observed for isotope i to the number of fissions needed to create the number of

      radioisotopes observed for isotope j.

r_p - the equivalent spherical particle radius

S_i - the fraction of fissions in the ith mass chain that appears with constant specific

      Activity

S – Sources and Sinks

t - time

u_i - the wind velocity in the i direction

URDR – Unit-Time Reference Dose Rate

v_D - downward velocity of particles

v_g - particle fall speed due to gravity

W - weapon yield in kilotons

x_c, y_c, z_c - the location of the Gaussian puff centroid

Y_i - the cumulative fission yield of isotope i in mass chain m

z_{GZ} - the altitude of ground zero

z_{HOB} - the altitude of the height of burst above ground zero

β - the natural logarithm of the standard deviation

α_0 - the natural logarithm of the median diameter in microns

λ - the radioactive decay constant

ξ - the direction transverse to the constant wind

ρ_a - air density

ρ_p - particle material density

ς - molecular diffusivity

σ_h - the standard deviation of a Gaussian puff in the horizontal axis

σ_i - the standard deviation of the $\log_{10}$(diameter) for the ith population

σ_z - the standard deviation of a Gaussian puff in the vertical axis

τ_R - washout time scale

ϕ_i - the percentage of mass for the ith population

$\bar{x}_i$ - the $\log_{10}$ of the average diameter in microns for the ith population

χ - the $\log_{10}$ of the diameter in microns

ψ_i - the slope of the Freiling plot for isotope i

ω_s – washout timescale

Appendix A: Converting a Log_{10} distribution to a Ln Distribution

The general equation for a Log_{10} distribution

$$N(d) = \frac{1}{\sqrt{2\pi}\sigma \ln 10d} \exp\left[-\frac{1}{2}\left(\frac{Log_{10}d - \chi}{\sigma}\right)^2 dd\right]$$

(A-1)

where

   d is diameter

   σ is Logarithmic standard deviation

   χ is the Log_{10} of the median particle diameter.

First transform the Logarithmic standard deviation, σ, into the Lognormal standard

deviation, β. Heft defines σ as

$$\sigma = \frac{Log_{10}d_{max} - Log_{10}d_{min}}{6}$$

(A-2)

It should be noted that

$$Log_{10}d = \frac{\ln d}{\ln 10}$$

(A-3)

Substituting A-3 into A-2 yields

$$\sigma = \frac{\ln d_{max} - \ln d_{min}}{6\ln 10}$$

(A-4)

Let $\beta = \dfrac{\ln d_{max} - \ln d_{min}}{6}$ therefore

$$\sigma = \frac{\beta}{\ln 10}$$

(A-5)

Next we transform the exponential from Log_{10} to $\ln$

$$\frac{Log_{10}d - Log_{10}d_{0.5}}{\sigma} = \frac{\dfrac{\ln d}{\ln 10} - \dfrac{\ln d_{0.5}}{\ln 10}}{\dfrac{\beta}{\ln 10}} = \frac{\ln d - \ln d_{0.5}}{\beta}$$

(A-6)

Finally, combining all these things together

$$N(d) = \frac{1}{\sqrt{2\pi}\,\dfrac{\beta}{\ln 10}\ln 10}\exp\left[-\frac{1}{2}\left(\frac{\ln d - \ln d_{0.5}}{\beta}\right)^2\right]$$

which equals

$$\frac{1}{\sqrt{2\pi}\beta}\exp\left[-\frac{1}{2}\left(\frac{\ln d - \ln d_{0.5}}{\beta}\right)^2 dd\right]$$

(A-7)

Appendix B: Summarization of Freiling Ratios and Heft Distributions

Fission produces over 300 different types of fission fragments that go through a series of β/γ decays until they reach stable isotopes. The series of atoms formed through the fission fragments decay are known as mass chains. Freiling ratios help to characterize these mass chains in terms of how volatile or refractory they are as a whole.

Freiling ratios are based on the results of radiochemical analysis of fallout particles. Both the total number of atoms and the number of atoms of each radioisotope are counted in each fallout particle. The first long lived radioisotope of a given mass chain is chosen to represent the mass chain.

The number of fissions needed to create the number of radioisotopes observed in the fallout particle is:

$$f_i = a_i / Y_i \qquad\qquad \text{(B-1)}$$

where

a_i is the number of atoms of isotope i in a sample

Y_i is the cumulative fission yield of isotope i in mass chain m (7:1994).

A purely volatile isotope, ^{89}Sr, is used to reference against other isotopes. A ratio of any isotope is then set up against ^{89}Sr (7:1995):

$$r_{i,89} = \frac{f_i}{f_{89}} . \qquad\qquad \text{(B-2)}$$

If the fallout particle had all of the fission-fragment isotopes in the same ratios as what can be expected from fission, then $r_{i,89}$ would equal one. If the isotope i were distributed in the same proportion as ^{89}Sr in the fallout particle, then isotope i would be

volatile. However, because fractionation alters the isotope proportions, this will not be the case.

Freiling chose ^{95}Zr to represent a purely refractory isotope. This leads to a refractory to volatile ratio (7:1994)

$$r_{95,89} = \frac{f_{95}}{f_{89}}.$$ (B-3)

For each isotope of interest (and by extension each mass chain of interest), $r_{i,89}$ and $r_{95,89}$ are determined for each fallout particle size group. $r_{i,89}$ is then plotted on the ordinate and $r_{95,89}$ is plotted on the abscissa for each mass chain of interest. A straight line is then fit to the data. The slope of this line determines the classification of the mass chain. Mass chains with Freiling ratio slopes between 0.98 and 1.0 are considered refractory. If the slope is between 0.0 and 0.02, the mass chain is considered to be purely volatile and slopes between 0.02 and 0.98 are considered mixed chains (6:6).

Heft Characterization of Radioactive Particles from Nuclear Tests

In his article "The Characterization of Radioactive Particles from Nuclear Weapons Tests", Heft analyzed samples taken from stabilized clouds following nuclear explosions. Heft proposed a series of logarithmic distributions to fit the particle sizes that he observed from differing types of nuclear bursts. He created different particle distributions for airburst detonations, Coral Island surface bursts and cratering detonations. I will briefly consider Heft's Coral Island surface distributions and then focus on his cratering detonation distributions.

Heft asserts that for land surface bursts the particle population divides into two distinct components, which Heft referred to as crystalline and glass particles. The

crystalline particles are made up of soil material which entered the fireball at a later time and hence were never melted. Because these particles arrived at a later time, the activity associated with them is exclusively surface distributed volatiles. Since the crystalline particles are soil material that has surface deposition of radionuclides from the bomb debris, the density of the crystalline particles is identical to that of the soil material.

Heft defines the glass population as soil material which entered the fireball at a time earlier to the crystalline material. As a result the glass particles were at least partially melted. In addition, the amount of soil material that would be considered glass particles is much greater than the amount of soil material that would result in crystalline particles. As a result of increased material and time in the fireball, the mean diameter of a glass particle is larger than the mean diameter of a crystalline particle. Also, since glass particles are local soil material that is partially or fully melted, the density of the glass particles is the same or slightly less than the density of the local soil (12:255-256).

For a land subsurface burst in which the fireball is not contained, Heft adds a third particle population called local fallout. Heft describes this population as "soil material which interacted with the fireball at high temperature but which was separated from the fireball early, before the temperature had fallen below the melting point of the soil" (12:256). The density of the local particles is much lower than that of the local soil and the range of particle diameters for the local particles is much greater than the diameter range for either the crystalline or glass particles. Interestingly, Heft contends that the relative abundance of radionuclides in the local fallout is independent of particle size and is constant between samples of local fallout (12:256).

Shifting back to the two-component lognormal surface burst distribution, Heft makes Freiling plots of the isotopes found in the aerial filters from the Coral Island detonations. Heft normalizes the isotopes with a reference refractory isotope according to the equation:

$$r_{i,ref} = \frac{f_i}{f_{ref}} \qquad (B\text{-}4)$$

It should be noted that instead of normalizing the isotope of interest, A, against a reference volatile as Freiling does, Heft normalizes the reference isotope against a reference refractory, ^{155}Eu. Instead of generating $r_{i,89}$ and $r_{95,89}$ as Freiling does, Heft instead uses ^{155}Eu as a reference refractory and ^{137}Cs as a reference volatile to generate $r_{i,155}$ (which Heft calls r^A) and $r_{137,155}$ (which Heft calls r^{137}). This means that the slope values are reversed for the mass chains, or in other words, a slope of one represents a purely volatile mass chain whereas a slope of zero represents a purely refractory mass chain. Heft finds the slope of each isotope using the following formula:

$$\psi_i = \frac{1}{5} \sum_{k=1}^{5} \left(\frac{r_{i,155} - 1}{r_{137,155} - 1} \right) \qquad (B\text{-}5)$$

where

ψ_i is the slope of the Freiling plot for isotope i (12:259) and

k is an index used to reference the different aerial filters from which the particles were collected.

The normalized isotopic ratios were calculated at all five aerial filters and plotted vs. the normalized isotopic ratios for ^{137}Cs. Heft's results are shown in Figure 3.
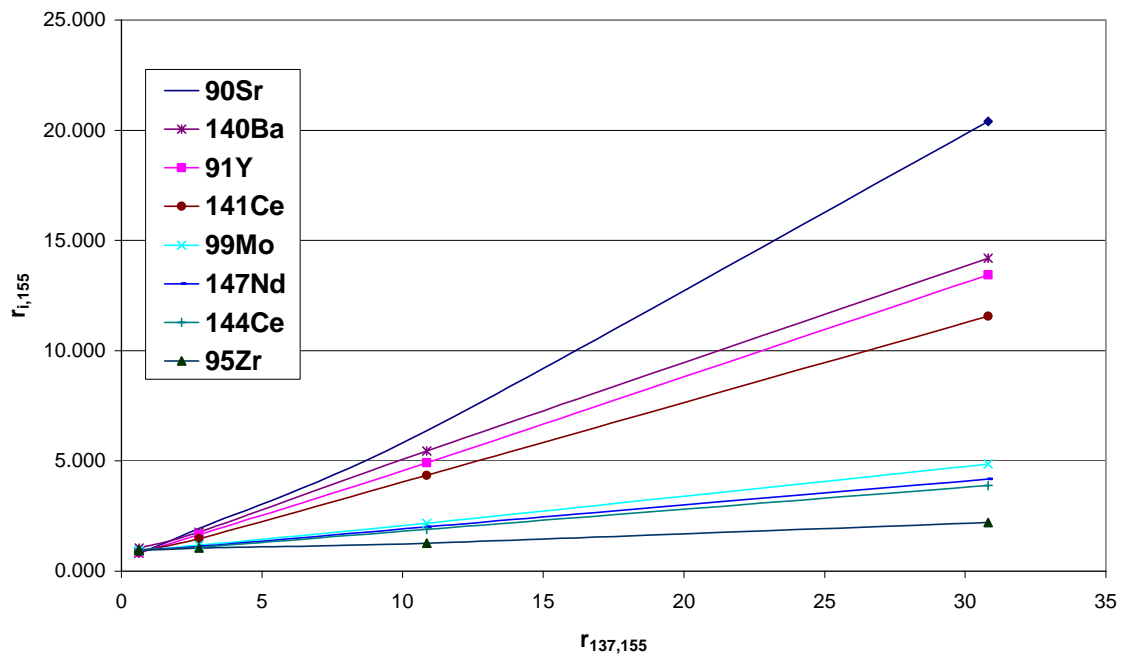
Figure 80: Freiling Ratios for Land Surface Detonation Fallout Particles

Heft notes that when the Freiling ratios are plotted, every $r_{i,155}$ for the normalized isotopes crosses one when $r_{137,155}$ crosses one. Although there is not any actual fallout particle analyzed where $r_{137,155}$ is one, when $r_{137,155}$ equals one indicates that the volatile ^{137}Cs and the refractory ^{155}Eu are present in the same proportions as they were created due to the fission of the weapon fuel. In other words, there is no fractionation of either isotope at this particular point on the graph. It follows that if $r_{i,155}$ also is one when $r_{137,155}$ is unity, then isotope i is also in the same proportion in which it was created and therefore not fractionated.   The significance of every isotope's $r_{i,155}$ and $r_{137,155}$ all crossing at (1,1) is that it indicates the particle populations collected by the aerial filters are representative of the entire population. In other words, all of the isotopes are accounted for within the

particle sample. If there were a class of fallout particles not collected by the filters, then the absence of the isotopes in this missing particle class would become apparent on the Freiling plot. This absence would be indicated by the $r_{i,155}$ vs $r_{137,155}$ of the varying isotopes not intersecting at the point (1,1) (12:259-260).

The data presented above fits the linear relationship:

$$r_{i,155} = (1-\psi_i) + \psi_i r_{137,155}.$$ (B-6)

Heft suggests that this is evidence that the aerial filters suggest a two-component isotopic distribution (12:260).

Heft measured the specific activity of his reference refractory, ^{155}Eu, and plotted this against the harmonic mean particle diameter <D> of the particle ranges from the particles collected from the filters.

When specific activity varies by 1/<D>, this implies that the radioisotopes are being surface distributed onto the particles. There are clearly two regions on Figure 81 where this occurs, 1 to 2 microns and greater than 30 microns. From 1 to 2 microns, Heft theorizes that the 1/<D> slope can be attributed to late condensation of volatiles onto the crystalline particles. The 1/<D> slope at the larger mean particle diameters (30 microns and greater) is attributed to surface attachment of refractories onto glass particles that entered the cloud earlier than the crystalline particles. The area in between the two areas of linearity is thought to be either volume distribution of the isotopes or the mixing of surface deposited particles from both glass and crystalline particles (12:260-262).
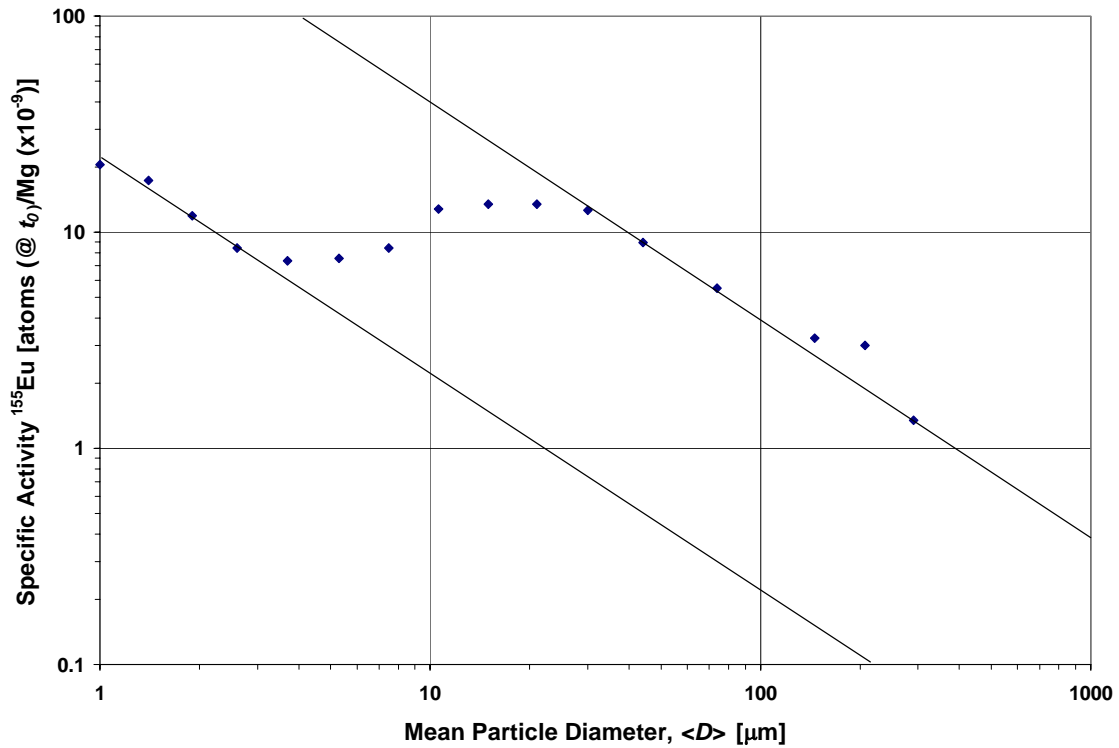
Figure 81: Specific Activity vs Mean Particle Diameter

Heft also looked at the mass of the particle population from the second coral island aerial filter and from this data was able to fit the following lognormals in Figure 82.

Based on the linearity of the Freiling data, the specific activity data and the mass distribution data, Heft concludes that there are two particle populations (crystalline and glass) which he represents by equation B-7:
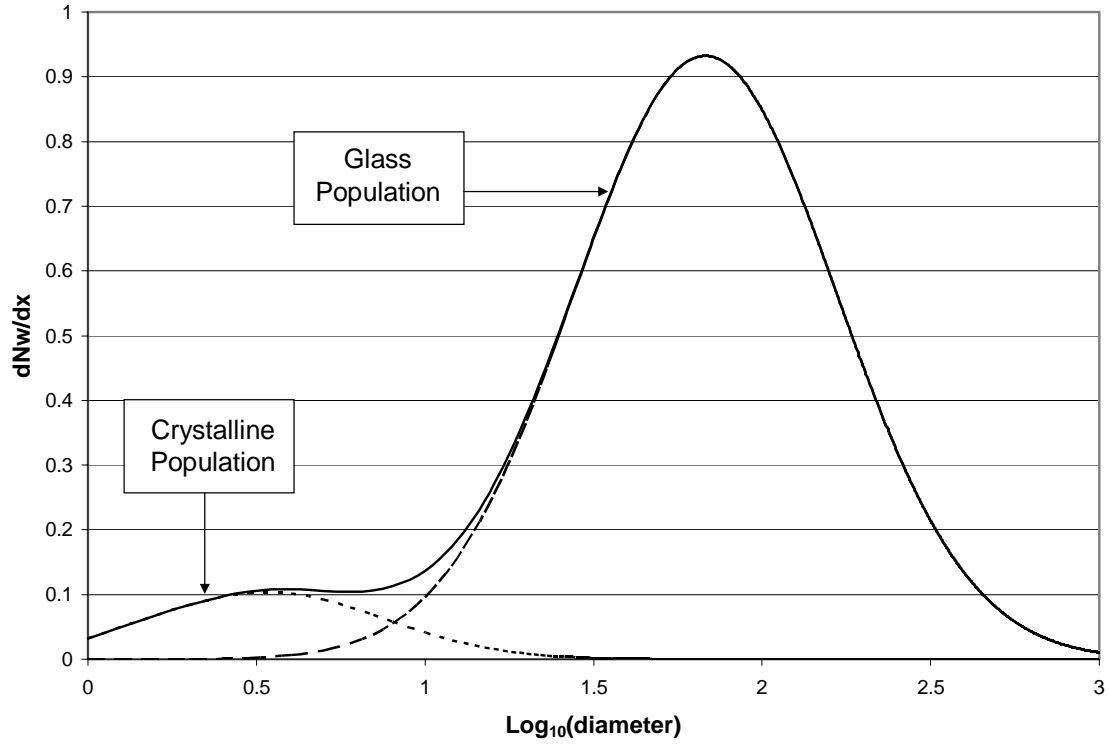
Figure 82: Mass Distribution for Heft Two-Component Surface Burst Fallout Particles

$$\frac{dF_m}{dx} = \frac{\phi_1}{\sqrt{2\pi}\sigma_1}\left[\exp\left(\frac{\left(\overline{x_1}-x\right)^2}{2\sigma_1^2}\right)\right] + \frac{\phi_2}{\sqrt{2\pi}\sigma_2}\left[\exp\left(\frac{\left(\overline{x_2}-x\right)^2}{2\sigma_2^2}\right)\right] \qquad \text{(B-7)}$$

where

F_m is the fraction of mass

ϕ_1 is the percentage of mass for the glass population, 0.91

σ_1 is the standard deviation of the $\log_{10}$(diameter) for the glass population, 0.3895

$\overline{x_1}$ is the $\log_{10}$ of the average diameter in microns for the glass population, 1.8315

χ is the $\log_{10}$ of the diameter in microns

ϕ_2 is the percentage of mass for the crystalline population, 0.09

σ_2 is the standard deviation of the $\log_{10}$(diameter) for the crystalline population, 0.3641

$\overline{x_2}$ is the $\log_{10}$ of the average diameter in microns for the glass population, 0.5299 (12:265).

Heft also examined fallout particles collected from test shots in the Nevada desert. Heft looked at fallout particles taken close to ground zero as well as six aerial filters taken in the aerial cloud at successively later times and a final set of fallout particles taken from the ground at a location distant from ground zero.

Unlike his analysis of the surface burst, Heft changes the atom ratio to:

$$r_{i,1} = \frac{f_{i,147}}{f_{i,147}^1} \tag{B-8}$$

where

$f_{i,147}^1$ is the atom ratio for isotope i relative to the reference refractory ^{147}Nd for the fallout particles close to ground zero (12:268).

The numerator for the above equation is the fraction ratio observed from the aerial filter while the denominator is the fraction ratio from the local fallout. This means that if the numerator is the close in fallout instead of fallout samples from the aerial filter, $r_{i,1}$ is always equal to one for all isotopes. The aerial filters and the remote fallout are then plotted in a modified Freiling plot. The modified Freiling plot for ^{137}Cs is shown in Figure 83.
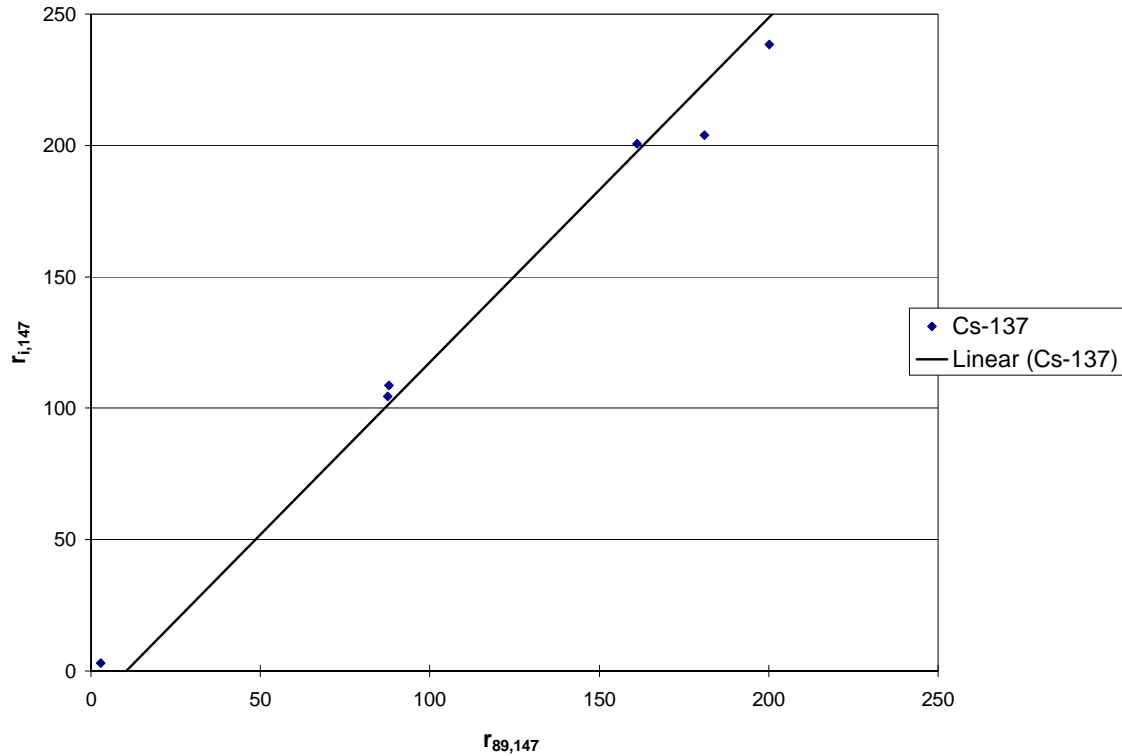
Figure 83: Modified Freiling Plot for ^{137}Cs from Aerial Filters of Surface Burst

As is evident from the modified Freiling plot, the trendline for r^{137} vs. r^{89} does not cross at (1,1). This is true for all the other isotopes sampled in the aerial filters as well. This indicates that the sample from the aerial filters does not represent the complete particle population; therefore the local fallout must be its own particle distribution. If the close-in fallout particles at (1,1) are treated separately from the modified aerial filter Freiling ratios then the data fits a linear relationship similar to the surface burst data above. Once again, this suggests that the particles in the aerial filter have a two-component isotopic distribution (12:268-269).

Heft also looked at the data for particle mass, treating the close-in fallout particles as their own distribution and fit the following logarithmic distributions to the data.
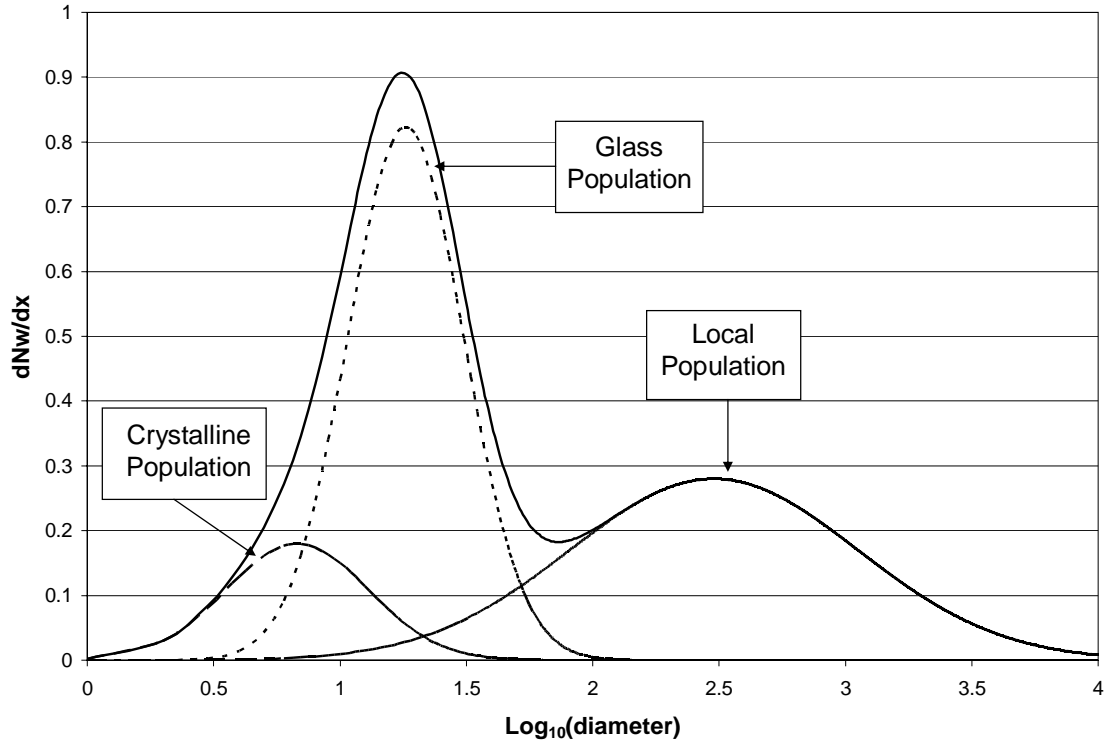
Figure 84: Mass Distribution for Heft Three-Component Surface Burst Fallout Particles

Heft gives the following equation to describe this distribution:

$$\frac{dF_m}{dx} = \sum_{i=1}^{3} \left(\frac{\phi_i}{\sigma_i \sqrt{2\pi}} \right) \exp\left[-\left(\frac{\overline{x_i} - x}{\sigma_i \sqrt{2}} \right)^2 \right]$$ (B-9)

where

ϕ_i is the percentage of mass for the ith population

σ_i is the standard deviation of the $\log_{10}$(diameter) for the ith population

$\overline{\chi_i}$ is the $\log_{10}$ of the average diameter in microns for the ith population

χ is the $\log_{10}$ of the diameter in microns (12:274).

The parameters of the Heft distribution functions (mass, volatiles and refractories) are listed in Table 10.

Table 10: Parameters of Heft Tri-Component Distributions (12:274)

Quantity	Mass	Volatile (^{137}Cs)	Refractory (^{147}Nd)
ϕ_1 (Local)	0.400	0.153	0.924
σ_1	0.570	0.570	0.570
x_1	2.480	2.480	2.480
$<D>_1$ (μ)	302	302	302
(Atoms/Mg)$_1$ x 10^{-6}	--	0.55	1.05
ϕ_2 (Glass)	0.474	0.48	0.076
σ_2	0.23	0.23	0.23
x_2	1.260	1.138	1.138
$<D>_2$ (μ)	18.2	13.7	13.7
(Atoms/Mg)$_2$ x 10^{-6}	--	1.87	0.052
ϕ_3 (Crystalline)	0.126	0.367	0.00
σ_3	0.280	0.280	--
x_3	0.830	0.649	--
$<D>_3$ (μ)	6.8	4.5	--
(Atoms/Mg)$_3$ x 10^{-6}	--	0.55	0.00

It should be noted that the crystalline component contains no refractories. This supports the crystalline population entering the fireball at a later time after all of the refractories have been scavenged and the temperature of the fireball has dropped below the melting temperature of the local soil material.

The Heft subsurface volatile and refractory distributions use the parameters in the volatile and refractory columns respectively of Table 10. The volatile and refractory distributions are shown in Figure 85 and Figure 86 respectively.
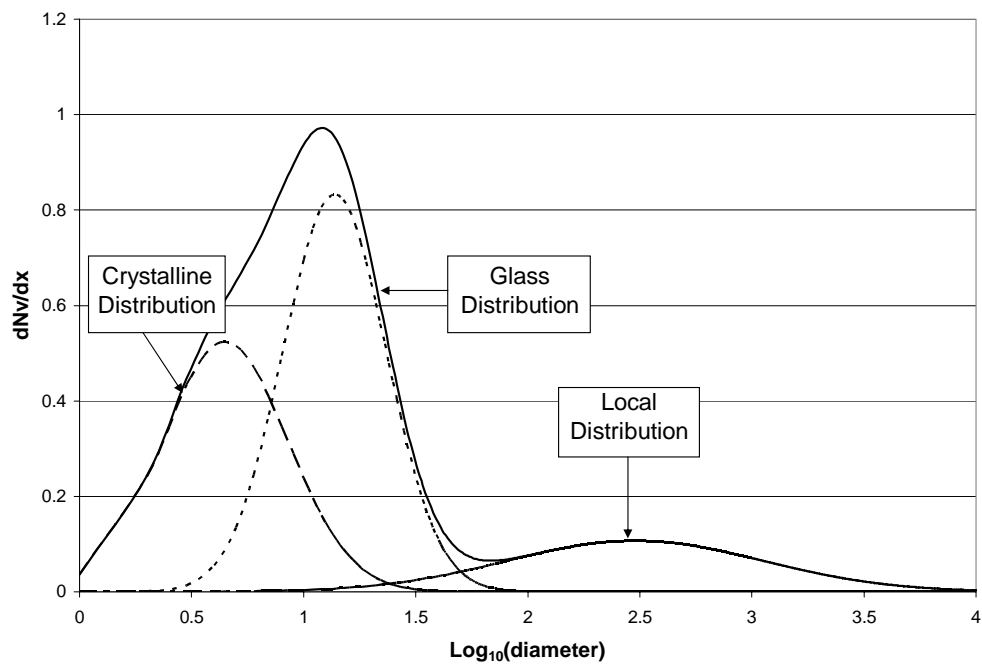
Figure 85: Volatile Distribution for Heft Tri-Component Surface Burst Fallout Particles
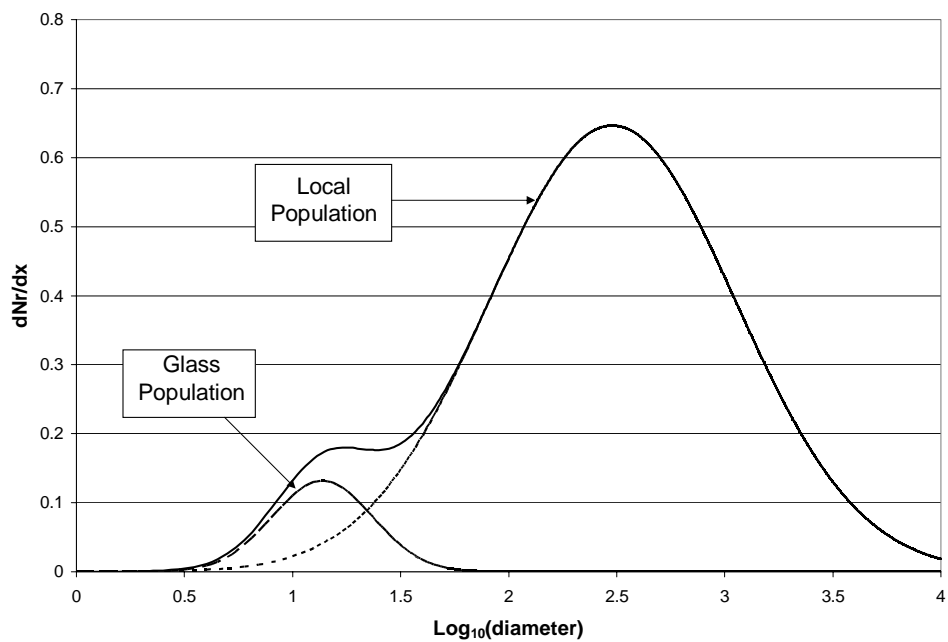
Figure 86: Refractory Distribution for Heft Tri-Component Subsurface Burst Fallout Particles

103

While the local distribution is only approximately 40% of the mass as compared with 47.4% for the glass distribution, it dominates the refractories, giving the local distribution more activity per unit mass than the glass distribution. In addition, the Heft distribution minimizes the amount of activity associated with the crystalline distribution by not giving it any activity at all from refractories and only 36.7% of the activity associated with the volatiles even though the crystalline distribution is 17% of the activity.

Appendix C. Summary of Surface Effects in SCIPUFF

The conservation of mass equation used by SCIPUFF is

$$\frac{dQ}{dt} = -\left(F_s + F_R\right) \qquad\qquad (C\text{-}1)$$

where

Q is mass,

t is time,

F_s is the flux of particles at the surface,

F_R is the flux of particles due to rain scavenging (21:56)

The flux of particles at the surface is defined by:

$$F_s = v_D \int_{z=0} c\, dA .$$

where

v_D is the downward velocity which for particulates is a summation of the average

fall speed of the particle, v_g, and the deposition velocity of the particle, v_d (21:56).

For larger particles, v_D is dominated by the average fall speed of the particles.

The deposition velocity becomes more important the smaller the particle is.

Dry deposition takes into account mechanisms other than gravity and precipitation

that deposit particles from the Gaussian puffs transported by SCIPUFF to the ground or

other surface such as vegetation. Dry deposition is described using the deposition

velocity, v_d. The deposition velocity is defined at a specific reference height which is

either the vegetative canopy or a height above the surface. For particles, the dry

deposition velocity is found using the following equation:

$$v_d = E\left(u_*^2 + \overline{v_*}^2\right)^{1/2} \frac{\kappa}{\ln\left(1 + \dfrac{z_r - z_d}{z_0}\right)} \qquad \text{(C-2)}$$

where

u_* is the surface friction velocity,

v_* is the average local friction speed,

κ is the Von Karmans constant (0.4),

z_r is the reference height,

z_0 is the surface roughness length,

z_d is the displacement length (20:52).

Finally, E is the collection efficiency which is defined by

$$E = 1 - \left(1 - E_B\right)\left(1 - E_{IN}\right)\left(1 - E_{IM}\right) \qquad \text{(C-3)}$$

where

E_B is the efficiency of the viscous sublayer flow within a millimeter of the surface

elements,

E_{IN} is the particle interception,

E_{IM} is particle impaction (21:52).

The variables that make up the collection efficiency are dependent upon the

surface over which the particles are falling. For vegetative canopies, such as leaves or

grass, where Brownian motion is important, the variables are defined as follows

$$E_B = f_D Sc^{-0.7} \qquad \text{(C-4)}$$

where

f_D is the ratio of the viscous drag to the total canopy drag including pressure forces. This is assumed to be 1/3,

Sc is the Schmidt number (21:53).

$$E_{IN} = \left[f\left(\frac{r_p}{r_p + A_s}\right) + (1-f)\left(\frac{r_p}{r_p + A_L}\right) \right]$$ (C-5)

where

f is the fraction of total particles intercepted by collectors,

r_p is the radius of the particle,

A_s is the characteristic radius of small collectors such as vegetative hairs and

A_L is the characteristic radius of large collectors.

SCIPUFF assumes a value of 0.01 for f, 10 μm for A_s and 100 μm for A_L (21:54).

$$E_{IM} = \frac{St^2}{1 + St^2}$$ (C-6)

where

St is the Stokes number (21:54).

SCIPUFF makes a simplifying assumption and finds the average collection efficiency, $\overline{E}$, in order to find the average local deposition rate.

$$\overline{E} = \frac{E}{(1-\beta)E + \beta}$$ (C-7)

where

β is a coefficient between 0.1 and 0.3 that varies with canopy type and velocity profile (21:54).

In addition to the special formulas for collection efficiency SCIPUFF assumes for vegetative canopies, SCIPUFF assumes the following relationships for vegetative canopies:

$$z_d = \frac{h_c}{2} \tag{C-8}$$

$$z_r = 2h_c \tag{C-9}$$

where

h_c is the height of the vegetative canopy (21:55).

For rough surfaces that do not include a vegetative canopy, such as bare soil, rock, etc., there is no interception, so E_{IN} is zero. The other collection efficiency terms are defined as follows (21:55):

$$E_B = 0.8Sc^{-0.7} \tag{C-10}$$

$$E_{IM} = \frac{A_{IM}}{1 + A_{IM}} \tag{C-11}$$

where

$$A_{IM} = 0.08St\left(1 - e^{-0.42St}\right) \tag{C-12}$$

For a rough surface, z_d is assumed to be zero and z_r is assumed to be 10m (21:55). The end result of the dry deposition processes is that the deposition velocity is then added to the fall velocity and thereby impacts the mass flux at the surface which is used by SCIPUFF in its conservation of mass equation.

HPAC offers several surfaces over which fallout particles may fall. These surfaces along with relevant data associated with each surface are presented in table C-1

Table C-1: HPAC Surface Parameters

Surface	Canopy Height or Surface Roughness	Bowen Ratio	Albedo
Desert	0.01 m	4.0	0.3
Urban	0.5 m	1.5	0.16
Cultivated	1 m	0.6	0.16
Grassland	0.25 m	0.9	0.2
Forest	10.0 m	1.0	0.12
Water	Roughness = 0.0005 m	0.11	0.12

The Albedo is a measure of the reflectivity of a surface. Specifically, it is the measure of the radiation of the sun that is reflected to that incident upon a surface. Albedo is a fraction between 0 and 1. The more reflective a surface is, the higher the albedo it has. Therefore snow, which tends to reflect a good portion of the sun's radiation incident upon it, usually has an albedo of about 0.9. In the realm of fallout transport, a low albedo would indicate that a surface is likely to retain radiation from the sun and therefore warm up. This increased temperature at the surface will cause small thermals which would keep the smaller particles suspended for a longer period of time than would otherwise occur.

The Bowen Ratio is the ratio of heat conduction to evaporative flux at the air-water interface. This indicates how much moisture is at the surface compared with the amount of heat conduction. A high Bowen ratio is usually fairly typical of dry surfaces while a low Bowen ratio is more typical of moist surfaces.

The single most important factor for the surfaces considered here is the canopy height of the surface. The friction that resists a passing wind encounters is directly proportional to the canopy height. This friction causes things such as eddies and turbulence which in turn slows down the rate of travel of the transported puffs. A higher friction therefore acts to enhance the particle collection efficiency of surfaces with high canopies. Thus, the higher the canopy is for a particular surface, the more concentrated the fallout will be over that surface.

Appendix D. Code for Calculating g(t)

```
!*****************************Program HPAC G(t) Maker*****************************

Program HPAC_G_t_Maker

!*******************************************************************************
        ! Programer: Timothy Skaar
        ! Purpose:  This program calculates approximate G(t) for HPAC constant wind dose rate fallout
                !contour
        ! Last updated 16 November 2004
                ! Last update was to improve integration scheme from Trapezoid to
        ! Last updated 19 November 2004
                ! EW resolution problem found and fixed.
        ! Updated 23 Nov 2004 - Integration Schemes updated
        ! Updated 1 Dec 2004 - Lat/Long output fixed
        ! Updated 16 Dec 2004 - New Lat/Long coordinates added to 1kt Heft to account for Change in
        Spatial Domain
        ! Updated 22 Dec 2004 - New Lat/Long coordinates added for 100kt Heft & DELFIC

Use Kinds

Implicit None

Character(len=40)::filename, output_filename
Real(dp)::North_Lat
Real(dp)::South_Lat
Real(dp)::East_Long
Real(dp)::West_Long
Real(dp)::Grd_Zero_Long
Real(dp)::Grd_Zero_Lat
Real(dp)::x_resolution, y_resolution
Real(dp)::dose_rate_time                                ! Time dose rate evaluated at in HPAC run
Real(dp)::kph                                           ! Wind Speed used in
HPAC run
Real(dp)::Yield                                        ! [kilotons]
Real(dp)::NS_Resolution, EW_resolution        ! Resolution (miles then later km)
Real(dp)::Longitude_Resolution                 ! Resolution of Longitude
Real(dp)::Starting_Longitude          ! Longitude when time is started after grd zero
Integer::Long_index                           ! Index which relates Starting_longitude to
dose rate
Integer::G_Counter, G_index                    ! Used for reading 4.03 files
Integer::Dimension_Choice
Real(dp)::NS_distance, EW_distance             ! Dimensions of fallout grid in miles
Real(dp),parameter::deg_per_rad = 57.29577951_dp
Real(dp)::A,B,C,D                              ! These are used in lat/long to dist equation
Character(len=40)::scratch,scratchdos,scratchtres, scratchquatro
Character(len=10)::First_Point
Real(dp)::scratch1, scratch2, scratch3
Integer::i,j
Integer::ierror
```

```fortran
Real(dp), allocatable, dimension(:,:)::dose_rate                         ![rad/hr]
Real(dp), allocatable, dimension(:)::Integrate_URDR ! Integrated Unit Reference Dose Rate [R/hr/km]

Real(dp), allocatable, dimension(:,:)::Unit_Reference_Dose_Rate
!Real(dp), parameter::k=8445._dp                        ! Surface normalization value [r-km^2/hr-KT]
        ! There are several possible options for this value.  See Bridgman 436
Real(dp)::k
Real(dp), allocatable, dimension(:)::G_t        !Fractional arrival rate of activity [1/hr]
Real(dp), allocatable, dimension(:)::t                ! Time [hr]
Real(dp)::Distance                                                        ! [km]
Integer::HPAC_Version
Real(dp)::h,XI0, XI1, XI2, X                                ! Variables for Composite Simpson's rule
Integer::Simpson_index
Real(dp)::Integrate_G_t
Real(dp)::Test_Integrate

! Note 1 R=0.88rad


!*******************************************************************************
************
        !The following section of code inputs the long/lat field and calculates resolution and dist.
Write(*,*)"Enter Dimension Choice"
Write(*,*)"1) 1kt Delfic DR"
Write(*,*)"2) 1kt Heft DR"
Write(*,*)"3) 10kt Delfic DR"
Write(*,*)"4) 10kt Heft DR"
Write(*,*)"5) 100kt Delfic DR"
Write(*,*)"6) 100kt Heft DR"
Write(*,*)"7) User Input Dimension"
Read(*,*) Dimension_Choice

Select Case (Dimension_Choice)

        Case(1) !1 kt Delfic DR


                North_Lat = 33.58611_dp
                East_Long = -82.91225_dp
                South_Lat = 33.31649_dp
                West_Long = -84.26616_dp

        Case(2) !1 kt Heft DR

                North_Lat = 33.54073_dp
                East_Long = -82.92603_dp
                South_Lat = 33.35937_dp
                West_Long = -84.25365_dp

        Case(3) ! 10kt Delfic DR

                North_Lat = 33.69978_dp
                East_Long = -81.60902_dp
                South_Lat = 33.16964_dp
```

West_Long = -84.29636_dp

Case(4) ! 10kt Heft DR

North_Lat = 33.62621_dp
East_Long = -82.78434_dp
South_Lat = 33.27465_dp
West_Long = -84.25769_dp

Case(5) ! 100kt Delfic DR

North_Lat = 34.101_dp
East_Long = -79.5_dp
South_Lat = 32.79871_dp
West_Long = -84.34637_dp

Case(6) ! 100kt Heft DR

North_Lat = 33.93053_dp
East_Long = -80.84596_dp
South_Lat = 32.98986_dp
West_Long = -84.34596_dp

Case (7)

Write(*,*)"Enter Northern Latitude"
Read(*,*)North_Lat
Write(*,*)"Enter Eastern Longitude"
Read(*,*)East_Long
Write(*,*)"Enter Sourthern Latitude"
Read(*,*)South_Lat
Write(*,*)"Enter Western Longitude"
Read(*,*)West_Long

End Select

Write(*,*)"North Lat is",North_Lat
Write(*,*)"East Long is", East_long
Write(*,*)"South Lat is", South_lat
Write(*,*)"West Long is",West_Long

Write(*,*)"Enter Ground Zero Latitude"
Read(*,*)Grd_Zero_Lat
Write(*,*)"Enter Ground Zero Longitude"
Read(*,*)Grd_Zero_Long
Write(*,*)"Enter x resolution"
Read(*,*)x_resolution
Write(*,*)"Enter y resolution"
Read(*,*)y_resolution
Write(*,*)"Enter Yield"
Read(*,*)Yield
Write(*,*)"Enter time of dose rate (hrs)"
Read(*,*)dose_rate_time
Write(*,*)"Enter wind speed (kph)"

Read(*,*)kph
Write(*,*)"Enter source normalization constant [(R/hr)km^2 per KT at 1 hr](k)"
Read(*,*)k

!***
****
      ! This section is if several runs are to be done and user doesn't want to constantly input data
      ! Make sure you turn of the read statements in the above section if user wants to use this

Grd_Zero_Long=-84.23_dp
Grd_Zero_Lat=33.45_dp
!x_resolution=150._dp
!y_resolution=150._dp
!dose_rate_time=23.01_dp
!kph=10._dp
!Yield=10._dp

!***
****

North_Lat=North_Lat/deg_per_rad
South_Lat=South_Lat/deg_per_rad
East_Long=East_Long/deg_per_rad
West_Long=West_Long/deg_per_rad

! Find North South Distance in miles
A = North_Lat
B = East_Long
C = South_Lat
D = East_Long !(all converted to radians: degree/57.29577951)

If (North_Lat==South_Lat) then
      NS_Distance=0._dp
ElseIf (SIN(A)*SIN(C)+COS(A)*COS(C)*COS(B-D) > 1._dp) THEN
      NS_Distance = 3963.1_dp * ACOS(1._dp) ! solved a prob I ran into. I haven't fully analyzed it yet
      NS_Distance=NS_distance*1.609344_dp   !Convert from miles to km
ELSE

      NS_Distance = 3963.1_dp*ACOS(SIN(A)*SIN(C)+COS(A)*COS(C)*COS(B-D))
      NS_Distance=NS_distance*1.609344_dp   !Convert from miles to km
End If

! Finds East West Distance in Miles
A = North_Lat
B = East_Long
C = North_Lat
D = West_Long !(all converted to radians: degree/57.29577951)

If (East_Long==West_Long) then
      EW_distance = 0._dp
ElseIf (SIN(A)*SIN(C)+COS(A)*COS(C)*COS(B-D) > 1._dp) THEN
      EW_Distance = 3963.1_dp*ACOS(1._dp) ! solved a prob I ran into. I haven't fully analyzed it yet
      EW_Distance = EW_distance*1.609344_dp !Convert from miles to km

114

```
ELSE

        EW_Distance=3963.1_dp*ACOS(SIN(A)*SIN(C)+COS(A)*COS(C)*COS(B-D))
        EW_Distance = EW_distance*1.609344_dp !Convert from miles to km
End If

Write(*,*)"NS Distance is", NS_Distance, "miles"
Write(*,*)"EW Distance is", EW_Distance, "miles"

Write(*,*)"NS distance is",NS_distance," EW distance is ",EW_distance
NS_Resolution = NS_distance/(y_resolution - 1._dp)
EW_Resolution = EW_distance/(x_resolution - 1._dp)

!*******************************************************************************
************
        ! This section of code reads in the input data

Write(*,*)"What Version of HPAC was used?"
Write(*,*)"1) 4.03 (Delfic Distribution)"
Write(*,*)"2) 4.04 (Heft Distribution)"
Read(*,*)HPAC_Version

Write(*,*)"Enter filename to read data from"
Read(*,*)filename

Allocate(dose_rate(1:Int(x_resolution),1:Int(y_resolution)))
Allocate(integrate_URDR(1:Int(x_resolution)))

Select Case (HPAC_Version)

Case(1)

        If (Int(x_resolution).le.100) then
                G_index = 1000
        Else if ((Int(x_resolution).gt.100).and.(Int(x_resolution).le.300)) then
                G_index = 10000
        Else
                G_index = 100000
        End if

        Open(unit=4, file=filename, status='old', action='read', iostat=ierror)

                If (ierror.ne.0) then

                        Write(*,*) "The output file is not opening"

                End if

                Do i=1,16
                        Read(4,*)scratch
                End Do

                Read(4,*)First_Point
```

```fortran
            Write(*,*)First_Point

            Backspace(4)

            Do i=1,Int(x_resolution)
                    Do j=1,Int(y_resolution)

                            If (j==1.and.First_Point.ne."G0") then

                                    G_counter = (Int(x_resolution)-1) - (i-1)

                            Elseif (j==1) then

                                    G_counter = i-1

                            Else

                                    G_counter = G_counter + Int(x_resolution)

                            End If

                    If (G_counter.lt.G_index) then

                            Read(4,*)scratch,scratchdos,scratch1,scratch2,dose_rate(i,j)
                            dose_rate(i,j)=dose_rate(i,j)/0.88_dp   ! converting from rad to R
                    Else
                            Read(4,*)scratch, scratch1, scratch2, dose_rate(i,j)
                            dose_rate(i,j)=dose_rate(i,j)/0.88_dp            ! converting from rad to R

                    End if

                    End Do
            End Do

    Close(4)

Case(2)

    Open(unit=4, file=filename, status='old', action='read', iostat=ierror)

    If (ierror.ne.0) then

            Write(*,*) "The output file is not opening"

    End If

    Do i=1,27
            Read(4,*)
    End Do


    Do j=1,Int(y_resolution)
            Do i=1,Int(x_resolution)
```

116

```
                    Read(4,*)scratch, scratchdos, scratchtres, scratchquatro, dose_rate(i,j)
                    dose_rate(i,j)=dose_rate(i,j)/0.88_dp          ! Converting from Rad to R

             End Do
        End Do

        Close(4)

End Select



!*********************************************************************************
************
        ! The following section of Code takes the Way-Wigner approximation to find the unit
        ! time reference Dose Rate
Allocate(unit_reference_dose_rate(1:Int(x_resolution),1:Int(y_resolution)))

Do i=1,Int(x_resolution)
        Do j=1,Int(y_resolution)
                    Unit_Reference_Dose_Rate(i,j) = (Dose_Rate(i,j)/dose_rate_time**-1.2_dp)
        End Do
End Do

!*********************************************************************************
***********
        !This section of code integrates the dose using trapazoid method

Write(*,*) "Starting Trapezoid Method"

integrate_URDR=0._dp
Do i=1,Int(x_resolution)
        Do j=2,Int(y_resolution)

                    integrate_URDR(i) = integrate_URDR(i) + (NS_resolution/2._dp)*&
                            &(Unit_Reference_Dose_rate(i,j-1) + Unit_Reference_dose_rate(i,j))

        End Do
End Do


!*********************************************************************************
***********
        ! This section of code integrates the dose using composite simpson's method
        ! See Burden & Faires Pg 199

        Write(*,*)"Starting Simpson's method"

        h = NS_distance/(y_resolution-1)

        Simpson_index=Int(y_resolution)

        If ((Real(Simpson_index, dp)/2._dp)==Real((Simpson_index/2),dp)) then
                    Simpson_index=Simpson_index-1
```

117

```
        End if

        Do i=1, Int(x_resolution)

                !Write(*,*)"I is",i

                XI0 = Unit_Reference_dose_rate(i,1) + Unit_Reference_dose_rate(i, Simpson_Index)
                XI1=0._dp
                XI2=0._dp

                Do j=1, Simpson_index-1

                !       Write(*,*)"j is",j

                        If ((Real(j, dp)/2._dp)==Real((j/2),dp)) then
                                XI2 = XI2 + Unit_Reference_dose_rate(i,j)
                        Else
                                XI1 = XI1 + Unit_Reference_dose_rate(i,j)
                        End if

                End Do

                XI0 = h*(XI0 + 2._dp*XI2 + 4._dp*XI1)/3._dp


                Integrate_URDR(i) = XI0

                If (Simpson_index.ne.Int(y_resolution)) then

                        Integrate_URDR(i)=Integrate_URDR(i) + (NS_resolution/2._dp)*&
                        &(Unit_Reference_Dose_rate(i,Int(y_resolution)-1) + &
                        &Unit_Reference_dose_rate(i,Int(y_resolution)))

                End if

        End Do


!********************************************************************************
***********
        !Starting Test integration to check value for k

Test_integrate=0._dp
Do i=2,Int(x_resolution)
        test_integrate=test_integrate+(EW_resolution/2._dp)*(Integrate_URDR(i-1)+&
                &Integrate_URDR(i))
End Do
Write(*,*)"The old test integrate value is",Test_Integrate


!********************************************************************************
************
        ! This section converts the Unit_Reference_Integrated_Dose_Rate to g(t) and sets up t(i)
```

```
Longitude_Resolution = ((West_Long-East_Long)*deg_per_rad)/x_resolution
Starting_Longitude = West_Long*deg_per_rad
Long_index=0

Do i=1, Int(x_resolution)
        Starting_Longitude = Starting_Longitude - Longitude_Resolution
        Long_index=Long_index+1
        If (Starting_Longitude.gt.Grd_Zero_Long) then
                Starting_Longitude=Starting_Longitude + Longitude_Resolution
                Long_index=Long_index-1
                Exit
        End If
End Do

Allocate(G_t(1:Int(x_resolution)))
Allocate(t(1:Int(x_resolution)))

Write(*,*)"Starting G_t calculation"

        G_t=0._dp
        t=0._dp
        Distance=0._dp

        !Write(*,*)"long index is",long_index

        Do i=Long_index,Int(x_resolution)
                !Write(*,*)"i is",i
                G_t(i)=(Integrate_URDR(i)/(Yield*k))*kph
                If (i.gt.Long_index) then
                        Distance=Distance + EW_resolution
                        t(i)=Distance/kph
                End If
        End Do

        Distance=0._dp
        Do i=Long_index-1,1,-1
                G_t(i)=(Integrate_URDR(i)/(Yield*k))*kph
                Distance=Distance - EW_resolution
                t(i)=Distance/kph
        End Do
!*******************************************************************************
**********
Test_integrate=0._dp
h = Abs(t(1)-t(Int(x_resolution)))/(x_resolution-1)
Do i=2,Int(x_resolution)
        test_integrate=test_integrate+(h/2._dp)*(g_t(i-1)+&
                &g_t(i))
End Do
Write(*,*)"The trap g(t) test integrate value is",Test_Integrate

!*******************************************************************************
************
        ! This section of code uses composite Simpson's rule to integrate G_t
```

```
Write(*,*)"Starting G_t integrate routine"

h = Abs(t(1)-t(Int(x_resolution)))/(x_resolution-1)



        !Write(*,*)"I is",i

        XI0 = g_t(1) + g_t(Int(x_resolution))
        XI1=0._dp
        XI2=0._dp

Do i=1, Int(x_resolution) - 1

        !        Write(*,*)"j is",j

        If ((Real(i+1, dp)/2._dp)==Real(((i+1)/2),dp)) then
                XI2 = XI2 + G_t(i+1)
        Else
                XI1 = XI1 + G_t(i+1)
        End if

End Do

XI0 = h*(XI0 + 2._dp*XI2 + 4._dp*XI1)/3._dp

Integrate_G_t = XI0


!*****************************************************************************
************
        ! This writes the output file

Write(*,*)"Enter output filename"
Read(*,*)output_filename

Open(unit=5, file=output_filename, status='new', action='write', iostat=ierror)

        If (ierror.ne.0) then

                Write(*,*) "The output file is not opening"

        End if

Do i=1,Int(x_resolution)
        Write(5,2001)t(i), g_t(i)
        2001 Format(2es16.7)
End Do

Write(5,*)"Integrate G_t is",Integrate_G_t
Write(5,*)"The file data was read from is",filename
Write(5,*)"South Lat is",South_Lat*deg_per_rad
Write(5,*)"West Long is",West_Long*deg_per_rad
Write(5,*)"North Lat is",North_Lat*deg_per_rad
```

```
Write(5,*)"East Long is",East_Long*deg_per_rad
Write(5,*)"Yield is",yield
Write(5,*)"Dose Rate Time is ",Dose_rate_time
Write(5,*)"Source Normalization constant is ",k
Write(5,*)"This run was completed on 30 Nov 04"

Close(5)


!***********************************************************************************
***********

End Program HPAC_G_t_Maker
```

Appendix E. Code for Calculating the Grounded Source Normalization Constant

```
Program HPAC_k_maker

! Programer Timothy Skaar
        ! Purpose: Input dose rate field from HPAC and calculate grounded source normalization constant
        ! Created on 22 Nov 04
        ! Updated 30 Nov 04 - Added Lat/Long field to output

Use Kinds
Use Lat_Long_converter
Use HPAC_Input

Implicit None

!*****************Variables used in Subroutine
HPAC_Parameters*****************************
Real(dp)::North_Lat
Real(dp)::South_Lat
Real(dp)::East_Long
Real(dp)::West_Long
Real(dp)::Grd_Zero_Long
Real(dp)::Grd_Zero_Lat
Real(dp)::x_resolution, y_resolution
Real(dp)::kph                                                    ! Wind Speed used in
HPAC run
Real(dp)::Yield                                                  ! [kilotons]
Real(dp)::dose_rate_time
!*********************************************************************************
***********
Real(dp)::NS_Resolution, EW_resolution           ! Resolution (miles)
Real(dp)::NS_distance, EW_distance       ! Dimensions of fallout grid in miles

Real(dp)::Longitude_Resolution           ! Resolution of Longitude in whatever units Longitude is in
Real(dp)::Starting_Longitude             ! Longitude which time is started at (closest long to grd zero)
Integer::Long_index                      ! Index which relates Starting_longitude to dose rate

Integer::i,j
Real(dp), allocatable, dimension(:,:)::dose_rate                 ![rad/hr]
Real(dp), allocatable, dimension(:,:)::Unit_Reference_Dose_Rate
Real(dp)::Distance                                              ! [km]

Call HPAC_Parameters(North_Lat,South_Lat, East_Long, West_Long, Grd_Zero_Long,Grd_Zero_Lat,&
                                        &x_resolution, y_resolution,
dose_rate_time, yield)

Write(*,*)"Finished HPAC Parameters Subroutine"

NS_distance=Lat_Long_Distance(North_Lat,East_Long,South_Lat, East_Long)*1.609344_dp
EW_distance=Lat_Long_Distance(North_Lat,East_Long,North_Lat,West_Long)*1.609344_dp
```

```fortran
NS_Resolution = NS_distance/(y_resolution - 1._dp)
EW_Resolution = EW_distance/(x_resolution - 1._dp)

Allocate(dose_rate(1:Int(x_resolution), 1:Int(y_resolution)))

Write(*,*)"Starting HPAC Dose Rate Reader Subroutine"

Call HPAC_Dose_Rate_Reader(dose_rate, x_resolution, y_resolution, yield)

Write(*,*)"Finished Reading input"

!*****************************************************************************
************
        ! The following section of Code takes the Way-Wigner approximation to find the unit
        ! time reference Dose Rate
Allocate(unit_reference_dose_rate(1:Int(x_resolution),1:Int(y_resolution)))

Write(*,*)"Finished Allocating URDR"

Do i=1,Int(x_resolution)
        Do j=1,Int(y_resolution)

                Unit_Reference_Dose_Rate(i,j) = (Dose_Rate(i,j)/dose_rate_time**-1.2_dp)

        End Do
End Do

Write(*,*)"Finished creating unit_reference_dose_rate"

!*****************************************************************************
************

Call Integrate(EW_distance, NS_distance, EW_resolution, NS_resolution, Int(x_resolution), &
                                & Int(y_resolution), Unit_Reference_Dose_rate, Yield)

End Program HPAC_k_maker

!*****************************************************************************
************

Subroutine Integrate(EW_distance, NS_distance, dgx, dgy, nxmap, nymap, Dose_Rate, Yield)

! Integrate routine is 2-D Simpson's from Burden and Faires

Implicit None

Integer, Parameter:: dp = Selected_Real_Kind(p=14)

Real(dp), Intent(in)::NS_distance    ! distance in kilometers from the map center to the left map edge
Real(dp), Intent(in)::EW_distance    ! distance in kilometers from the map center to the lower map edge
Real(dp), Intent(in)::dgx                       ! resolution in kilometers in the x-direction (left to right across
map)
Real(dp), Intent(in)::dgy                       ! resolution in kilometers in the y-direction (top to bottom
across map)
```

```fortran
Integer, Intent(in)::nxmap                         ! number of points in the x direction across the map
Integer, Intent(in)::nymap                         ! number of points in the y direction across the map
Real(dp), Dimension(nxmap,nymap), Intent(in)::Dose_Rate
Real(dp)::a,b,n,m
Real(dp)::h,x,y
Real(dp)::J1, J2, J3, HX
Real(dp)::K1, K2, K3
Real(dp)::ymax,xmax,ymin,xmin
Real(dp)::Q
Real(dp)::L
Real(dp)::J
Real(dp)::k_eff                                    ! Grounded Source Normalization Constant
Integer::i, z

ymin=0._dp
xmin=0._dp

a=xmin
b=EW_distance
n=Real(nxmap-1, dp)
m=Real(nymap-1, dp)

! Step One (Page 233)
h=(b-a)/n
J1=0._dp
J2=0._dp
J3=0._dp

! Step Two (Page 233)
Do i=0,n

        ! Step Three

        x=a+i*h
        ymax=NS_distance
        xmax=EW_distance
        HX = (ymax-ymin)/m
        K1=dose_rate(i+1,1) + dose_rate(i+1, nymap)
        K2 = 0._dp
        K3 = 0._dp

        ! Step Four
        Do z=1, m-1

                ! Step Five
                y = 0._dp + z*HX
                Q=dose_rate(i+1,z+1)

                ! Step Six
                If ((Real(z, dp)/2._dp)==Real((z/2),dp)) then
                        K2=K2+Q
                Else
                        K3=K3+Q
                End if
```

```
        End Do

        ! Step Seven
        L= (K1 + 2._dp*K2 + 4._dp*K3)*HX/3._dp

        ! Step Eight
        If (i==0.or.i==Int(n)) then
                J1=J1+L
        Else If ((Real(i, dp)/2._dp)==Real((i/2),dp)) then
                J2=J2+L
        Else
                J3=J3+L
        End if
End Do

! Step Nine
J=h*(J1+2._dp*J2+4._dp*J3)/3._dp

!J= dose

Write(*,*)"The integrated Dose Rate is ",J

k_eff=J/Yield

Write(*,*)"The Grounded Source Normalization Constant is",k_eff

Return

End Subroutine Integrate
```

```
Module HPAC_Input

! Modified 16 Dec 2004: Updated 1kt Heft Dimensions to reflect change in Spatial Domain

Use Kinds
Implicit None

Public::HPAC_Parameters, HPAC_Dose_Rate_Reader
Private

Contains

Subroutine HPAC_Parameters(North_Lat,South_Lat, East_Long, West_Long,
Grd_Zero_Long,Grd_Zero_Lat,&
                                                &x_resolution, y_resolution,
dose_rate_time, yield)

        Real(dp), intent(inout)::North_Lat
        Real(dp), intent(inout)::South_Lat
        Real(dp), intent(inout)::East_Long
        Real(dp), intent(inout)::West_Long
        Real(dp), intent(inout)::Grd_Zero_Long
        Real(dp), intent(inout)::Grd_Zero_Lat
        Real(dp), intent(inout)::x_resolution, y_resolution
        Real(dp), intent(inout)::dose_rate_time                  ! Time dose rate evaluated
at in HPAC run
        Real(dp), intent(inout)::yield
        Integer::Dimension_Choice

        Write(*,*)"Enter Dimension Choice"
        Write(*,*)"1) 1kt Delfic DR"
        Write(*,*)"2) 1kt Heft DR"
        Write(*,*)"3) 10kt Delfic DR"
        Write(*,*)"4) 10kt Heft DR"
        Write(*,*)"5) 100kt Delfic DR"
        Write(*,*)"6) 100kt Heft DR"
        Write(*,*)"7) User Input Dimension"
        Read(*,*) Dimension_Choice

        Select Case (Dimension_Choice)

                Case(1) !1 kt Delfic DR

                !North_Lat = 33.60298_dp
                !East_Long = -82.93110_dp
                !South_Lat = 33.2173_dp
                !West_Long = -84.26808_dp
                North_Lat = 33.58611_dp
                East_Long = -82.91225_dp
                South_Lat = 33.31649_dp
                West_Long = -84.26616_dp

                Case(2) !1 kt Heft DR
```

126

```
                    ! Old Lat Long for HPAC default Spatial Domain
                    !North_Lat = 33.54320_dp
                    !East_Long = -82.90273_dp
                    !South_Lat = 33.32721_dp
                    !West_Long = -84.32642_dp

                    ! New Lat Long for HPAC with User Adjusted Spatial Domain
                    North_Lat = 33.54073_dp
                    East_Long = -82.92603_dp
                    South_Lat = 33.35937_dp
                    West_Long = -84.25365_dp

          Case(3) ! 10kt Delfic DR

                    North_Lat = 33.69978_dp
                    East_Long = -81.60902_dp
                    South_Lat = 33.16964_dp
                    West_Long = -84.29636_dp

          Case(4) ! 10kt Heft DR

                    North_Lat = 33.62621_dp
                    East_Long = -82.78434_dp
                    South_Lat = 33.27465_dp
                    West_Long = -84.25769_dp

          Case(5) ! 100kt Delfic DR

                    !North_Lat = 33.89648_dp
                    !East_Long = -80.22811_dp
                    !South_Lat = 33.01025_dp
                    !West_Long = -84.34988_dp

                    North_Lat = 34.101_dp
                    East_Long = -79.5_dp
                    South_Lat = 32.79871_dp
                    West_Long = -84.34637_dp

          Case(6) ! 100kt Heft DR

!                   North_Lat = 33.70267_dp
!                   East_Long = -81.41802_dp
!                   South_Lat = 33.18209_dp
!                   West_Long = -84.29610_dp

                    North_Lat = 33.93053_dp
                    East_Long = -80.84596_dp
                    South_Lat = 32.98986_dp
                    West_Long = -84.34596_dp

          Case (7)

                    Write(*,*)"Enter Northern Latitude"
                    Read(*,*)North_Lat
```

127

```fortran
                        Write(*,*)"Enter Eastern Longitude"
                        Read(*,*)East_Long
                        Write(*,*)"Enter Sourthern Latitude"
                        Read(*,*)South_Lat
                        Write(*,*)"Enter Western Longitude"
                        Read(*,*)West_Long

                End Select

        Write(*,*)"North Lat is",North_Lat
        Write(*,*)"East Long is", East_long
        Write(*,*)"South Lat is", South_lat
        Write(*,*)"West Long is",West_Long

        Write(*,*)"Enter Ground Zero Latitude"
        !Read(*,*)Grd_Zero_Lat
        Write(*,*)"Enter Ground Zero Longitude"
        !Read(*,*)Grd_Zero_Long
        Write(*,*)"Enter x resolution"
        Read(*,*)x_resolution
        Write(*,*)"Enter y resolution"
        Read(*,*)y_resolution
        Write(*,*)"Enter Yield"
        Read(*,*)Yield
        Write(*,*)"Enter time of dose rate (hrs)"
        Read(*,*)dose_rate_time
        Write(*,*)"Enter wind speed (kph)"
        !Read(*,*)kph

        !*****************************************************************************
*********************
                ! This section is if several runs are to be done and user doesn't want to constantly input
data
                ! Make sure you turn of the read statements in the above section if user wants to use this

        Grd_Zero_Long=-84.23_dp
        Grd_Zero_Lat=33.45_dp
        !x_resolution=150._dp
        !y_resolution=150._dp
        !dose_rate_time=23.01_dp
        !Yield=10._dp

        !*****************************************************************************
*********************

        Return

End Subroutine HPAC_Parameters

Subroutine HPAC_Dose_Rate_Reader(dose_rate, x_resolution, y_resolution, yield)

        ! This subroutine reads in the Dose Rate from HPAC (which is given in rads) and returns
        ! the dose rate array to the Main Program in Renken
```

```fortran
        Real(dp), intent(in)::x_resolution, y_resolution
        Real(dp), dimension(x_resolution,y_resolution), intent(inout)::dose_rate
        Real(dp), intent(in)::Yield
        Integer::HPAC_Version
        Character(len=40)::filename
        Integer::G_Counter, G_index                                      ! Used for reading 4.03
files
        Integer::ierror
        Integer::i,j
        Character(len=40)::scratch,scratchdos,scratchtres, scratchquatro
        Real(dp)::scratch1, scratch2, scratch3
        Character(len=10)::First_Point

        Write(*,*)"What Version of HPAC was used?"
        Write(*,*)"1) 4.03 (Delfic Distribution)"
        Write(*,*)"2) 4.04 (Heft Distribution)"
        Read(*,*)HPAC_Version

        Write(*,*)"Enter filename to read data from"
        Read(*,*)filename

        Select Case (HPAC_Version)

        Case(1)

                If (Int(x_resolution).le.100) then
                        G_index = 1000
                Else if ((Int(x_resolution).gt.100).and.(Int(x_resolution).le.300)) then
                        G_index = 10000
                Else
                        G_index = 100000
                End if

                Open(unit=4, file=filename, status='old', action='read', iostat=ierror)

                        If (ierror.ne.0) then

                                Write(*,*) "The output file is not opening"

                        End if

                        Do i=1,16
                                Read(4,*)scratch
                        End Do

                        Read(4,*)First_Point

                        Write(*,*)First_Point

                        Backspace(4)

                        Do i=1,Int(x_resolution)
                                Do j=1,Int(y_resolution)
```

```fortran
                    If (j==1.and.First_Point.ne."G0") then

                            G_counter = (Int(x_resolution)-1) - (i-1)

                    Elseif (j==1) then

                            G_counter = i-1

                    Else

                            G_counter = G_counter + Int(x_resolution)

                    End If

                    If (G_counter.lt.G_index) then

Read(4,*)scratch,scratchdos,scratch1,scratch2,dose_rate(i,j)
                            dose_rate(i,j)=dose_rate(i,j)/0.88_dp
! Converts from rad to R
                            !Write(*,*)"G counter is",G_counter
                            !Write(*,*)scratch
                    Else
                            Read(4,*)scratch, scratch1, scratch2, dose_rate(i,j)
                            dose_rate(i,j)=dose_rate(i,j)/0.88_dp
! Converts from rad to R
                            !Write(*,*)scratch
                            !Write(*,*)"G counter is",G_counter
                    End if

            End Do
        End Do

    Close(4)

Case(2)

    Open(unit=4, file=filename, status='old', action='read', iostat=ierror)

    If (ierror.ne.0) then

            Write(*,*) "The output file is not opening"

    End If

    Do i=1,27
            Read(4,*)
    End Do


    Do j=1,Int(y_resolution)
            Do i=1,Int(x_resolution)

                    Read(4,*)scratch, scratchdos, scratchtres, scratchquatro, dose_rate(i,j)
```

130

```
                    dose_rate(i,j)=dose_rate(i,j)/0.88_dp                    ! Converts from
rad to R

                End Do
            End Do

            Close(4)

        End Select

        Return

    End Subroutine HPAC_dose_rate_reader

End Module HPAC_Input
```

```
Module Lat_Long_Converter

Use Kinds
Implicit None

Public::Lat_Long_Distance
Private

Contains

Function Lat_Long_Distance(Lat1,Long1,Lat2, Long2) Result(distance)

! Purpose
        ! This subroutine takes a pair of longitude/latitude points and finds the distance
        ! between them.
        ! Note 1: Longitude and Latitude points should be input as degrees.
        ! Note 2: Latitude should always be input as N.  Therefore, 33.4S should be input as -33.4N
        ! Note 3: Longitude should always be input as E.  Therefore, 84.23W should be input as -84.23E
        ! Note 4: Output distance is miles.  To convert to kilometers, multiply by 1.609344

        Real(dp),parameter::deg_per_rad = 57.29577951_dp
        Real(dp), intent(in)::Lat1,Long1,Lat2,Long2          ! Latitude and Longitude for points 1 and 2
        Real(dp)::Distance
        Real(dp)::A,B,C,D                                                          ! Local
Variables

        A=Lat1/deg_per_rad
        B=Long1/deg_per_rad
        C=Lat2/deg_per_rad
        D=Long2/deg_per_rad

        If (A==C.and.B==D) then
                Distance=0._dp
        ElseIf (SIN(A)*SIN(C)+COS(A)*COS(C)*COS(B-D) > 1._dp) THEN
                Distance = 3963.1_dp * ACOS(1._dp)

        ELSE

                Distance = 3963.1_dp*ACOS(SIN(A)*SIN(C)+COS(A)*COS(C)*COS(B-D))

        End If

End Function Lat_Long_Distance

End Module Lat_Long_Converter
```

```fortran
Module Kinds
Implicit None
        Integer, Parameter:: dp = Selected_Real_Kind(p=14)

        Real(dp), Parameter::Pi=3.14159265359_dp

End Module Kinds
```

Bibliography

1.   Atchison, J. and J.A.C. Brown. *The Lognormal Distribution.* Cambridge, MA: Cambridge University Press, 1957.

2.   Bridgmann, Charles J. *Introduction to the Physics of Nuclear Weapon Effects.* Alexandria, VA: DTRA, 2001.

3.   Burden, Richard L. and J. Douglas Faires *Numerical Analysis* Seventh Edition Pacific Grove, CA: Brooks/Cole, 2001.

4.   Chancellor, Richard M. *A Comparison of Hazard Prediction and Assessment Capability (HPAC) Software Dose Rate Contour Plots to a Sample of Local Fallout Data from Test Detonations in the Continental United Stated, 1945-1962* MS Thesis, AFIT/GNE/ENP/05M-02. Wright-Patterson AFB, OH: Graduate School of Engineering, Air Force Institute of Technology, March 2005.

5.   Eisenbud, Merril and Thomas, Gesell. *Environmental Radioactivity From Natural, Industrial, and Military Sources.* San Diego: Academic Press, Fourth Edition. 1997.

6.   Freiling, E.C., Kay, M.A. and J.V. Sanderson. *Fractionation IV: Illustrative Calculations of the Effect of Radionuclide Fractionation on Exposure-Dose Rate from Local Fallout.* San Francisco, CA: U.S. Naval Radiological Defense Laboratory, 1968.

7.   Freiling, E.C. "Radionuclide Fractionation in Bomb Debris," *Science*, 133: 1991-1998 (June 1961).

8.   Glasstone, Samuel and Philip J. Dolan *The Effects of Nuclear Weapons.* Washington, DC: U.S. Government Printing Office, Second Edition, 1962.

9.   Glasstone, Samuel and Philip J. Dolan *The Effects of Nuclear Weapons.* Washington, DC: U.S. Government Printing Office, Third Edition, 1977.

10. Hawthorne, Howard A., Ed. *Compilation of Local Fallout Data from Test Detonations 1945-1962 Extracted from Dasa 1251: Volume II – Oceanic U.S. Tests.* Washington, D.C.: Defense Nuclear Agency, 1979.

11. *Hazard Prediction and Assessment Capability (HPAC): User's Guide Version 4.0* San Diego, CA: SAIC Corporation, August 2001.

12. Heft, Robert E. "The Characterization of Radioactive Particles from Nuclear Weapons Tests," *Radionuclides in the Environment.* Washington DC: American Chemical Society, 1970.

13. Krieser, Curtis R. *A Rain Scavenging Model for Predicting Low Yield Airburst Weapon Fallout for Operational Type Studies* MS Thesis, AFIT/GNE/PH/84M-9. Wright-Patterson AFB, OH: Graduate School of Engineering, Air Force Institute of Technology, Mar 1984.

14. McGahan, Joseph T. Engineer, SAIC, Washington D.C. Personal Correspondance. 13 October 2004.

15. McGahan, Joseph T. "In Cloud Scavening for Low-Intermediate Yields Preliminary," Microsoft PowerPoint Presentation, 21 October 2003.

16. McGahan, Joseph T. "Newfall Users Guide and Reference Manual Version 7.5," 5 March 1996.

17. Morris, Douglass B. *A Predictive Technique for Forecasting the Isotopic Composition of Radioactive Fallout*. PhD. dissertation, AFIT/DS/ENP/04-02. Wright-Patterson AFB, OH: Graduate School of Engineering, Air Force Institute of Technology. December 2004.

18. Norment, H.G., Ing, W.Y.G. and J. Zuckerman *Department of Defense Land Fallout Prediction System: Volume II – Initial Conditions* Edgewood Arsenal, MD: Defense Atomic Support Agency, 1966.

19. Norment, H.G. *DELFIC: Department of Defense Fallout Prediction System Volume I – Fundamentals*. Bedford, MA: Atmospheric Science Associates, 1979.

20. Parker, Edward N. *DASA-1188: Radioactive Fallout from Nuclear Explosions* Washington, D.C.: Defense Atomic Support Agency, 1960.

21. Sykes, R.I., Parker, S.F. , Henn, D.S., Cerasoli, C.P. and L.P. Santos *PC-SCIPUFF Version 1.2PD Technical Documentation*. Princeton, NJ: Titan Corporation, 1998.

22. Tompkins, Robert C. *DASA 1800-V: Department of Defense Land Fallout Prediction System Volume V – Particle Activity*. Edgewood Arsenal, MD: 1968.

23. Wallace, John M. and Peter V. Hobbs *Atmospheric Science: An Introductory Survey*. San Diego, CA: Academic Press, 1977.

REPORT DOCUMENTATION PAGE

The public reporting burden for this collection of information is estimated to average 1 hour per response, including the time for reviewing instructions, searching existing data sources, gathering and maintaining the data needed, and completing and reviewing the collection of information. Send comments regarding this burden estimate or any other aspect of this collection of information, including suggestions for reducing the burden, to the Department of Defense, Executive Services and Communications Directorate (0704-0188). Respondents should be aware that notwithstanding any other provision of law, no person shall be subject to any penalty for failing to comply with a collection of information if it does not display a currently valid OMB control number.

PLEASE DO NOT RETURN YOUR FORM TO THE ABOVE ORGANIZATION.

1. REPORT DATE *(DD-MM-YYYY)*	2. REPORT TYPE	3. DATES COVERED *(From - To)*

4. TITLE AND SUBTITLE

5a. CONTRACT NUMBER

5b. GRANT NUMBER

5c. PROGRAM ELEMENT NUMBER

6. AUTHOR(S)

5d. PROJECT NUMBER

5e. TASK NUMBER

5f. WORK UNIT NUMBER

7. PERFORMING ORGANIZATION NAME(S) AND ADDRESS(ES)

8. PERFORMING ORGANIZATION REPORT NUMBER

9. SPONSORING/MONITORING AGENCY NAME(S) AND ADDRESS(ES)

10. SPONSOR/MONITOR'S ACRONYM(S)

11. SPONSOR/MONITOR'S REPORT NUMBER(S)

12. DISTRIBUTION/AVAILABILITY STATEMENT

13. SUPPLEMENTARY NOTES

14. ABSTRACT

15. SUBJECT TERMS

16. SECURITY CLASSIFICATION OF:			17. LIMITATION OF ABSTRACT	18. NUMBER OF PAGES	19a. NAME OF RESPONSIBLE PERSON
a. REPORT	b. ABSTRACT	c. THIS PAGE			
					19b. TELEPHONE NUMBER *(Include area code)*